

Structural and Mineralogical Controls  
on the Formation of the 'Inter-lens' at  
the Ernest Henry Deposit,  
Queensland.

Thesis submitted in accordance with the requirements of the University of  
Adelaide for an Honours Degree in Geology

Shaun Patrick O'Brien  
November 2016



THE UNIVERSITY  
*of* ADELAIDE

## **STRUCTURAL AND MINERALOGICAL CONTROLS ON THE FORMATION OF THE 'INTER-LENS' AT THE ERNEST HENRY DEPOSIT, QUEENSLAND.**

### **INTER-LENS: CHARACTERISATION AND CONTROLS.**

#### **ABSTRACT**

The Ernest Henry Iron-oxide Copper Gold (IOCG) deposit is by far the largest in the Eastern Succession of the Mount Isa Inlier. In the current genetic model, the release of CO<sub>2</sub> from fluids sourced from enriched mantle was critical to brecciation and mineralisation. However, a weakly -mineralised and -brecciated shear zone within the orebody named the 'Inter-lens' separates the orebody into two distinct lenses. The Inter-lens was not well reported early in the life of the mine and has not been taken into account in the current ore deposit models. Establishing the relative timing of the Inter-lens structure provides strong geological constraints for the formation of the orebody. In this study, optical petrographic investigation, Scanning Electron Microscopy (SEM) and Mineral Liberation Analysis (MLA) were used to investigate the protolith. Key mineral relationships and textures were assessed to reveal the paragenesis of the Inter-lens. Structural observations in oriented drill core complimented underground mapping of exposures of the Inter-lens to reveal the deformational history of the Inter-lens with respect to the Ernest Henry orebody. The protolith was revealed to be Mount Fort Constantine Metavolcanics that have undergone intense deformation with a metasomatic evolution broadly consistent with the main ore-body. Mineralisation stages overprinted tectonic fabrics via veining, replacement and infill, providing direct evidence that the Inter-lens is a pre-mineralisation structure. Preservation of the Inter-lens during brecciation and mineralisation of the Ernest Henry deposit requires that the currently accepted 'explosive' breccia model must be revised.

**KEYWORDS**

Mount Isa Inlier, Cloncurry, IOCG, Ernest Henry, Structural, Mineralogical, Paragenesis, Alteration.

## TABLE OF CONTENTS

Structural and Mineralogical Controls on the Formation of the 'Inter-lens' at the Ernest Henry Deposit, Queensland. ....	i
Abstract.....	i
Keywords.....	ii
List of Figures and Tables .....	4
Introduction.....	5
Project Aims .....	7
Background and Geological Setting .....	8
Regional Geology.....	8
Tectonic History and Stratigraphy of the Eastern Succession.....	8
Isan Orogeny.....	9
Cloncurry Iron Oxide Copper Gold (IOCG) mineral systems.....	11
Local Geology .....	11
Location and discovery.....	11
Host Rocks – Mount Fort Constantine Volcanics .....	12
Ernest Henry deposit.....	13
Inter- lens .....	14
hydrothermal alteration and paragenesis .....	15
Stage 1- Regional Sodid and Sodid-Calcic .....	16
Stage 2- Pre-mineralisation (Dark-rock and Red-rock).....	16
Stage 3- Cu-Au Mineralisation.....	17
Methods .....	19
Petrography and optical microscopy .....	22
Scanning Electron Microscope (SEM) and Mineral Liberation Analysis (MLA) .....	22
observations and Results.....	23
Inter- lens contacts .....	23
Structure.....	26
Oriented Core Summary .....	27
Rocks of the Inter- lens .....	32
Porphyritic Meta-andesite.....	32
Tectonic fabrics .....	33
Biotite-magnetite anastomosing foliation.....	34
Biotite-Garnet-Magnetite veining.....	36
Elongate breccia clasts in quartz-calcite-rich matrix.....	39



Quartz-calcite veining (and wall-rock Replacement) .....	43
Calcite birds-wings .....	45
Alteration Stages and Mineral Textures .....	46
Albitisation .....	46
Magnetite + Biotite (replacement of albite).....	46
Potassic feldspar .....	47
Biotite + Magnetite (rims of breccia clasts) .....	47
Cu-mineralisation .....	49
Sericite .....	52
Chlorite .....	53
Mineral Liberation analysis (MLA) Maps .....	55
EH889_04 .....	58
EH889_08 .....	58
EH760_11 .....	58
Discussion.....	59
Hypothesis 1: The protolith of the Inter-lens is the same protolith as the Ernest Henry orebody (Mount Fort Constantine Volcanics). .....	59
Hypothesis 2: The paragenesis of the Inter-lens is consistent with paragenesis of the Ernest Henry deposit.....	60
Hypothesis 3: The formation of the Inter-lens post-dates mineralisation of the Ernest Henry deposit.....	62
Does understanding of the Inter-lens have any implications for the genetic models for the Ernest Henry orebody? .....	63
Conclusions.....	65
Acknowledgments .....	66
References.....	66
Appendix A: Description of host rocks at Ernest Henry. ....	68
Appendix B: Extended Methods.....	69
Core orientation .....	70
Structural measurements from oriented core .....	70
Core Logging .....	72
Underground .....	73
Petrography and optical microscopy .....	73
Scanning Electron Microscope (SEM) and Mineral Liberation Analysis (MLA) .....	74
Appendix C: Oriented Drillhole Structural Data .....	75
Appendix D: SAmples and descriptions. ....	77
Appendix E: Core logging summary .....	95

Appendix F: Graphical drillhole logs. ....	96
EH640 .....	96
EH656 .....	109
EH680 .....	116
EH760 .....	120
EH764 .....	128
EH889 .....	131

## LIST OF FIGURES AND TABLES

Figure 1: 3-dimensional Ernest Henry deposit model .....	6
Figure 2: Regional geology and study location .....	10
Figure 3: Interpreted Ernest Henry basement geology model .....	13
Figure 4: Representative images of host rocks and distribution at Ernest Henry .....	15
Figure 5: Paragenetic sequence Stages 1, 2 and 3 of Ernest Henry .....	18
Figure 6: Plan of study area in section view .....	19
Figure 7: Underground mapping of level 1500 .....	20
Figure 8: Underground mapping of level 1525 .....	21
Figure 9: South-facing exposure of Inter-lens contact on level 1525 .....	23
Figure 10: Samples of clast supported breccia within Inter-lens contact zone .....	24
Figure 11: Inter-lens contacts in drill core .....	25
Figure 12: Equal area projection of measured Inter-lens contacts .....	26
Figure 13: Overlaying underground mapping of levels 1500, 1525 and 1550 .....	27
Figure 14: Equal area projection displaying poles to structural measurements .....	28
Figure 15: Poles to foliation in oriented drill core .....	29
Figure 16: Poles to foliation measurements taken underground .....	30
Figure 17: Representative examples of tectonic fabrics of the Inter-lens .....	31
Figure 18: Biotite-magnetite altered, porphyritic metavolcanic rock .....	33
Figure 19: Anastomosing biotite-magnetite foliation .....	35
Figure 20: Garnet-biotite-magnetite gash-style vein .....	37
Figure 21: Petrographic transect of bt-gt vein to qtz-cal matrix .....	38
Figure 22: Typical examples of elongate breccia clasts in calcite-rich matrix .....	40
Figure 23: Clast supported variation of elongate clasts in quartz-calcite-rich matrix ....	41
Figure 24: Quartz-calcite veining to wall-rock replacement .....	44
Figure 25: Representative image of 'birds-wing' tension vein textures .....	46
Figure 26: Representative images of alteration styles observed in the Inter-lens. ....	48
Figure 27: Representative examples of brecciated porphyritic meta-andesites .....	50
Figure 28: Chalcopyrite replacement textures. ....	50
Figure 29: Chalcopyrite infill textures .....	51
Figure 30: Chalcopyrite mineralisation cross cutting pre-existing fabrics. ....	51
Figure 31: Mineralisation stage calcite textures .....	52
Figure 32: Representative examples of chlorite alteration .....	53
Figure 33: MLA map of EH889_04 .....	55
Figure 34: MLA map of EH889_08 .....	56
Figure 35: MLA map of EH760_11. ....	57
Figure 36: Paragenesis of the Inter-lens w.r.t. Mark et al. (2006). ....	61
Figure 37: Basic geological model representing Inter-lens deformation and overprinting relationships. ....	64
Table 1: 760_06 Key mineralisation sequence and associate alteration stages .....	38
Table 2: 889_04 Mineralisation sequence and associate alteration stages .....	42
Table 3: EHM_21955 Mineralisation sequence and associate alteration stages .....	42
Table 4: EHM_21954 Mineralisation sequence and associate alteration stages .....	45
Table 5: Distribution of 'birds-wings' tension veins .....	45
Table 6: Summary of alteration stages and mineral textures .....	54

## INTRODUCTION

The discovery of the Ernest Henry Cu-Au deposit, approximately 35km northeast of the township of Cloncurry, was made in 1991 beneath >30m of Phanerozoic sedimentary cover. The magnetite dominated pipe-like breccia is hosted in Proterozoic, Mount Fort Constantine (intermediate) Volcanics and minor metasediments (Williams et al., 2005) bound at the hanging wall and footwall contacts by the NE-trending Hanging Wall Shear Zone (HWSZ) and Footwall Shear Zone (FWSZ) dipping ~40° towards SSE. The pre-mining resource of 167 Mt at 1.1% Cu and 0.54 ppm Au (Mark, Oliver, & Williams, 2006) is the largest deposit in the Eastern Succession of the Mount Isa Inlier. The Ernest Henry discovery inspired exploration strategies which commonly targeted significant magnetic anomalies. However, uneconomical or barren magnetite-bearing 'ironstones' continue to be discovered, which raises questions of the validity of contemporary geological models. Importantly, Cu-Au mineralisation at Ernest Henry occurs as hydrothermal breccia infill and minor alteration in a magnetite dominated breccia and as such, resolving the mechanisms of brecciation is essential.

The currently accepted model of the Ernest Henry deposit proposes that release of CO<sub>2</sub> from fluids sourced from enriched mantle or mafic magmas was critical to brecciation and mineralisation. Scavenging of ore components from local mafic wall rocks preceded the release of CO<sub>2</sub> under immense pressure (Oliver et al., 2006). This is interpreted to have generated 'explosive' fluidised (transport) breccia in a model similarly applied to describe phenomena such as kimberlite dykes (Oliver et al., 2006). However, an alternative hypothesis in favour of chemical milling processes is also supported. In this scenario, breccias developed through repeated interaction with fluids which 'digested'

wall-rock and clast boundaries along strongly structurally controlled pathways into dilatant structures (Baker, 1998; Pollard, 2006; Austin & Blenkinsop, 2008).

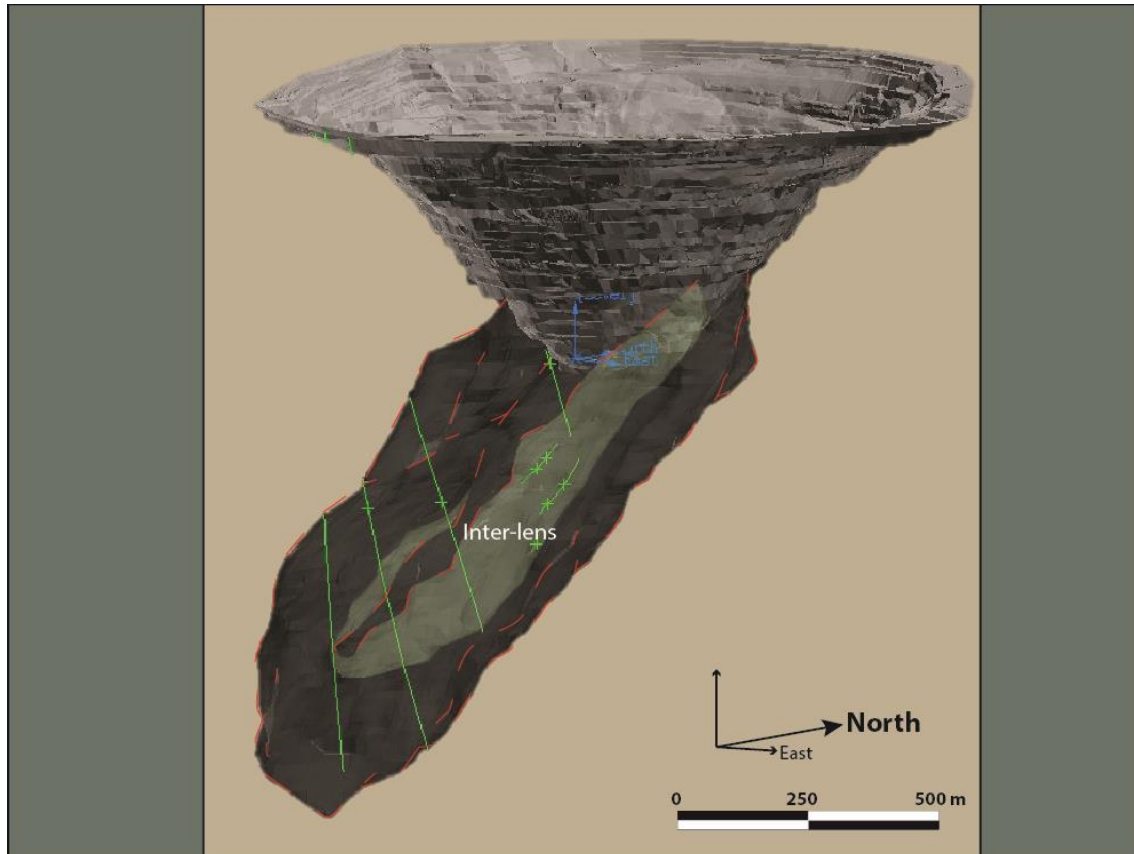


**Figure 1: 3-dimensional Ernest Henry deposit modelled on 1% cu grade shell using Surpac software 2016, Inter-lens in green.**

Extensive work by Mark et al. (2006) has revealed great detail of the metasomatic evolution of the Ernest Henry mineral system, although a definitive genetic model remains contentious. Adding to the complexity at Ernest Henry, exploration drilling and underground development has identified a weakly mineralised and weakly brecciated zone within the orebody named the 'Inter-lens' which separates the orebody into two distinct lenses. The Inter-lens was not well reported early in the life of the mine and its presence has not been taken into account in the current ore deposit models. Preliminary

inspection reveals a persistent shear fabric, although the timing and nature of Inter-lens deformation is unconstrained. Until now, no formal study has been undertaken to characterise the mineralogical and structural relationships between the Inter-lens and the main ore body, which are currently poorly understood. Establishing the relative timing of the Inter-lens structure will provide strong geological constraints for the formation of the orebody and it is hoped that the results will aid exploration targeting at mine and regional scales. In this paper, petrographic investigation and structural observations using drill core and mapping of underground exposures will investigate the protolith, paragenesis and deformational history of the Inter-lens with respect to the Ernest Henry orebody.

### **Project Aims**

The study aims to resolve the following hypotheses:

- Hypothesis 1: The protolith of the Inter-lens is the same protolith as the Ernest Henry orebody (Mount Fort Constantine Volcanics).
- Hypothesis 2: The paragenesis of the Inter-lens is consistent with paragenesis of the Ernest Henry deposit.
- Hypothesis 3: The formation of the Inter-lens post-dates mineralisation of the Ernest Henry deposit.

## **BACKGROUND AND GEOLOGICAL SETTING**

### **Regional Geology**

The Paleoproterozoic Mount Isa Inlier of northwest Queensland, Australia (Figure 2), is a globally significant mineral province containing Ag-Pb-Zn, Cu, IOCG and U deposits (Austin & Blenkinsop, 2009). The Mount Isa Inlier is divided into three N-S trending domains, the Western Fold Belt, Kalkadoon-Leichardt Belt and the Eastern Fold Belt/Succession. These divisions are defined by geological features such as bounding faults (e.g. the Pilgrim Fault defines the western boundary of the Eastern Succession) and variations in lithology, metamorphic grade and deformation style (Blake et al., 1990; Foster & Austin, 2008; Williams et al., 2015).

### **TECTONIC HISTORY AND STRATIGRAPHY OF THE EASTERN SUCCESSION**

The Eastern Succession exhibits the most intense deformation and metamorphism of the Mount Isa Inlier (Blenkinsop et al., 2008). The N-S trending, Pilgrim Fault Zone marks the western boundary of the Eastern Fold Belt (Spikings et al., 2001) which is subdivided into the Mary Kathleen-Wonga, Quamby-Malbon and Cloncurry-Selwyn zones (Blake et al., 1990; Denaro et al., 2007). Volcano-sedimentary Cover Sequences One, Two and Three (Blake et al., 1990) overlay Proterozoic basement rocks as unconformably stacked packages of intercalated metasediments and metavolcanics (Page, 1988; M. R. Williams et al., 2015). Each cover sequence is attributed to a discrete, post-Barramundi, intracratonic rift phase between 1850 to 1610 Ma (Blenkinsop et al., 2008; Foster & Austin, 2008; M. R. Williams et al., 2015). Cover Sequence 2 (CS2) and Cover Sequence 3 (CS3) are exposed in the Eastern Succession. CS2 deposited *ca.* 1780 – 1760 Ma consists of widely distributed, shallow water

calcareous sedimentary rocks with bimodal volcanics (Blake et al., 1990; Page & Sweet, 1998; Mark et al., 2006; Austin & Blenkinsop, 2009) and is extensively deformed and metamorphosed to upper amphibolite facies in parts. CS3 was unconformably deposited onto CS2 *ca.* 1680 – 1610 Ma (Blenkinsop et al., 2008) with W-E lateral facies change (Austin & Blenkinsop, 2009). CS3 is characterised by mostly finer grained siliclastic sedimentary and carbonate units with subordinate volcanics *ca.* 1675 – 1590 (Page & Sweet, 1998; Mark et al., 2006).

## ISAN OROGENY

The Isan Orogeny at *ca.* 1600 – 1500 Ma terminated deposition of CS3 (Blenkinsop et al., 2008). This regional polyphase deformation event was dominated by E-W compression and associated with widespread igneous intrusions, regional metamorphism, metasomatism and mineralisation (Mark et al., 2006).  $D_n$  terminology ( $D_1$ ,  $D_2$ ,  $D_3$ ) is conventionally used to describe regionally recognised stages of deformation through the Isan Orogeny (Foster & Austin, 2008). The waning stages of the Isan Orogeny broadly coincides with the post-metamorphic emplacement of the Williams-Naraku batholiths, local felsic intrusions, regional scale (several 100 km<sup>2</sup>) Na and Na-Ca alteration and a major Cu-Au mineralisation period ( Oliver et al., 2004; Blenkinsop et al., 2008; M. R. Williams et al., 2015).

N-S compression during  $D_1$  at *ca.* pre-1595 Ma resulted in localised early EW trending thrusting, folding and axial planar foliation (Baker, 1998; Oliver et al., 2004; Blenkinsop et al., 2008).  $D_2$  at *ca.* 1600-1580 Ma (Blenkinsop et al., 2008) produced dominant and pervasive deformation which is recognised throughout the Mount Isa Inlier. Major E-W compression produced widespread km-scale, N-S upright folds and axial planar upright cleavage (Baker, 1998; Oliver et al., 2004; Blenkinsop et al., 2008).



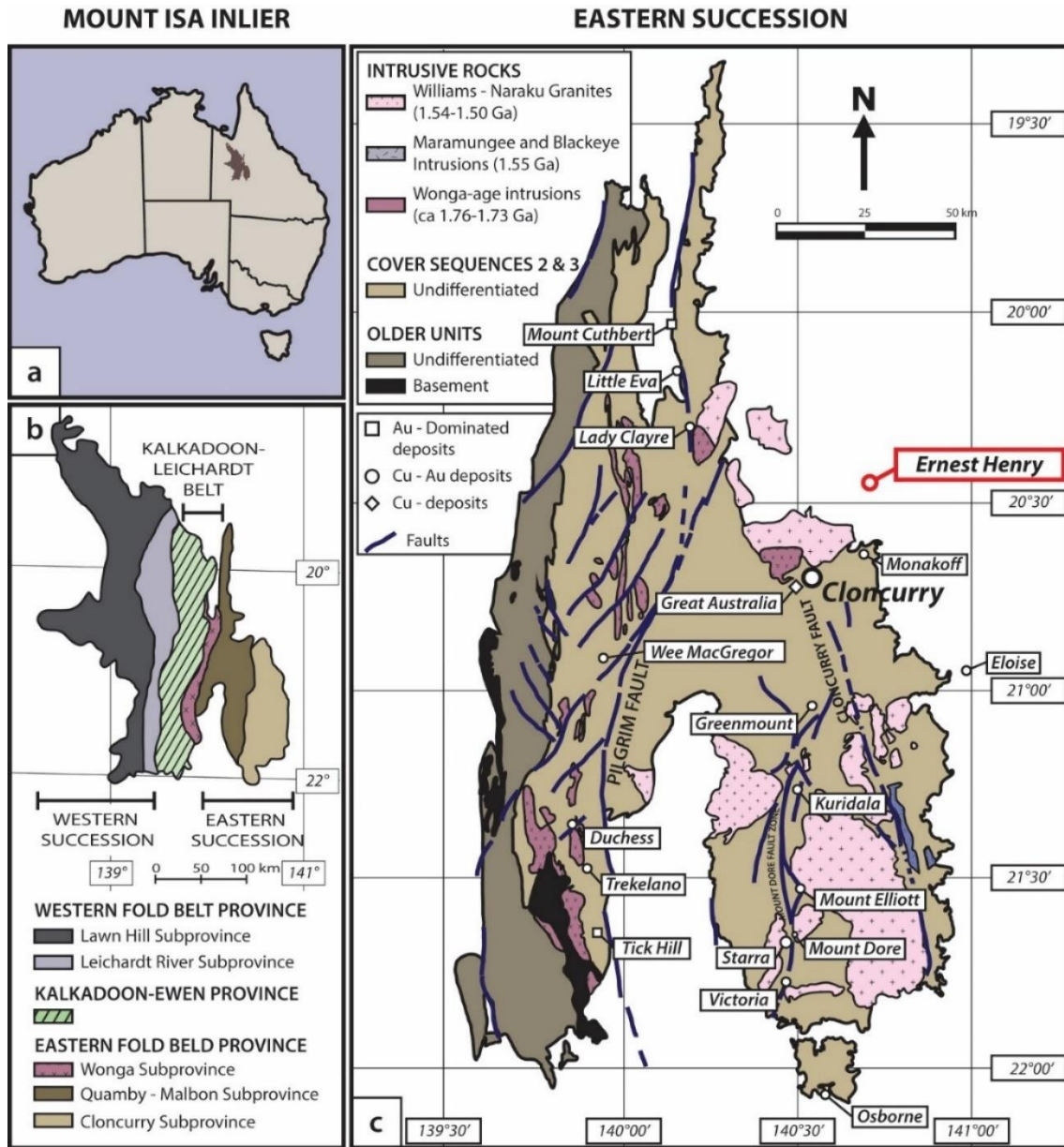


**Figure 2: Regional geology and study location; a) location of Mount Isa Inlier; b) sub provinces of the Mount Isa Inlier, adapted from Denaro et al. (2007); c) Simplified geology and mineral deposits of Eastern Succession including various deposits and faults adapted from Mark et al. (2006).**

D<sub>2</sub> was coincidental with peak metamorphism of greenschist to upper amphibolite grade and potentially minor partial melting in the lower crust (Page & Sun, 1998). D<sub>3</sub> ~1527 Ma is characterised by N to NE upright folding, crenulations and local reactivation of local D<sub>2</sub> fabrics (Blenkinsop et al., 2008).

## CLONCURRY IRON OXIDE COPPER GOLD (IOCG) MINERAL SYSTEMS

IOCG describes a diverse class of ore systems based on geochemical features.

Cloncurry hosts numerous significant IOCG deposits (including Osborne, Eloise, Monakoff, El and Ernest Henry) which display a diverse set of deposit-scale characteristics (Mark et al., 2006; M. R. Williams et al., 2015). The Cloncurry mineral system is geologically and metasomatically complex, although a consistent number of regional controls have been established. The emplacement of predominantly potassic and magnetite-bearing, A-type Williams-Naraku batholiths during the waning of the Isan Orogeny *ca.* 1550 – 1490 Ma (Oliver et al., 2004; Page & Sun, 1998) coincides with a metasomatic sequence which becomes increasingly structurally focussed. Regional scale Na and Na-Ca 'albitisation' alteration (Page & Sun, 1998) affects all rock indiscriminately, becoming locally overprinted by a distinctive 'dark-rock' biotite and/or biotite-magnetite alteration early in the hydrothermal evolution. Subsequent 'red-rock' K-feldspar alteration paired with a major Cu-Au mineralisation period is intensely structurally focused, commonly in breccias (Baker, 1998; Blenkinsop et al., 2008; Mark et al., 2006; Pollard, 2006; Austin & Blenkinsop, 2009; M. R. Williams et al., 2015).

### **Local Geology**

#### LOCATION AND DISCOVERY

The Ernest Henry IOCG deposit is located approximately 35km northeast of the township of Cloncurry. The drilling of a significant, coincidental aeromagnetic and ground-derived Transient Electromagnetic (TEM) anomaly led to the discovery by WMC Ltd. in 1991 beneath 30-60m of mainly undeformed Mesozoic to recent

sedimentary cover (M. R. Williams et al., 2015). The deposit is hosted in Proterozoic aged, brecciated felsic to intermediate Mount Fort Constantine Volcanics and minor metasediments (Figure 3, Figure 4) which experienced a complex series of structurally and lithologically controlled overprinting to amphibolite-magnetite-rich assemblages (Page & Sun, 1998; Mark et al., 2006; M. R. Williams et al., 2015).

#### HOST ROCKS – MOUNT FORT CONSTANTINE VOLCANICS

Mount Fort Constantine Volcanics of *ca.* 1745 Ma (Page & Sun, 1998) outcrop 7 km to the SW of the Ernest Henry deposit with unknown lateral extent (K. L. Blake, Pollard, & Xu, 1997). These meta-andesites preserve a variety of glomeroporphyritic, porphyritic, seriate to non-porphyritic textures. Phenocrysts are predominantly subhedral to euhedral plagioclase with fine grained groundmass. The environment of meta-andesite emplacement is unclear as extrusive-related textures such as flow top breccias are not present or preserved (Mark et al., 2006). Texturally, they are similar to the volcanic host sequence present at Ernest Henry, leading authors to interpret them as the host rocks (e. g. K. L. Blake et al. (1997); Mark et al. (2006); M. R. Williams et al. (2015)). The age and metamorphic grade indicate they are from Cover Sequence 2 (CS2) and have been assigned to the Mary Kathleen Group (K. L. Blake et al., 1997; Cleverley & Oliver, 2005), overlapping with the Wonga extensional event of *ca.* 1750-1735 Ma (Blenkinsop et al., 2008).

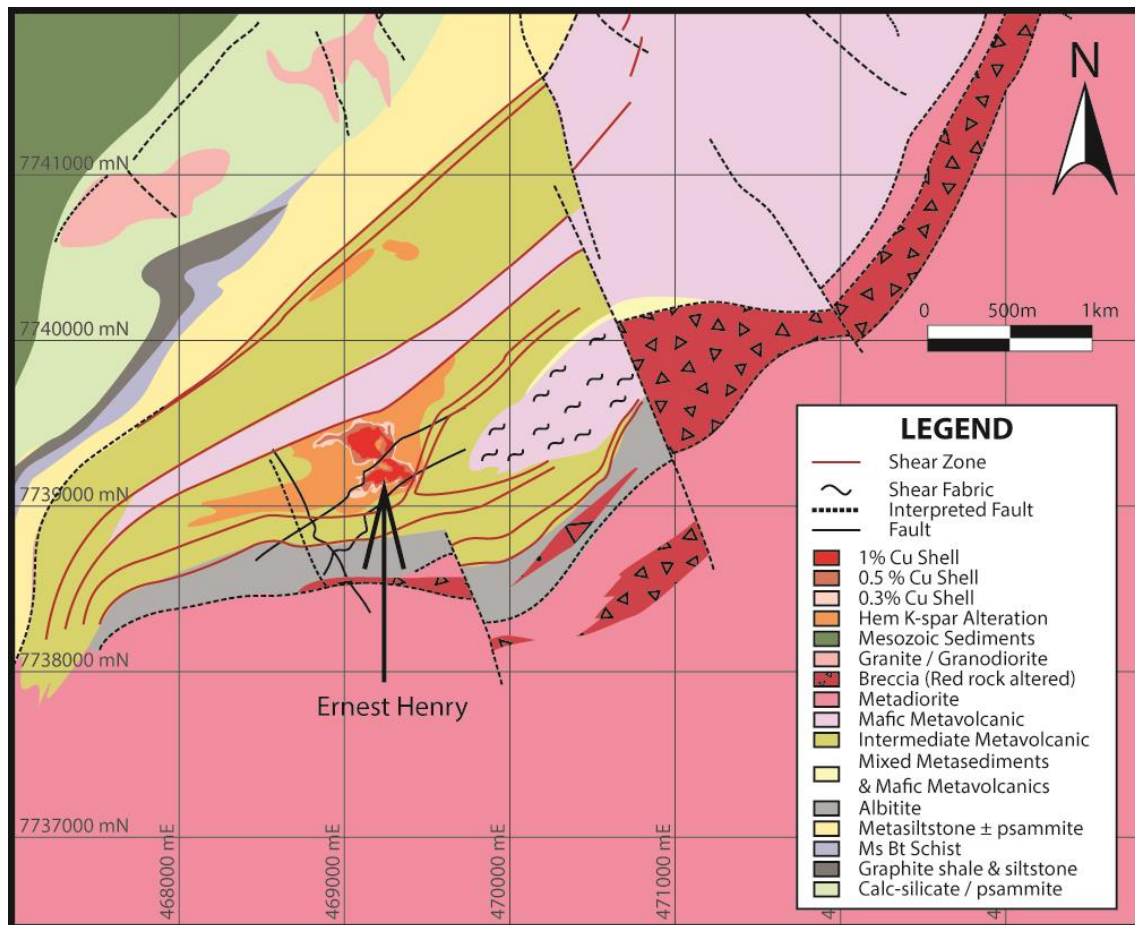


**Figure 3: Interpreted Ernest Henry basement geology model, after Mount Isa Mines internal report.**

### ERNEST HENRY DEPOSIT

The Ernest Henry orebody is situated at the core of a proximal alteration zone dominated by K-feldspar ‘red-rock’ alteration which overprints earlier Na-Ca ‘albitisation’ alteration and biotite-magnetite (K-Fe) ‘dark-rock’ alteration (Mark et al., 2006; M. R. Williams et al., 2015). Host rocks (Figure 4) are predominantly plagioclase-phyric meta-andesites intercalated locally with a minor component of metasediments. Intrusive metadiorites have demonstrated lithological control on hydrothermal alteration (Cleverley & Oliver, 2005; Mark et al., 2006). Metasediments are mainly carbonaceous metasiltstones and calc-silicates with minor biotite psammite, typically located at deposit peripherals and in particular the deposits upper hanging wall

(Mark et al., 2006; M. R. Williams et al., 2015). Local terms have been developed to describe the host rock lithologies which are outlined in greater detail in Appendix A. Two shear zones referred to as the Hanging Wall Shear Zone (HWSZ) and Footwall Shear Zone (FWSZ) are associated with the upper and lower contacts of the orebody. Biotite-rich rocks within these shear zones display strong tectonic fabrics. Main foliations, shear zones and faults dip moderately ( $\sim 40^\circ$ ) toward the south east (Twyerould, 1997). The Cu-Au orebody forms a pipe-like breccia bound by these fabrics, and slopes down dip (Mark et al., 2006). The most intensely mineralised parts of the ore zone are characterised by a matrix dominated breccia with a co-precipitated breccia matrix of magnetite, minor specular hematite, and chalcopyrite. Brecciation of the orebody grades outwards into a narrow zone of clast-supported breccia and onwards into a crackle breccia proximal to the bounding shear zones.

## INTER-LENS

Exploration drilling and underground development has identified a weakly mineralised and weakly brecciated zone within the orebody named the 'Inter-lens' which separates the orebody into two distinct lenses (Figure 4). Preliminary inspection reveals a persistent shear fabric in weakly mineralised and weakly brecciated, biotite rich rocks. The Inter-lens appears to be enveloped by the Ernest Henry ore breccia, yet lacks obvious 'red-rock' alteration. The Inter-lens structure was not well reported early in the life of the mine and its presence has not been taken into account in the current ore deposit models. The timing and nature of Inter-lens deformation is currently unconstrained and mineralogical and structural relationships with the main ore body are poorly understood.



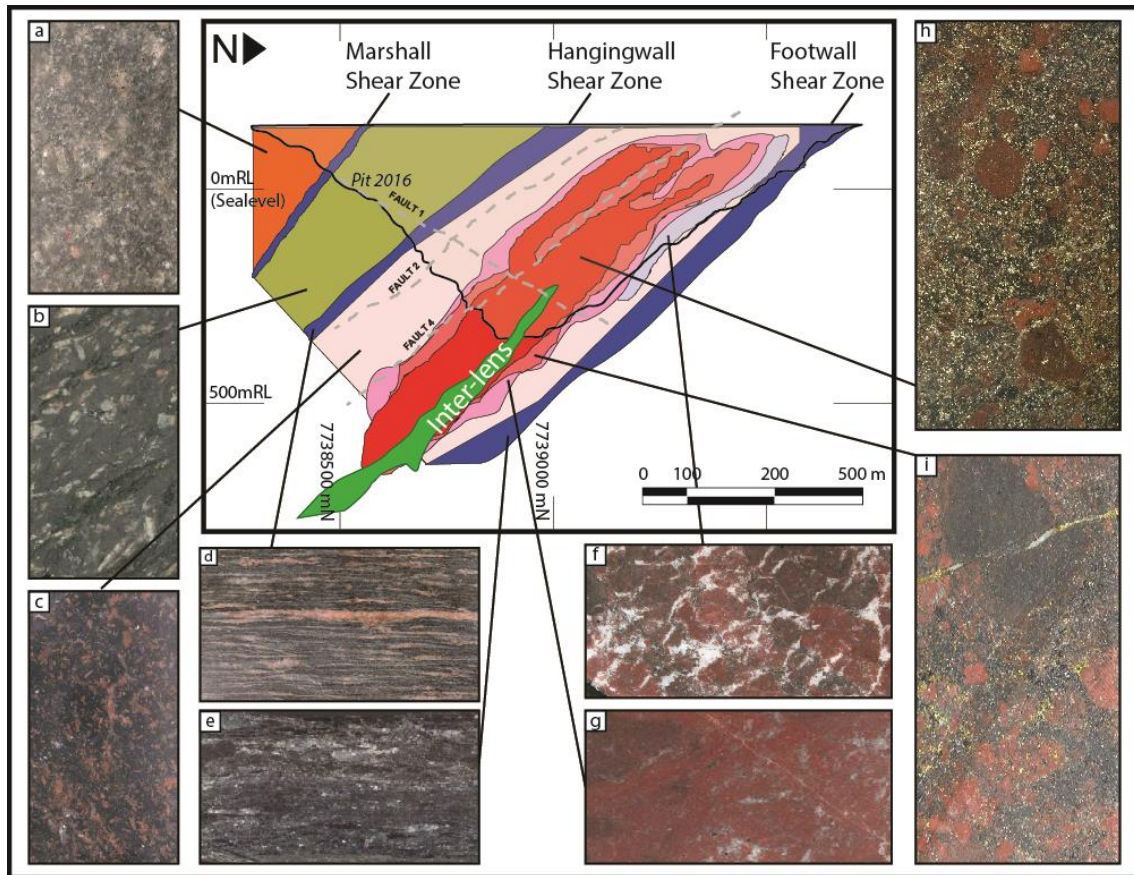


**Figure 4: Representative images of host rocks and distribution at Ernest Henry adapted from internal reports, Ernest Henry Mining. a) altered metadiorite (not mineralised); b) albitite (not mineralised), Regional Stage 1 alteration; c) porphyritic intermediate volcanic, stage 2 alteration; d) foliated intermediate volcanic, Stage 2 alteration; e) foliated mafic volcanic (not mineralised) stage 2 alteration; f) ‘birds-wing’ tension veined, altered felsic volcanic, rarely mineralised, pervasive stage 4 alteration; g) Felsic volcanic, rarely mineralised, stage 2 & 3 alteration; h) Matrix supported high grade ore breccia (>1% Cu); i) clast supported low grade ore breccia (0.5-1.% Cu).**

#### HYDROTHERMAL ALTERATION AND PARAGENESIS

The metasomatic and alteration history of the Ernest Henry Mine Lease (Figure 5) has been described in great detail by Mark et al. (2006). The alteration and mineralisation sequence becomes increasingly structurally localised can be broadly divided into four stages:

### Stage 1- Regional Sodic and Sodic-Calcic

Intense, regional Na-Ca alteration referred to locally as 'albitisation' is preserved in veins, breccia, replacement features and fine-grained albitites focussed largely outside the mine lease in NE-trending fault zones (Mark et al., 2006). Within the orebody, relict albite grains rarely occur within K-feldspar altered breccia clasts, localised along shear zones and faults. A regional red-rock event associated with Stage 1 developed through hematite staining of albite that is seen mostly distal from mineralisation (Ryan, 1998).

### Stage 2- Pre-mineralisation (Dark-rock and Red-rock)

Pre-ore, K-(Mn-Ba)-rich biotite-magnetite alteration is termed locally as 'Dark Rock' due to the characteristic fine-grained biotite and magnetite-rich assemblages. Dark-rock alteration overprints albitisation most intensely in plagioclase-phyric meta-igneous and ferromagnesian-rich rocks to develop a significant, proximal halo feature of the Cu-Au orebody (Mark et al., 2006). Shear zones comprising of biotite-rich, potassic altered rocks bound Cu-Au mineralisation and hydrothermal brecciation of the orebody. Ore-associated potassic (K-feldspar) alteration overprints albitisation and dark-rock alteration preferentially in plagioclase phyric meta-andesites (Mark et al., 2006). It is strongly localised in brittle structures including in NE-trending fault zones, but occurs most intensely in the orebody (Mark et al., 2006). Hematite dusted K-feldspars with a distinctive brick-red colour (red-rock) are strongly spatially associated with mineralisation in the orebody. Magnetite altered to hematite occurs commonly in selvages and along grain boundaries of K-feldspar altered clasts.

### Stage 3- Cu-Au Mineralisation

The main ore minerals are hosted in hydrothermal breccias at the core of an intense, K-feldspar alteration halo associated with bend in the host Footwall (FWSZ) and Hanging Wall Shear Zones (HWSZ). Breccia grades out from zones of intense matrix-supported and clast supported breccias, tension veined volcanics through to crackle fracture veining and unbrecciated volcanic rocks. Hydrothermal mineral association is typically magnetite, calcite, pyrite, biotite, barite, chalcopyrite, quartz, specular hematite and K-(Ba) feldspar with accessory native gold-electrum (Mark et al., 2006). Sphalerite, arsenopyrite, apatite, fluorite and galena are present as accessory minerals in the main ore breccia. Carbonate-magnetite-sulphide replacement textures in breccia matrix transition to tension vein infill, progressing outward from carbonate-pyrite-magnetite ± chalcopyrite to carbonate-pyrite to carbonate (Ryan, 1998). Fine grained muscovite 'sericite' alteration occurred prior to and is observed proximal to high grades of Cu-Au mineralisation while some remnant fine grained biotite-magnetite and albite alteration is retained locally.





## METHODS

This study focussed primarily on detailed graphical logging of drill core and geological mapping underground at the Ernest Henry mine lease. Paragenesis of the Inter-lens was then compared with the Ernest Henry paragenesis by Mark et al. (2006). For extended methods, refer to Appendix B.

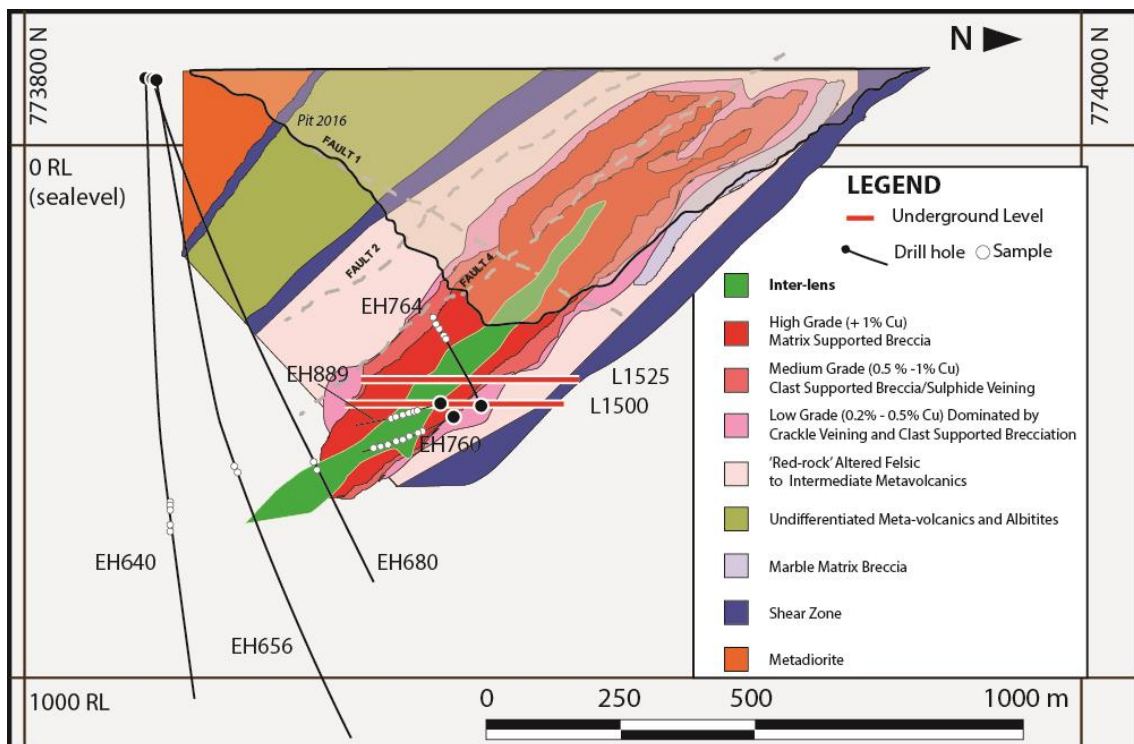


**Figure 6: Plan of study area in section view. Inter-lens geometry and location interpreted from voids within 0.7% Cu grade shell at Ernest Henry.**

Inter-lens geometry and location were estimated prior to the study using voids within 0.7% Cu grade shell at Ernest Henry and archived core photographs. Two underground levels and six drill holes were selected which provided a) good coverage along the strike of the Inter-lens structure and b) long intersections through the structure (Figure 6). Three oriented holes were identified (EH760, EH656, EH640).

Structural measurements from exposed features underground and in oriented drill core were measured with a magnetic declination of 6° E in Cloncurry. Effects of intense magnetite alteration underground was mitigated as best as practical using mine survey structural orientations, and by validating measurements of oriented samples at the surface.

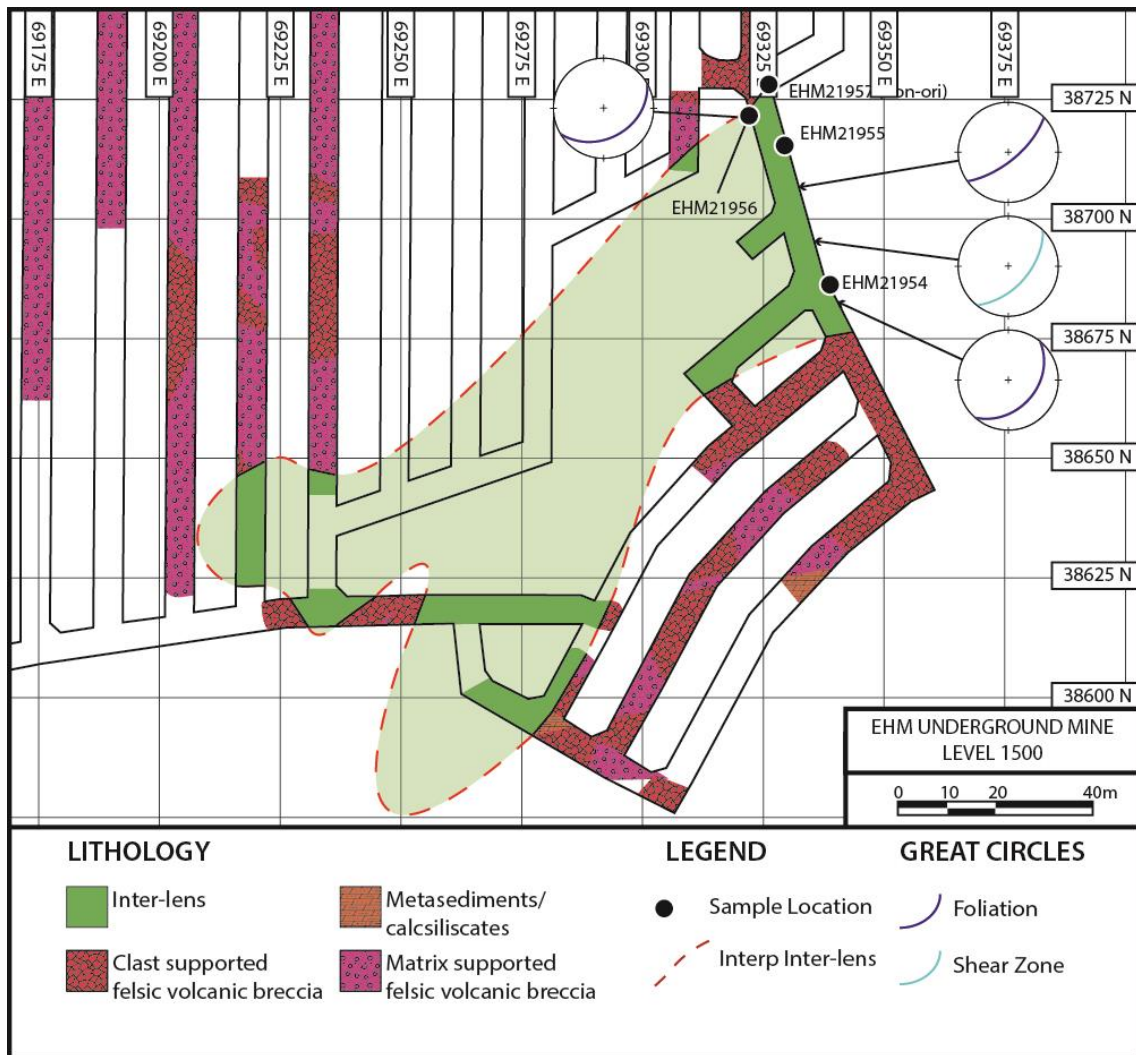


Figure 7: Underground mapping of level 1500 with interpreted Inter-lens and sample locations.

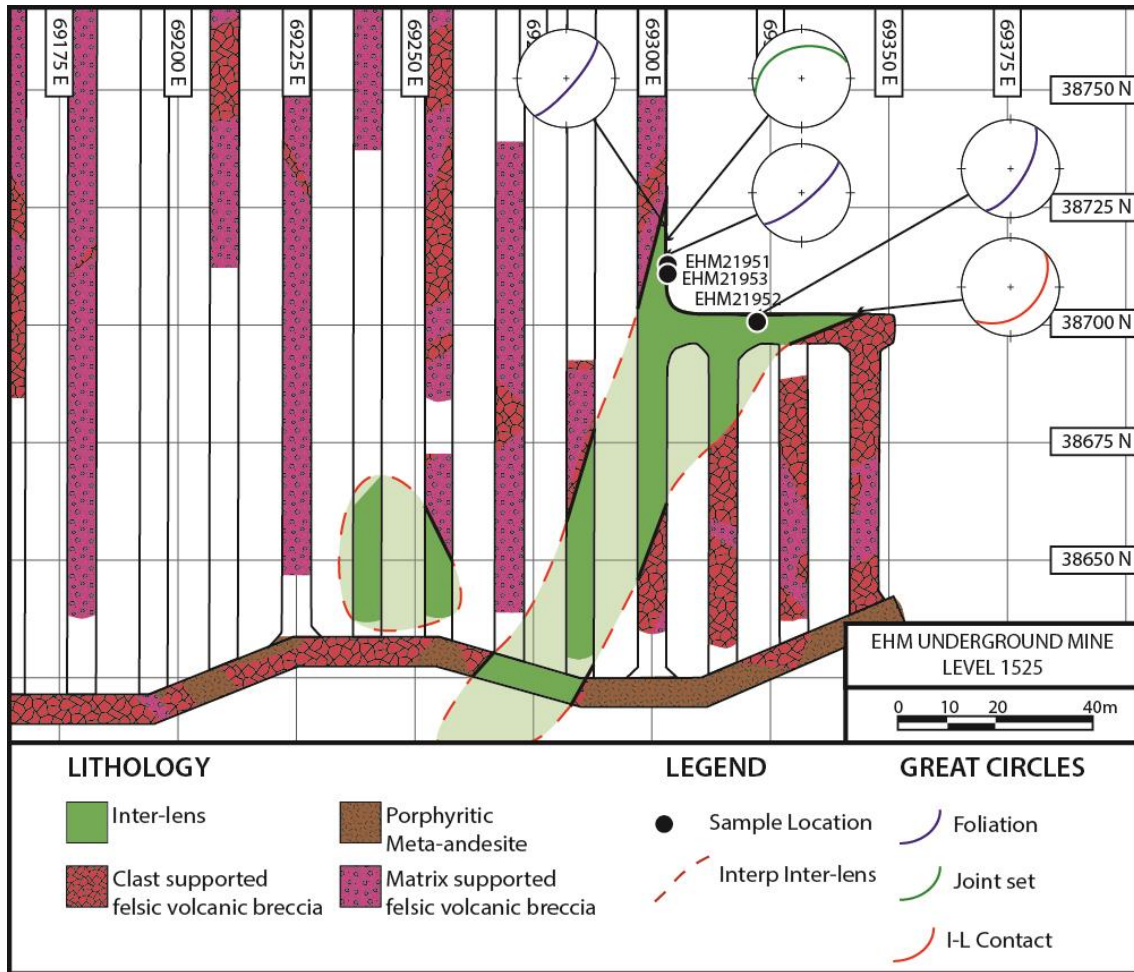


Figure 8: Underground mapping of level 1525 with interpreted Inter-lens and sample locations.

Replicating in-situ measurements in 3 oriented drill holes using a Marjex Core Orientation Frame was undertaken in a location shielded from magnetic sources. If a structure, such as a pervasive fabric, remained constant in its attitude, representative measurements were taken every 10-15m along a hole.

Alteration style was defined and recorded by identification in hand sample of indicator minerals, such as calcite, magnetite, biotite, hematite-stained K-feldspar and chlorite.

Rock textures were recorded with particular attention focused on foliation and brecciation. Mineral cross cutting relationships were examined, logged and photographed for detailed analysis. Samples representative of hydrothermal alteration

stages with clear textural relations were taken for paragenetic analysis from underground and drill core. Where permitted, oriented samples were taken from underground to prepare oriented thin sections to observe potential micro-scale kinematic indicators, and to observe hand samples in natural light.

### **Petrography and optical microscopy**

20 thin sections of the Inter-lens and surrounding ore breccia (11 unpolished, 9 polished) were generated by Ingham Petrographics, Ingham, Qld, from samples collected during March 2016. Photomicroscopy and viewing was undertaken at University of Adelaide using an Olympus BX51 System Microscope with a DP21 Microscope digital camera. Mineral identification in thin section was assisted by detailing optical properties as outlined by MacKenzie and Guilford (1980).

### **Scanning Electron Microscope (SEM) and Mineral Liberation Analysis (MLA)**

Mineralogical and textural analysis of protolith and alteration mineralogy was undertaken at Adelaide Microscopy using a FEI Quanta600 Scanning Electron Microscope with the Mineral Liberation Analysis (MLA). Semi-quantitative analysis was undertaken of 9 sections representative of host rock, veins and breccia matrix.



## OBSERVATIONS AND RESULTS

### Inter-lens contacts

In the underground environment, Inter-lens contacts are undulating and distinct, identified by a dramatic change in colour and texture of exposed rocks. Dip angle of the northern Inter-lens contact on level 1500 was observed to vary between 30° and 70° in the space of <5 meters while maintaining a broadly constant dip orientation of ~150° (Figure 7). On level 1525 (Figure 9) the contact is distinct and undulating. Clast supported breccia (hanging wall) has a distinct red colour due to K-feldspar alteration of breccia clasts, whereas the Inter-lens rocks are predominantly black, intensely foliated, and magnetite rich.

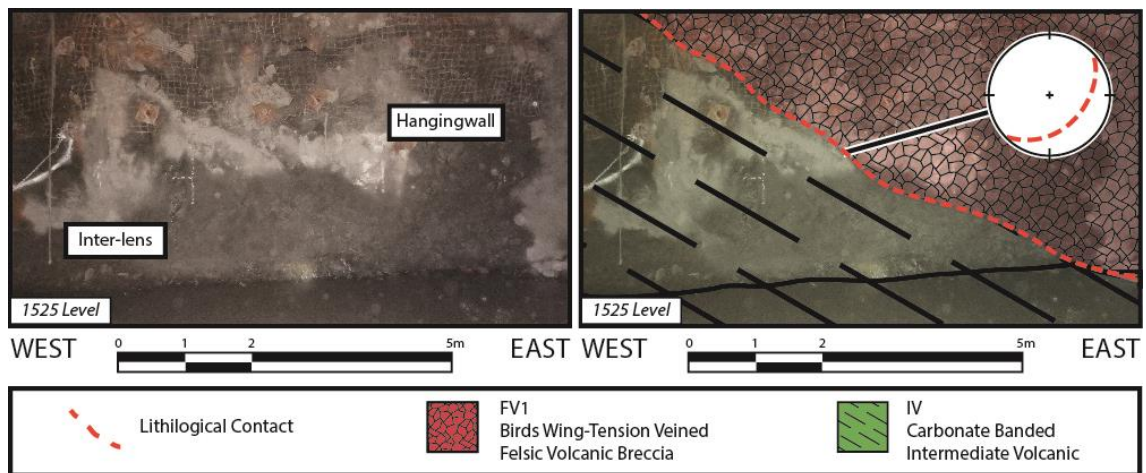


**Figure 9: South-facing exposure of Inter-lens contact on level 1525 a) Hanging wall clast supported breccia with low grade chalcopyrite mineralisation and calcite-rich ‘birds-wing’ textured tension veins; b) Interpretations and observations are superimposed. Inter-lens is distinctly foliated intermediate volcanics with foliation parallel calcite veins and lenses. Contact is distinct and undulate, dipping broadly parallel to the dominant mineral foliation at ~40/155.**

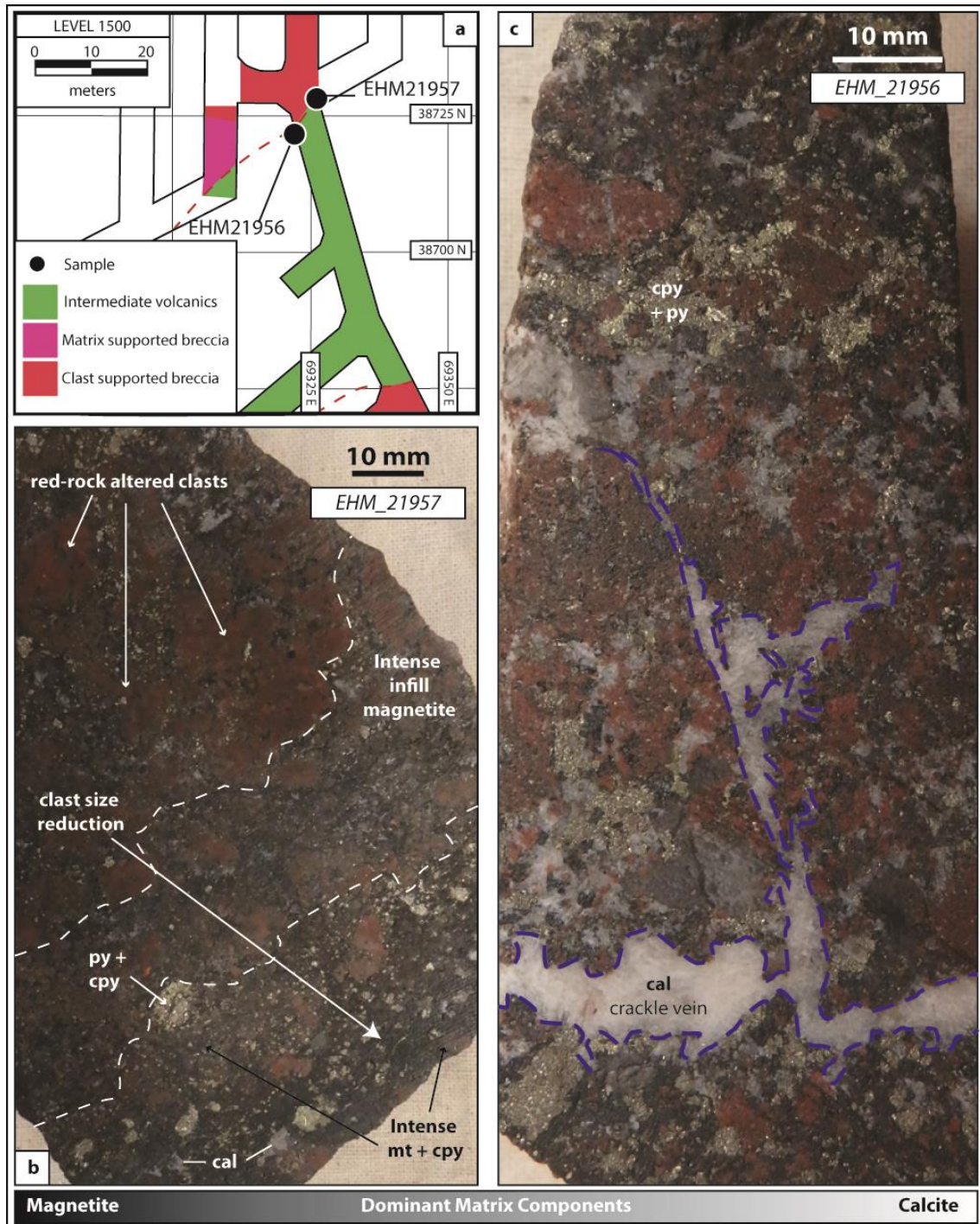


**Figure 10: Samples of clast supported breccia within Inter-lens contact zone. a) sample locations; b) Infilling magnetite (mt) dominates breccia matrix with varying amounts of infill pyrite (py) and chalcopyrite (cpy) in matrix support breccia. Infilling calcite (cal) increases to the right of the sample. C) Calcite ‘crackle’ veining cuts matrix supported breccias into secondary clasts. Infill calcite within the breccia matrix overwhelms magnetite, and is spatially associated with pyrite + chalcopyrite mineralisation.**



Contacts of the Inter-lens are associated with an increased abundance of calcite in the proximal red-rock altered breccias. Samples of clast supported breccia (EHM\_21956 and EHM21957, Figure 10) were collected from the outer limit and central zone of a narrow (<2m), gradational Inter-lens contact zone within the orebody (Figure 10a). Termed locally as FV1, these samples are typical of the low- to- medium-grade ore zone, and should not be considered Inter-lens rocks. Chalcopyrite mineralisation is strongest with more intense infill magnetite and reduced breccia clast size (Figure 10b). In the vicinity of the Inter-lens, calcite with associated pyrite and chalcopyrite mineralisation overwhelms magnetite as the dominant matrix infill mineral (Figure 10c). Calcite crackle veining lacking infill chalcopyrite imposes secondary brecciation chalcopyrite and is interpreted as a post-mineralisation feature.

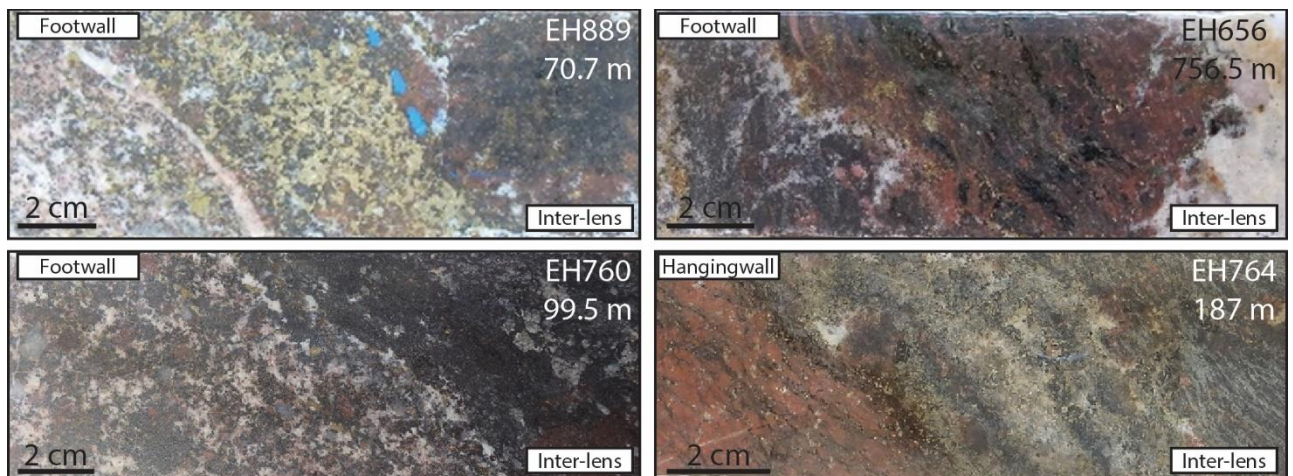


**Figure 11: Inter-lens contacts in drill core. Notice distinct textural contrasts and break in red-rock alteration.**

In drill core, Inter-lens contacts vary between distinct and gradational- to diffuse zones of intercalated red-rock and dark rock alteration (Figure 11). Contacts may be associated with thick (up to 20 cm) veins and lenses of massive calcite or quartz. In



more diffuse contact zones, biotite-magnetite foliation is partially preserved and is visible through overprinting by red-rock alteration. Contacts that were able to be measured dipped moderately south (mean = 35/178, Figure 12).

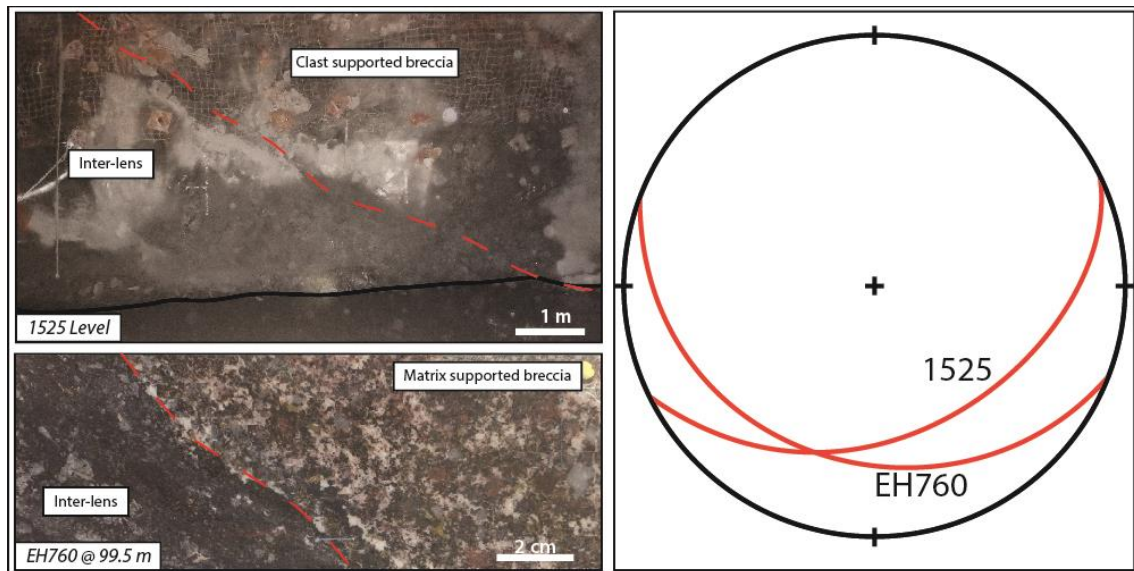


**Figure 12: Equal area projection of measured Inter-lens contacts. Inter-lens represents the footwall at contacts at underground level 1525 and in oriented drill core EH760 at 99.5m.**

## Structure

Interpreting Inter-lens contacts on multiple underground development levels produced a model feature which dips moderately south-southwest, sub-parallel to the orebody and broadening at depth (Figure 13). The interpreted geometry indicates that the Inter-lens could potentially intersect with, or anastomose with either the Footwall Shear Zone (FWSZ), the Hangingwall Shear Zone (HWSZ) or both.

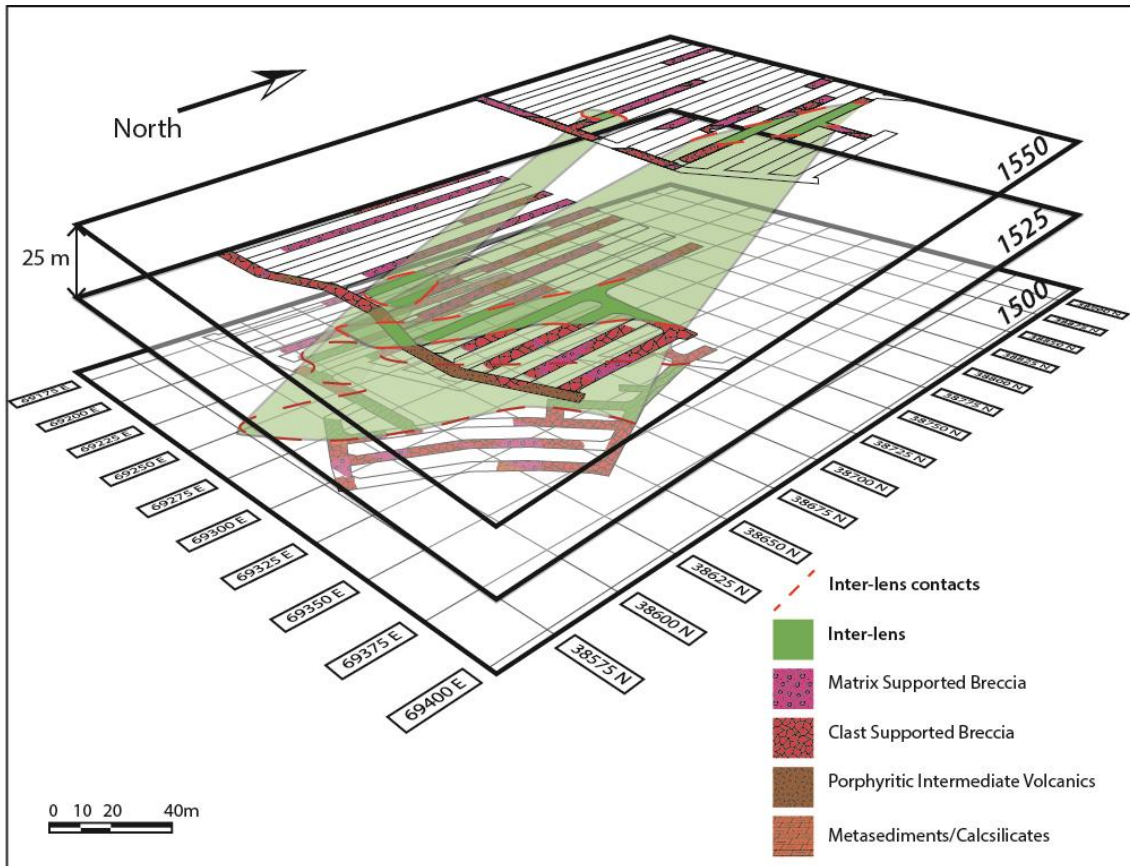


**Figure 13: Overlaying underground mapping of levels 1500, 1525 and 1550 with no vertical exaggeration. Inter-lens (green) is interpreted to be dipping moderately south, broadening with depth.**

### Oriented Core Summary

The dominant tectonic fabric observed is a pervasive biotite foliation in altered intermediate volcanic rocks dipping approximately 40/155. This fabric is interpreted to represent the earliest of the preserved fabrics within the Inter-lens based on textural observations and cutting relationships. Representative samples of tectonic fabrics are displayed in (Figure 17) Poles to foliation measurements are presented in Figure 14 Figure 15. Features shown to cluster within the same zone include alignment of garnet-biotite veins, subordinate quartz-calcite veining, breccia clast orientation and magnetite ( $\pm$  calcite) + chalcopryrite veins. For detailed graphical drill logs and summaries, refer to Appendices E and F.

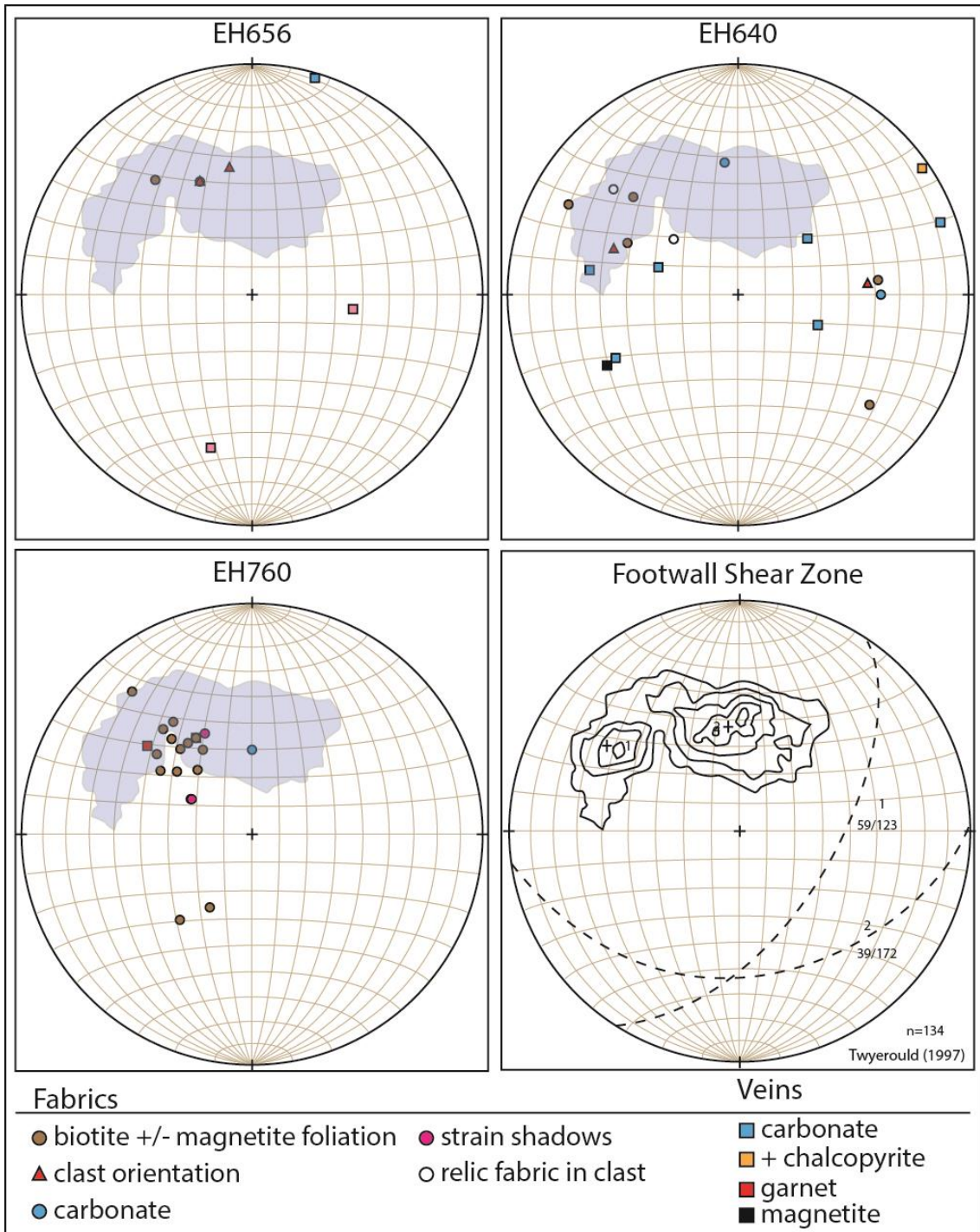


Figure 14: Equal area projection displaying poles to structural measurements taken in oriented drill core, dominant fabrics are represented with circles, veins with squares.

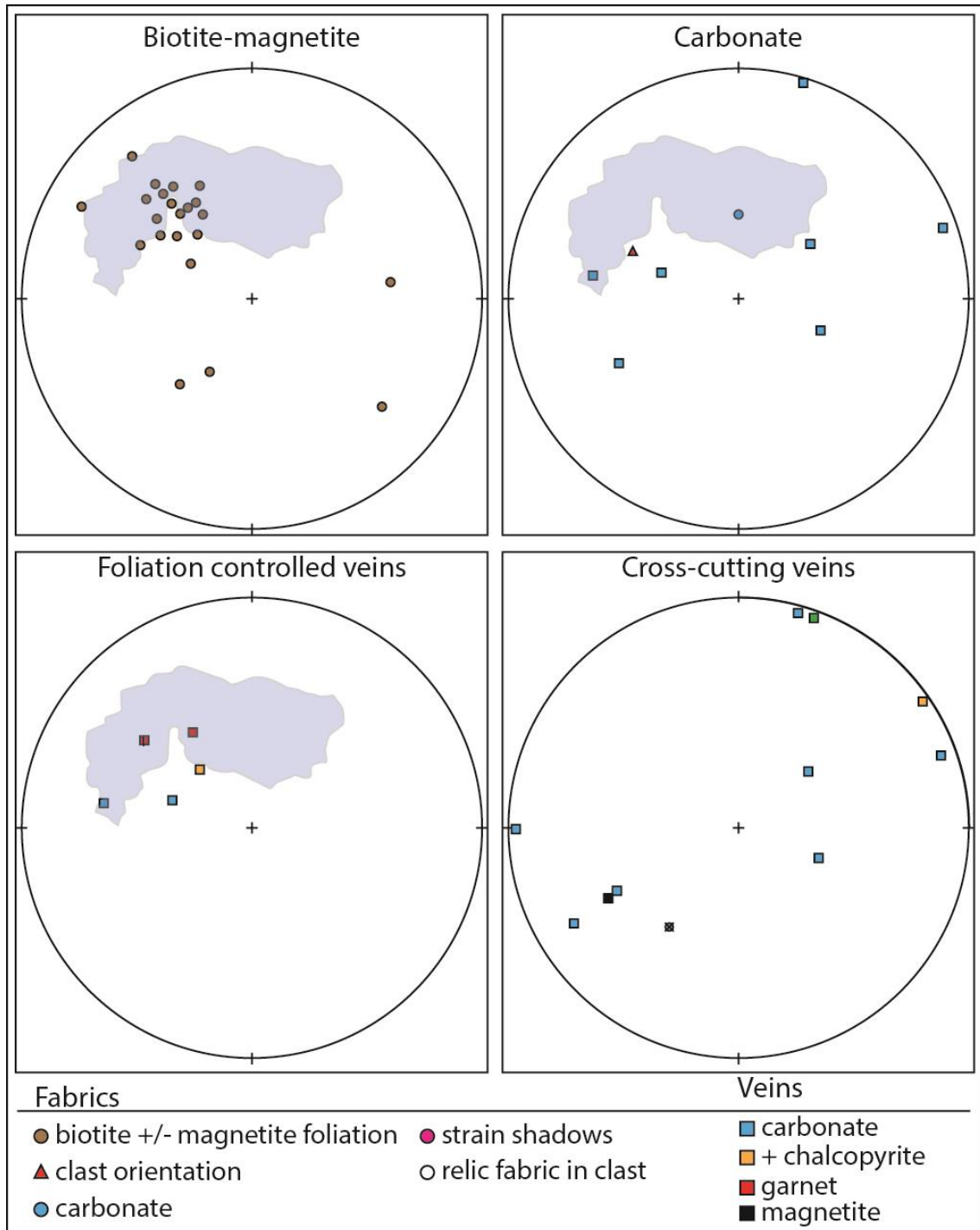
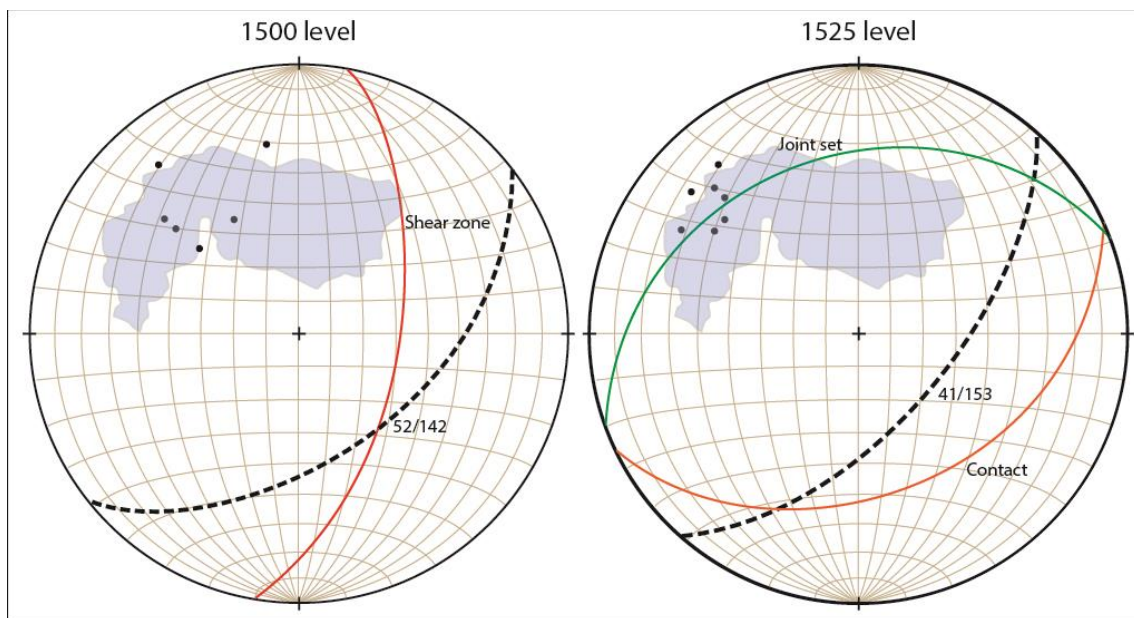


Figure 15: Poles to foliation in oriented drill core a) dominant biotite-magnetite foliation, b) calcite veins and replaced wall rock, c) foliation controlled veins, d) veins that cross-cut dominant fabrics. FWSZ data in blue (Twyerould, 1997).



Poles foliation measurements from the three oriented drill holes reveal persistent orientation, with mean orientation of 40/155. This distribution overlaps well with measurements of the Footwall Shear Zone by (Twyerould, 1997). When fabrics are isolated, the overlap of the dominant biotite-magnetite from the Inter-lens is consistent with the Footwall Shear Zone. Calcite fabrics and veins generally show poor overlap with the biotite-magnetite fabric. Veins are spread chaotically, and are seen to cross cut dominant fabrics regularly. Tectonic fabrics underground expressed predominantly as mineral foliation in intensely calcite veined, intermediate volcanic rocks. Mean foliation orientation (1500 = 52/142, 1525 = 41/153) overlapped strongly with the dominant foliation of the Footwall Shear Zone (Figure 16). Fabrics were cut by minor N-S trending shear zone and E-W trending joint set. Inter-lens contact on level 1525 was broadly parallel with the trend of the dominant foliation.



**Figure 16: Poles to foliation measurements taken underground within the Inter-lens. Dashed great circle represents mean.**

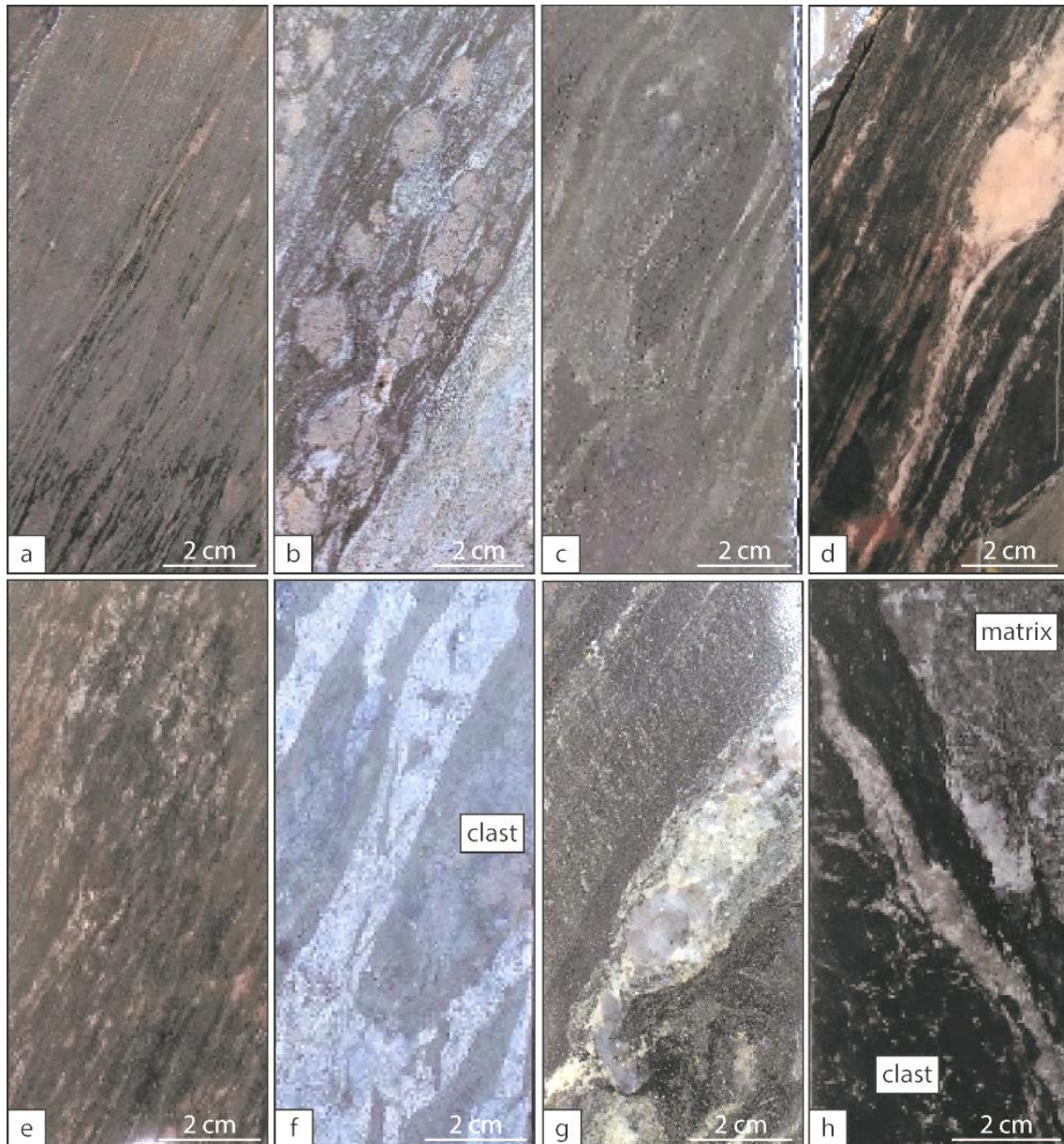


**Figure 17: Representative examples of tectonic fabrics of the Inter-lens. a) Biotite-magnetite lenses in intensely foliated intermediate volcanic; b) Garnet-magnetite-biotite veins in intermediate volcanic; c) Alignment of magnetite rimmed volcanic lenses in metasomatic breccia; d) Biotite- and magnetite-altered lenses intercalated with discontinuous calcite (+ quartz) veins. Coarse 15mm wide, feldspar porphyroblast has calcite tail extending to calcite veins aligned with foliation; e) Biotite- and magnetite-altered lenses intercalated with calcite; f) orientation of intermediate volcanic clasts in calcite-matrix breccia g) mineral banding in intermediate volcanic rock h) aligned breccia clasts and veining.**

## **Rocks of the Inter-lens**

The Inter-lens is dominated by intensely hydrothermally altered rocks affected by various styles and intensity of brecciation, veining and local crenulation. The identification and description of succinct lithologies is problematic due to the highly variable appearance, and complex overprinting textures observed in the rocks. Examples of identifiable rock types in the Inter-lens were typically altered meta-andesites.

### **PORPHYRITIC META-ANDESITE**

Volcanic rocks with Porphyritic textures with a fine-grained dark grey to black matrix were observed intermittently in the Inter-lens (Figure 18). Phenocryst abundance is variable and may be absent or less apparent in hand sample. Groundmass is typically rich in biotite and magnetite, overprinting fine grained to massive albite, generating a dark appearance. In sample 760\_10 (Figure 18a, b) there is a strongly defined shearing texture in the hand sample defined by anastomosing veins and elongate clasts of wall rock. Under thin section the groundmass texture appears to be mostly replaced by magnetite. Finer feldspar laths exhibit moderate alignment to define a fabric with interstitial magnetite and biotite. In some zones, clasts >10 cm across of weakly to non-foliated, porphyritic meta-andesites are present in a calcite rich matrix (Figure 18c). This unit is similar in appearance of the marble matrix breccia lithology at Ernest Henry.



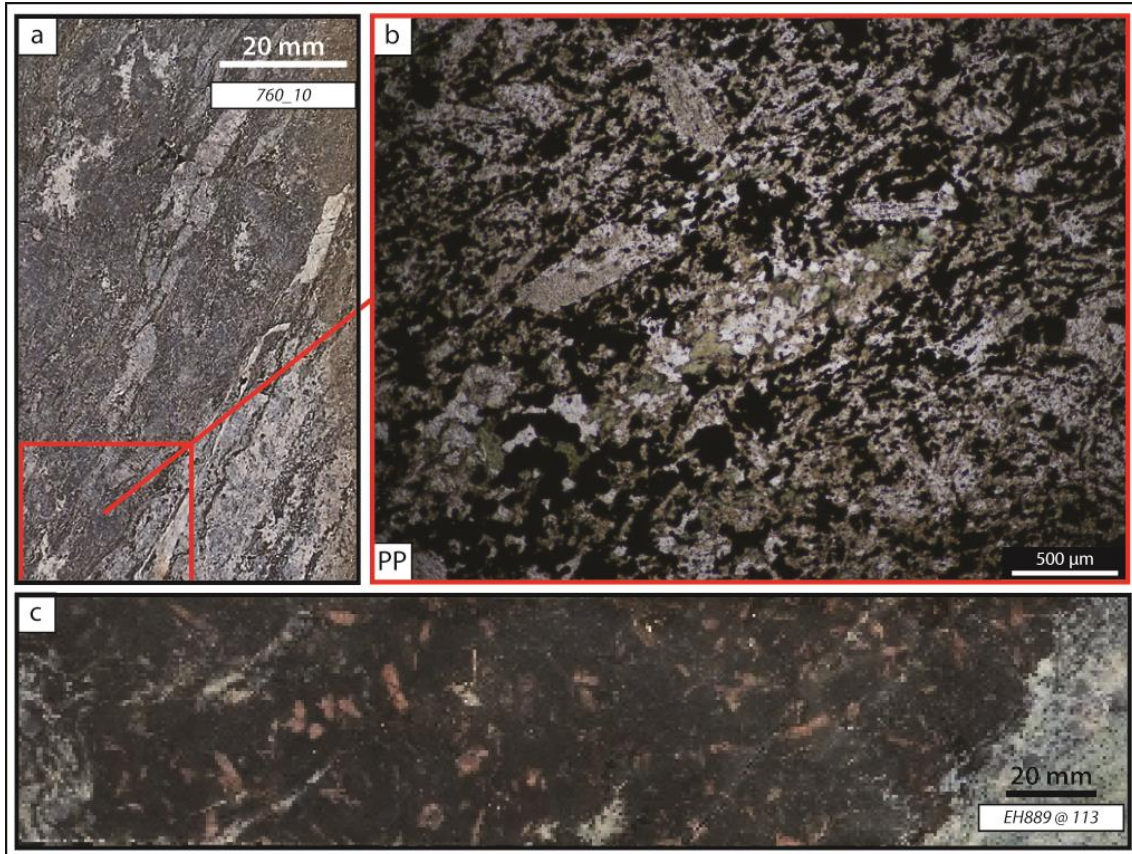


**Figure 18: a) Biotite-magnetite altered metavolcanic has porphyritic textures that are less apparent in hand sample. Lower portion of sample is dominated by thick foliation-parallel quartz-calcite gash veins with diffuse boundaries; b) Photomicrograph taken in plain polar (PP) reveals weak alignment of finer laths; c) Typical example of biotite-magnetite altered, porphyritic metavolcanic. Contains abundant pink coloured, altered feldspar phenocrysts and a dark grey to black groundmass.**

## Tectonic fabrics

Expression of tectonic fabrics observed in drill holes was variable and persistent (Figure 17) with five distinct fabrics identified in drill core.

1. Biotite-magnetite anastomosing cleavage
2. Biotite-garnet-magnetite veins
3. Calcite matrix through veining
4. Elongated breccia clasts
5. Calcite birds-wings.



Crosscutting relationships and replacement textures provide direct evidence for the relative timing of fabric development. Biotite-magnetite developed earliest, followed by subordinate calcite veining. Biotite-garnet veins were also shown to be parallel with the dominant fabric and replaced by calcite before quartz. Poles to the dominant foliation cluster within the same region as the dominant foliation of the Footwall Shear Zone (Twyerould, 1997). Quartz-calcite, magnetite and chalcopyrite bearing veins were shown to cross cut the dominant and subordinate foliations (Figure 14). Detailed logs are included in Appendix F.

#### BIOTITE-MAGNETITE ANASTOMOSING FOLIATION

The earliest and most common tectonic fabric observed is a pervasive biotite-magnetite mineral foliation of various intensity in sheared metavolcanic rocks (Figure 17a, d, e, Figure 19). A Weakly to- strongly-developed anastomosing cleavage defined by biotite-magnetite intercalated with albitised meta-volcanic lenses and discontinuous calcite (+ quartz) veins (Figure 19). Porphyroblasts are rare, but are observed at the macroscale in drill core (Figure 19c). Weak chalcopyrite mineralization may be present as a) disseminated throughout host rock associated with calcite and magnetite, b) in red selvages of calcite veins (notably the red colour is red calcite, not hematite stained K-feldspar) c) at intersections of calcite and anastomosing magnetite veins. The presence of chalcopyrite in magnetite-biotite places important constraints on the mineralogy in this fabric. It is interpreted that minerals of an original texture have been replaced by stage 3 magnetite-chalcopyrite assemblage.

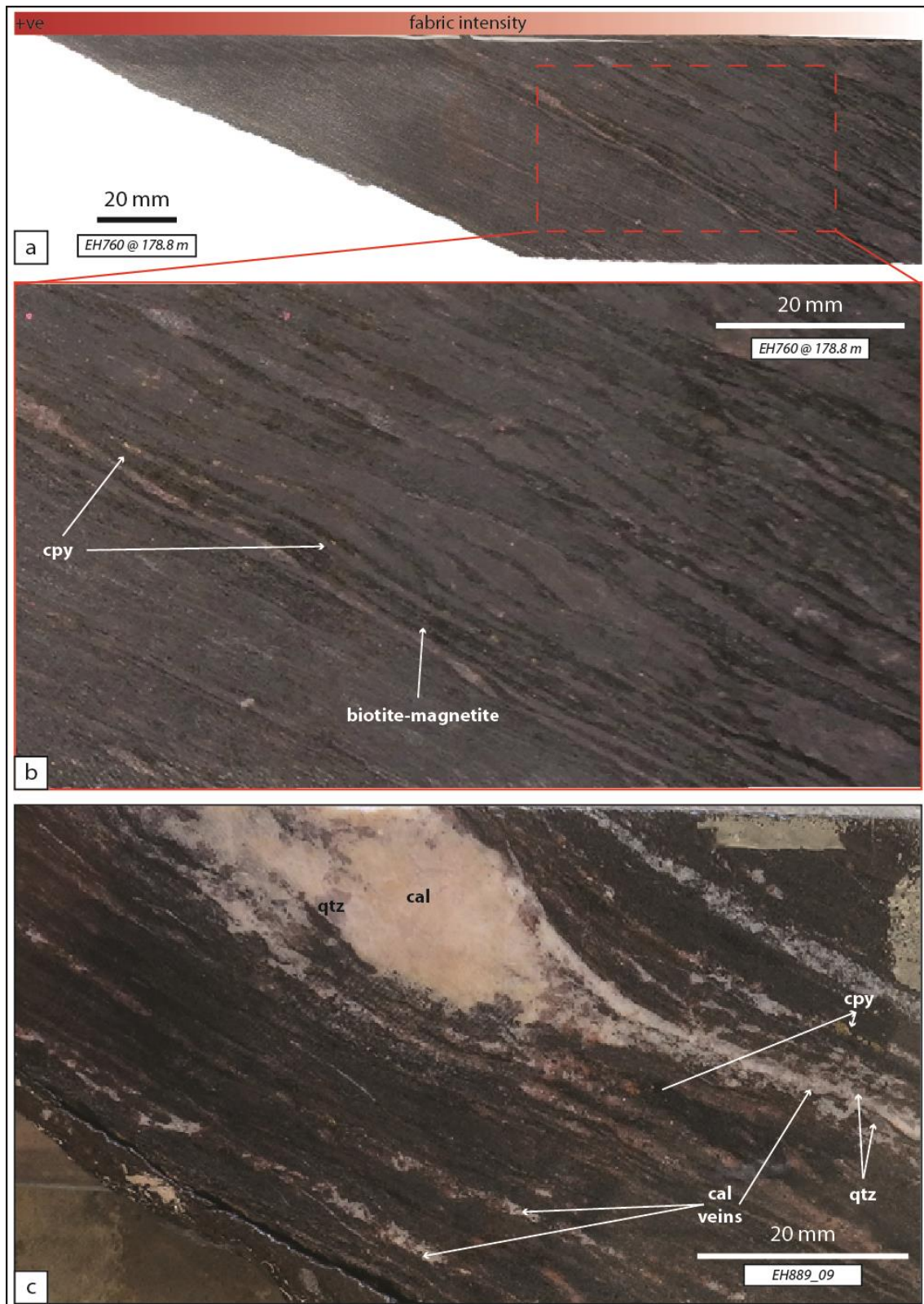


Figure 19: a) Biotite-magnetite vein abundance and length reduces with increased shearing; b) biotite-magnetite veins anastomose around lenses of altered metavolcanics, associated with minor infilling chalcopyrite (cpy) c) Biotite-magnetite fabric deviates around calcite porphyroblast. Clast tails extend into foliation-parallel calcite (cal) + chalcopyrite (cpy) veins.

## BIOTITE-GARNET-MAGNETITE VEINING

Pristine biotite associated defines a strongly schistose fabric in discontinuous sigmoidal shaped, gash-style veins (Figure 20a). Key mineral relations and textures are summarised in Table 1. Red, subhedral, coarse garnet porphyroblasts nucleate in series parallel to schistosity. Biotite foliation deviates around garnet grains and drapes garnets in syn-deformational textures (Figure 20d). Garnet and biotite growth were both syn-deformational. Garnets are fractured with varied intensity in alignment to fabric (Figure 20c) with no rotation. Proximal to vein boundaries, garnets are so intensely fractured they have the appearance of being sheared.

Euhedral magnetite overprints biotite and garnet in veins within fractured garnets. Magnetite abundance is greatest with the most intense fracturing of garnets (Figure 21). The core of the vein is predominantly biotite, transitioning to wholesale quartz composition over a distance of ~ 20cm. Outwards from the vein, relic biotite grains are observed to be chlorite altered and replaced by quartz (Figure 21c). Porphyroblastic K-feldspar grains are present aligned with the ghost biotite fabric. K-feldspar are also present and aligned in biotite veins, however their grain size increases with distance from garnets. Relic lenses of calcite in quartz are elongate broadly parallel to the dominant fabric. Biotite-garnet veins are probably a relic schist, perhaps with calcite layers, that have been hydrothermally replaced by calcite before quartz.



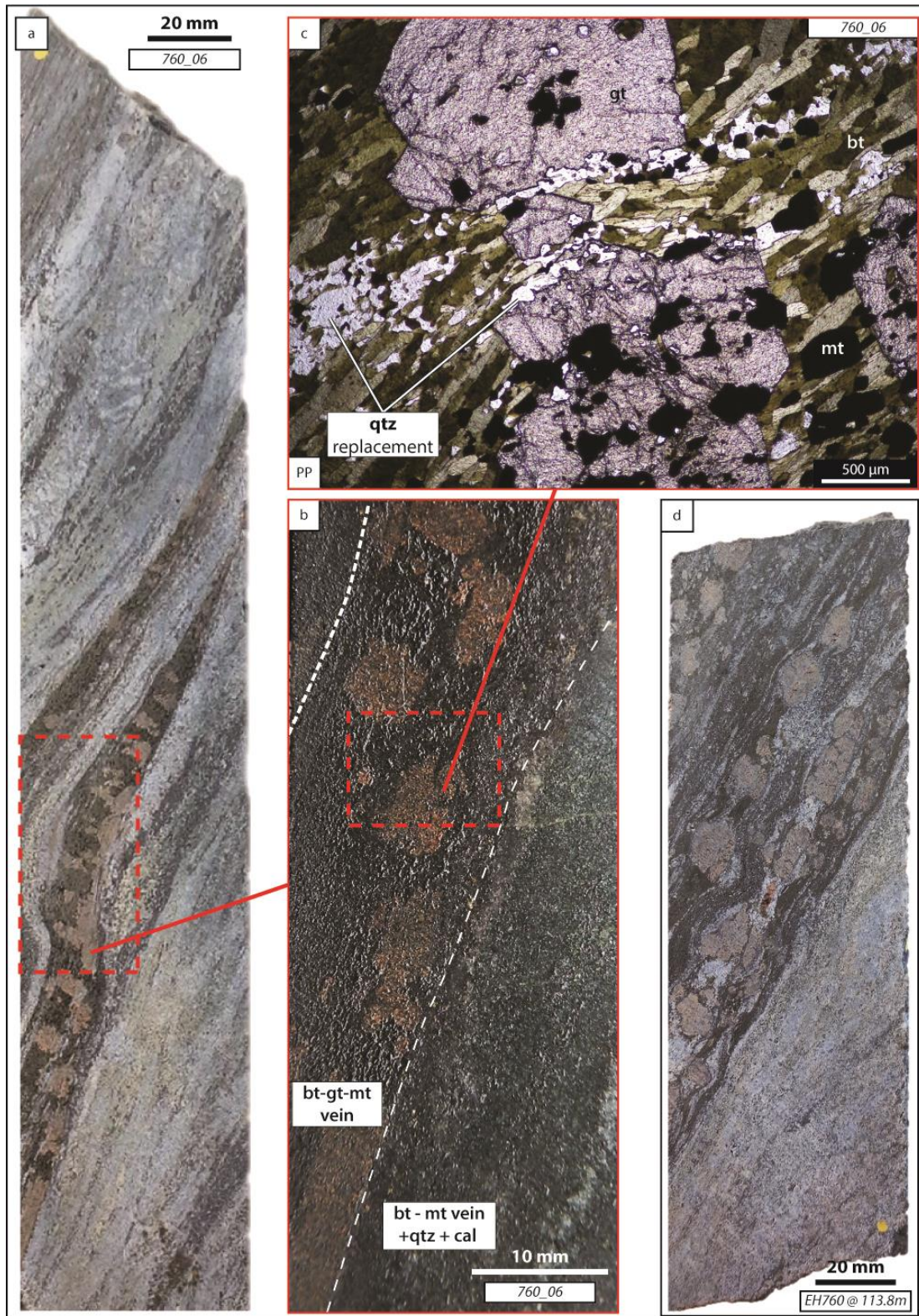


Figure 20: Representative garnet-biotite-magnetite gash-style vein. a); b) vein becomes progressively richer in quartz and calcite outwards; c) PP image of strained garnet (gt) in biotite (bt) vein. Biotite is undeformed and defines fabric. Magnetite (mt) is associated with veins in fractures in garnet grain. Secondary biotite vein and garnet growth accompanies deformation; d) Syn-deformational texture, biotite fabric intercalated with calcite drapes garnet grains.



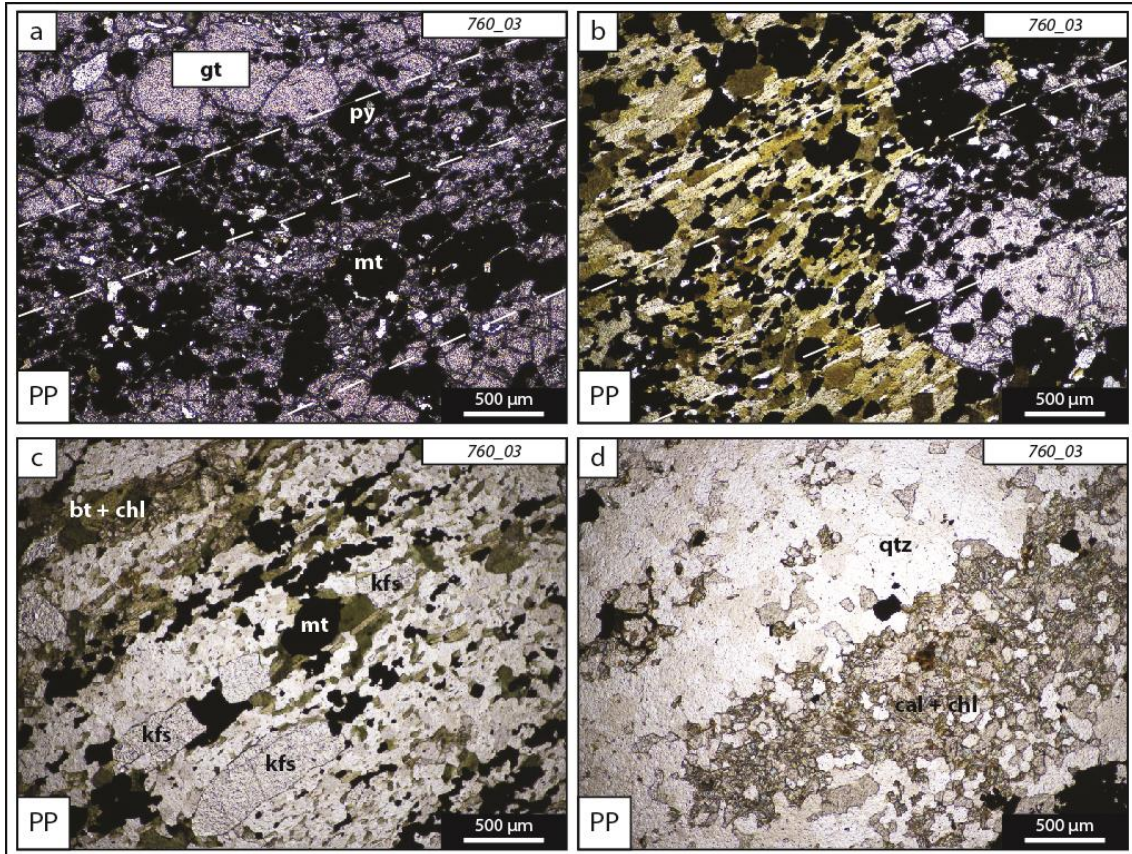


Figure 21: Transition from centre of biotite-garnet vein to quartz dominated host rock. a) Most intensely fractured zones are spatially associated with subhedral to euhedral pyrite (py) and magnetite (mt); b) magnetite vein and garnet fractures parallel with biotite fabric; c) elongate k-feldspar (kfs) grains are oriented with tectonic fabric. Grain size reduces closer to biotite (perimeter of quartz zone); d) relic biotite and calcite lens in quartz background aligned to fabric.

Table 1: 760\_06 Key mineralisation sequence and associate alteration stages

<i>Alteration Stage</i>	<i>Mineral</i>	<i>Field Relations</i>	<i>Textures</i>
<b>Stage 2</b>	Biotite	Defines primary fabric	schistose
<i>Pre-mineralisation</i>	Garnet	Porphyroblasts in biotite schist	fractured
<i>Potassic</i>	k-feldspar	porphyroblastic	euhedral
<b>Stage 3</b>			
<i>Mineralisation</i>	calcite	replaces biotite	replacement
	quartz	Indiscriminately texturally destructive	replacement
<i>Retrograde</i>	chlorite	Pseudomorph calcite	replacement

## ELONGATE BRECCIA CLASTS IN QUARTZ-CALCITE-RICH MATRIX

Lens-shaped clasts of porphyritic meta-volcanic wall-rock contain coarse plagioclase laths against a groundmass of fine grained K-feldspar + magnetite ± biotite ± pyrite (Figure 22). Key mineral relations and textures are summarised in Table 2. Albite is (rarely) preserved in phenocrysts and groundmass. Breccia texture varies between ductile, sigmoidal shaped clasts (Figure 22a) and brittle, angular clasts (Figure 22b). Clasts in both styles are typically elongate and in alignment with the fabric defined by the breccia matrix composed of calcite and quartz with minor, biotite, pyrite and chalcopyrite and porphyroblastic magnetite, k-feldspar and apatite. the quartz-calcite-rich matrix. Breccia clasts invariably have dark biotite-magnetite rims up to 5 mm thick. Biotite is typically pristine, stubby euhedral typical of strain-shadow infill. Minor chalcopyrite associated with magnetite in the strain shadows indicates some replacement or infill during Mineralisation stage. Remnant strain shadows containing fine grained biotite, magnetite and minor infill chalcopyrite are present as wisps in the quartz-calcite-rich matrix. Relic biotite grains in quartz-calcite matrix (Figure 22c) proximal to the clast demonstrates the replacement of biotite by calcite.



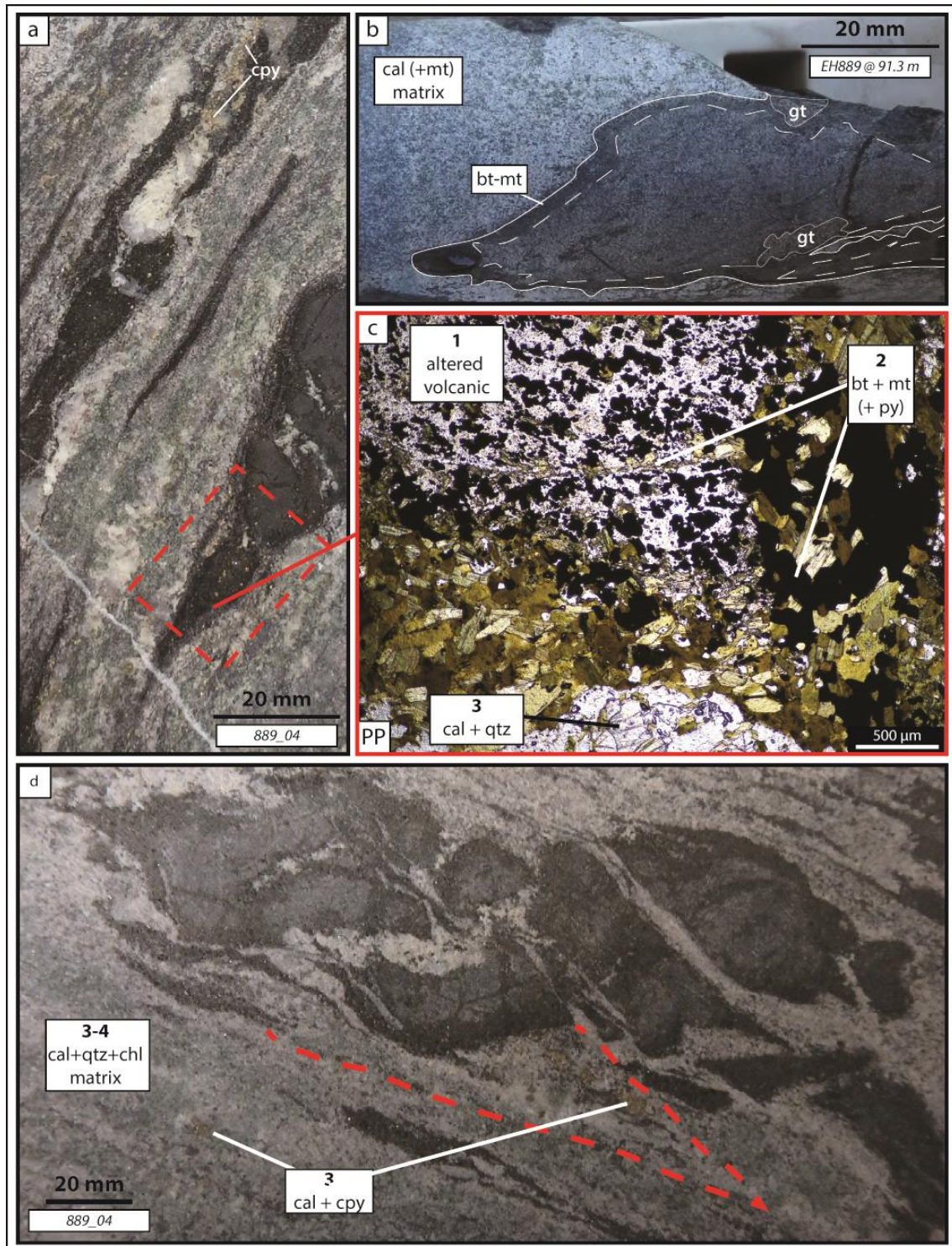


**Figure 22: Typical examples of elongate breccia clasts in calcite-rich matrix. a) sigmoidal-shaped clasts of albitised volcanic rock with distinctive magnetite-biotite rims. Clasts are aligned with fabric of quartz-calcite-rich matrix. Textures consistent with wall rock veining progressing to wall rock replacement; b) coarse angular clasts up to 10cm length; c) photomicrograph displays anastomosing rims and veins comprised of euhedral biotite (bt) + magnetite (mt). Magnetite is concentrated at the clast boundary; d) calcite and chalcopryrite are associated in strain shadow of clast (interpreted) which contains relic magnetite and biotite wisps. Chlorite (chl) alteration associated with calcite develops green colour in matrix. Numbers represent chronological order.**



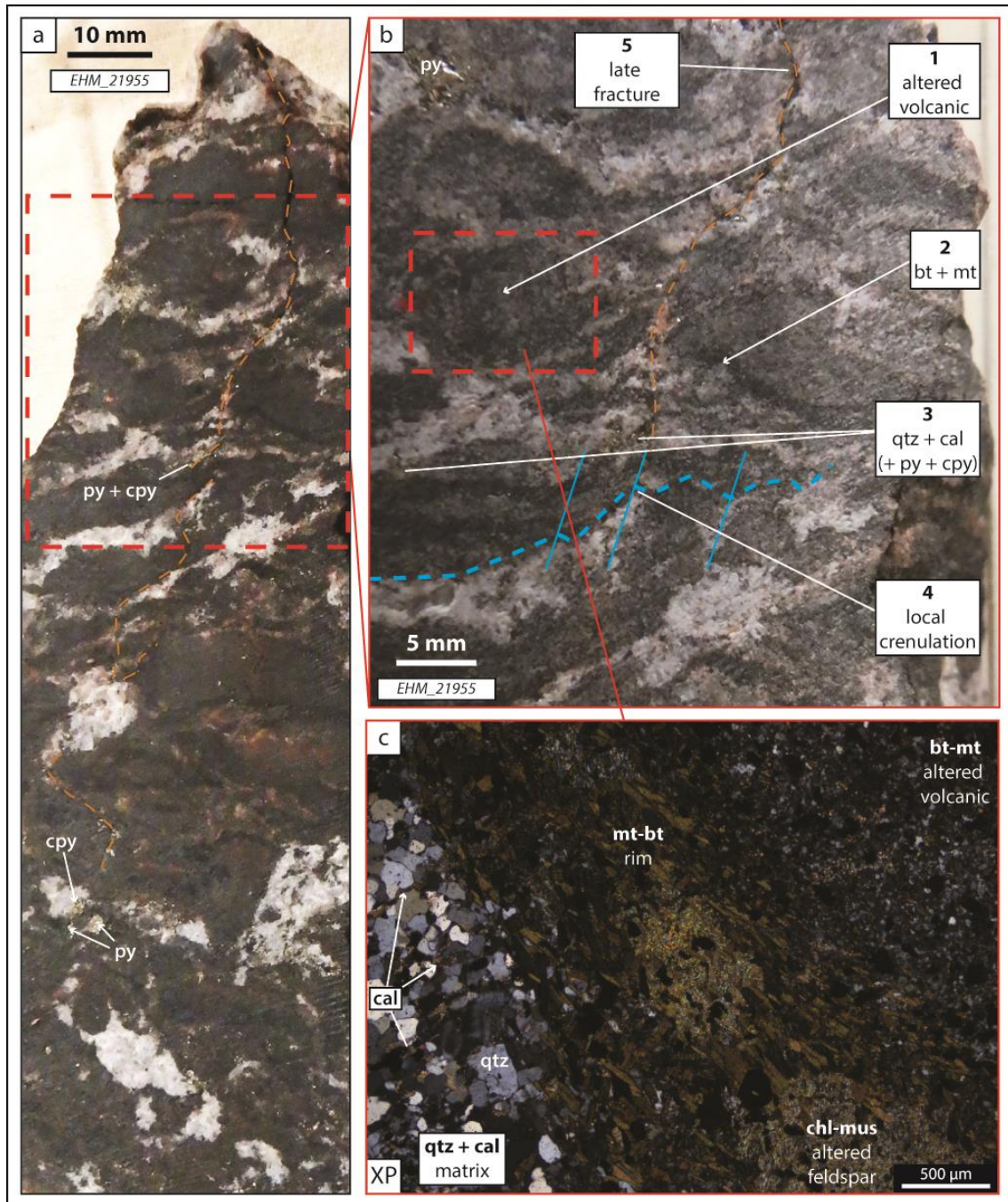


**Figure 23: Clast supported variation of elongate clasts in quartz-calcite-rich matrix. a) hand sample from underground within 1 m of Inter-lens contact, elongate volcanic clasts contain biotite-magnetite rims and local crenulation. Magnetite is present in late fracture (orange dashed line), minor infill pyrite (py) and chalcopyrite (cpy) are present where fracture intersects calcite; b) numbers represent chronological order. Minor infill chalcopyrite is associated with interface of calcite and magnetite, local crenulation in blue; axis is broadly parallel with orientation of fracture (orange dashed); c) Cross polar (XP) photomicrograph shows relic calcite in predominantly quartz matrix. Biotite defines fabric in alteration rim, associated with chlorite-muscovite (sericite) alteration of massive feldspar.**



**Table 2: 889\_04 Mineralisation sequence and associate alteration stages**

<i>Alteration Stage</i>	<i>Mineral</i>	<i>Field Relations</i>	<i>Textures</i>
<b>Stage 1</b> <i>Albitisation</i>	albite	Replacement of groundmass and phenocrysts	replacement
<b>Stage 2</b> <i>Pre-mineralisation</i> <i>Potassic</i>	biotite 1	Relic grains in clast groundmass	replacement
	magnetite	Subhedral in clast groundmass	replacement
	k-feldspar	Replaces biotite in groundmass	replacement
	biotite 2	Infills strain shadow	infill
<b>Stage 3</b> <i>Mineralisation</i>	Magnetite 2	Infill strain shadow and clast boundary assoc. with pyrite	replacement
	calcite	relic grains in quartz background replaces biotite	replacement
	pyrite	Euhedral associated with calcite	euhedral
	chalcopyrite	Anhedral grains with calcite and magnetite	infill
	quartz	Indiscriminately texturally destructive	replacement
<i>Retrograde</i>	chlorite	Pseudomorph calcite	replacement

**Table 3: EHM\_21955 Mineralisation sequence and associate alteration stages**

<i>Alteration Stage</i>	<i>Mineral</i>	<i>Field Relations</i>	<i>Textures</i>
<b>Stage 2</b> <i>Pre-mineralisation</i> <i>Potassic</i>	biotite 1	Relic grains in clast groundmass	anhedral
	magnetite	Subhedral in clast groundmass	replacement
	k-feldspar	Replaces biotite in groundmass	replacement
	biotite 2	defines fabric at clast boundary	schistose
<b>Stage 3</b> <i>Mineralisation</i>	calcite	relic grains in quartz background	infill
	pyrite	Euhedral associated with calcite	euhedral
	chalcopyrite	Anhedral grains with calcite	infill
	quartz	Indiscriminately texturally destructive	replacement
<i>Retrograde</i>	chlorite	Inter-grown	replacement
	muscovite	Pseudomorph feldspar	

Sample EHM\_21955 (1m from Inter-lens contact) represents clast dominated variety of aligned clast breccias. Key mineral relations and textures are summarised in Table 3.

Broadly aligned, magnetite-altered meta-volcanic clasts contain biotite-magnetite rims. Calcite is associated with minor infilling pyrite and chalcopyrite in a replacement quartz dominated matrix. Unlike clasts in sample EHM\_21954, biotite defines an intense fabric along the clast boundary (Figure 23c), groundmass is visibly rich in biotite and muscovite-chlorite has replaced massive feldspar (interpreted as recrystallised feldspar groundmass) within the biotite rim. The biotite rim developed on the clast surface as a shearing texture, not as infill as seen with more albite rich clasts (Figure 22). This may be attributed to more intense biotite alteration of the groundmass facilitating ductile deformation.

#### QUARTZ-CALCITE VEINING (AND WALL-ROCK REPLACEMENT)

Intense veining has developed zones of distinct mineralogical banding. Key mineral relations and textures are summarised in Table 4. Mineralogy of veins is typically biotite-magnetite with minor pyrite showing distinct to diffuse boundaries with quartz-calcite veins containing minor porphyroblastic k-feldspar, apatite (Figure 24) and infill magnetite and very minor chalcopyrite. These textures represent the most commonly mapped foliation underground. Fractured euhedral K-feldspar grains are fractured, fractures are infilled by chlorite altered calcite (Figure 24b). Biotite grains are aligned, the fabric deviates around porphyroblastic apatite (Figure 24c) indicating that these minerals grew synchronously during deformation. Biotite inclusions in calcite place calcite later in the sequence. Calcite is most commonly present as relic grains in a quartz background Magnetite forms parallel to lineation but exhibits infill textures between biotite grains, concentrated near the contact of biotite and quartz.

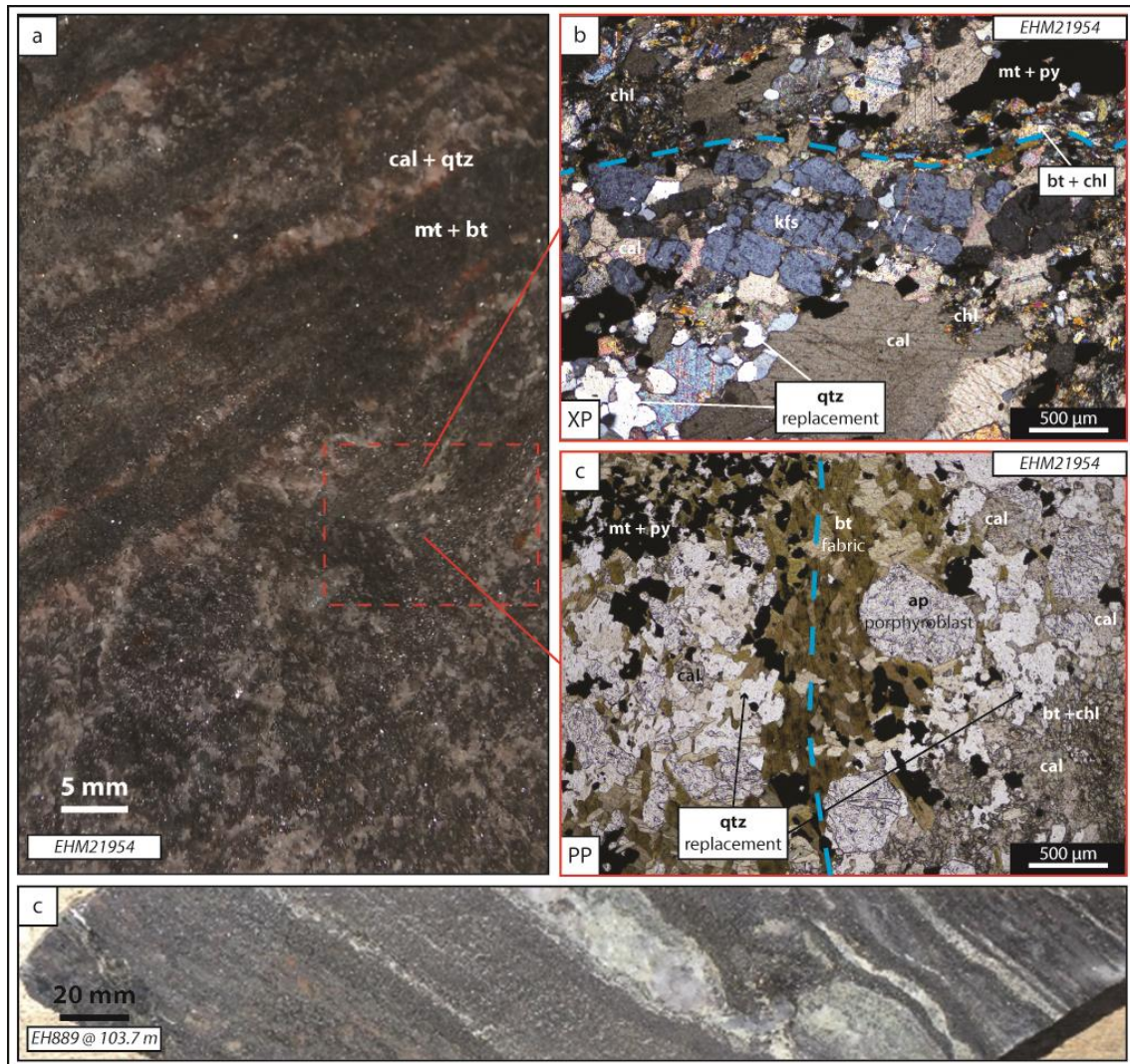


**Figure 24:**a) oriented hand sample of mineral banding collected underground; b) cross polar (XP) photomicrograph sliced parallel to foliation; c) plain polar (PP) photomicrograph sliced perpendicular to foliation and lineation; top-right sense of movement; K-feldspars and biotite are replaced by calcite (cal) and subsequently quartz (qtz). Fractures are infilled by calcite. Chlorite (chl) pseudomorphs calcite, developing a green colouration of calcite bands; d) representative image of mineral foliation bands in drill core.

The earliest minerals (Biotite, apatite and k-feldspar) express evidence of early deformation, overprinted by later minerals (calcite, quartz, magnetite, pyrite) via infill and replacement (Table 4), consistent with biotite-garnet sequences previously discussed. Replacement of biotite by calcite, and lack of volcanic protolith indicate that

these textures most likely represents intense veining progressing towards complete digestion and replacement of wall-rock.

**Table 4: EHM\_21954 Mineralisation sequence and associate alteration stages**

<i>Alteration Stage</i>	<i>Mineral</i>	<i>Field Relations</i>	<i>Textures</i>
<b>Stage 2</b> <i>Pre-mineralisation</i> <i>Potassic</i>	biotite	Defines earliest fabric	weakly schistose
	magnetite	Infills parallel to foliation/lineation	infill
	apatite	Porphyroblastic within biotite fabric	euhedral
	k-feldspar	Fractured, infilled by calcite	fractured
<b>Stage 3</b> <i>Mineralisation</i>	calcite	Infills fractured K-feldspars	infill
	pyrite	Euhedral associated with magnetite	euhedral
	chalcopryite	Anhedral grains with calcite	infill
<i>Retrograde</i>	quartz	Indiscriminately texturally destructive	replacement
	chlorite	Pseudomorph calcite	replacement

### Calcite birds-wings

‘Birds-wing’ tension veins are broadly parallel in orientation, typically cut existing fabrics and are not associated with chalcopryite mineralisation (Figure 25). Tension vein fabrics are observed mostly in gradual contact zones, proximal to the Inter-lens (Table 5)

**Table 5: Distribution of 'birds-wings' tension veins**

<i>Hole</i>	<i>Depth</i>	<i>Notes</i>
<i>EH680</i>	760-765m	Contact zone in the <b>hanging wall</b> unit to the Inter-lens
<i>EH656</i>	675- 685m	Contact zone in the <b>hanging wall</b> unit to the Inter-lens
<i>EH656</i>	762- 765 m	Contact zone in the <b>foot wall</b> to the Inter-lens
<i>EH640</i>	709-731 m	Contact zone in the <b>hanging wall</b> unit to the Inter-lens

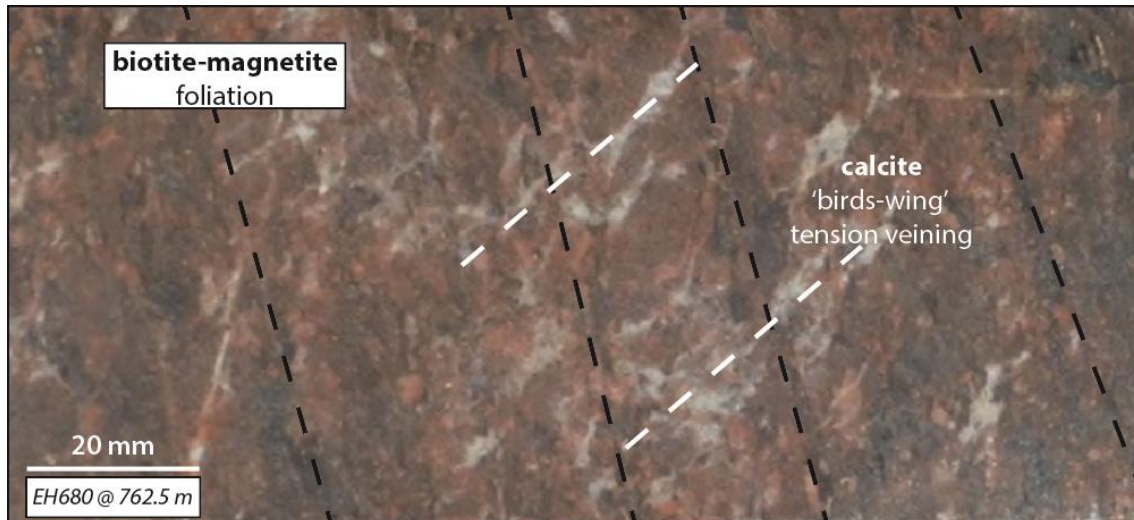


**Figure 25:** Representative image of 'birds-wing' tension vein textures. Sample is from gradual Inter-lens upper contact zone from interval 750m-768m. Tension veining has broadly parallel orientation, cutting dominant fabric defined by biotite and magnetite.

### Alteration Stages and Mineral Textures

Preservation of alteration styles, key mineral relationships and textures are summarised in Table 6. For detailed distribution of alteration styles, refer to detailed graphical drill logs in Appendix F

#### ALBITISATION

Albite replacement of primary volcanic rocks is preserved (rarely) in the feldspar groundmass and phenocrysts of the least altered metavolcanic rocks. Albite alteration was most commonly observed in breccia clasts (Figure 26a, b). SEM reveals complex alteration textures in feldspar phenocrysts which vary in Na and K response (Figure 29**Error! Reference source not found.**c, d) exposing sodic replacement of albite.

#### MAGNETITE + BIOTITE (REPLACEMENT OF ALBITE)

Magnetite-biotite alteration is pervasive throughout metavolcanic rocks of the Inter-lens. Magnetite is a dominant replacement groundmass mineral, seen to be replacing

albite, with anhedral habit. Biotite grains are typically subhedral to euhedral when well-preserved, grain habit defines a dominant tectonic fabric in most foliated rocks. Coarser feldspar phenocrysts contain rare inclusions of magnetite and biotite, appearing to be mostly resistant relative to the groundmass. Biotite is often pseudomorphed by chlorite and replaced by fine grained K-feldspar in the groundmass (Figure 26d).

#### POTASSIC FELDSPAR

Groundmass of volcanic clasts are most commonly potassic altered feldspar of variable recrystallization textures, most commonly masses of fine, euhedral grains. Replacement of biotite grains is commonly observed, leaving a ghost fabric (Figure 26d, e). Hematite staining (red-rock) is not observed.

#### BIOTITE + MAGNETITE (RIMS OF BRECCIA CLASTS)

Elongate and aligned breccia clasts are typically poor in groundmass biotite with distinct and well-developed biotite-magnetite rims. Replacement magnetite is moderate in the groundmass (Figure 22, Figure 33). Biotite is largely pristine with little to no alteration, enveloping k-feldspar and magnetite altered clasts, compared to groundmass biotite that is commonly replaced by k-feldspar. Biotite rim formation is most likely after K-feldspar alteration. It is interpreted that dilation along the dominant biotite-magnetite fabric around competent wall rock clasts has been infilled by biotite. Overprinting calcite and quartz preserve relic biotite grains at the outer portions of these rims.



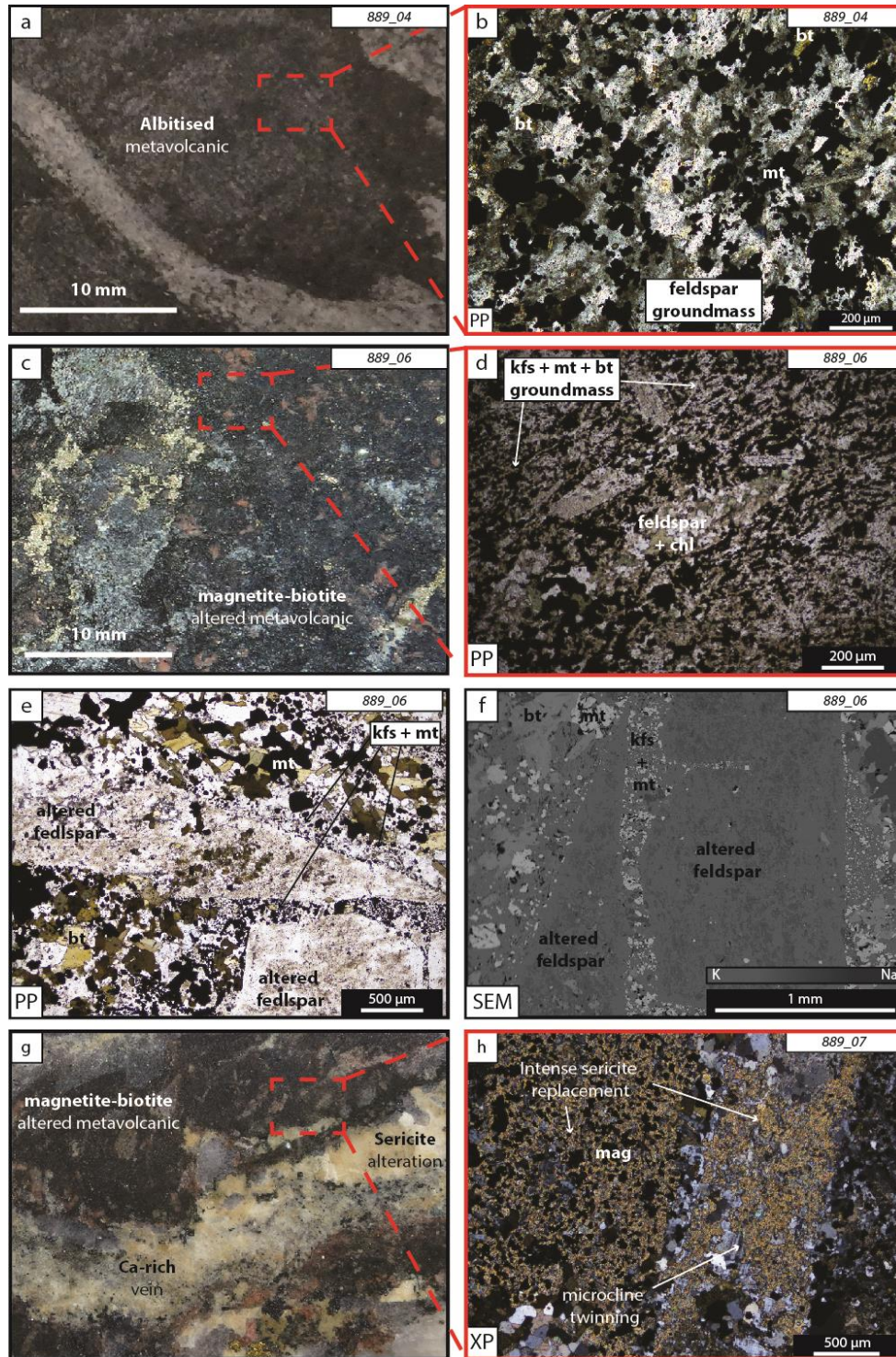


**Figure 26: Representative images of alteration styles observed in the Inter-lens. a) albitised metavolcanic clast in calcite-rich breccia; b) PP photomicrograph of clast in sample; c) Intensely magnetite-biotite altered porphyritic metavolcanic; d) PP photomicrograph of clast reveals intense chlorite alteration of feldspar phenocrysts and groundmass biotite. Replacement magnetite retains ghost fabric; e) PP image shows complex alteration textures on coarse feldspar phenocrysts; f) SEM image highlights variable Na and K response across feldspar surface; g) typical example of sericite alteration of calcite (ca) rich vein; h) XP photomicrograph shows intense replacement of coarse plagioclase phenocryst and feldspar groundmass with fine grain muscovite (sericite).**



## CU-MINERALISATION

Chalcopyrite associated with calcite veins and breccia matrix is the most common chalcopyrite association observed within the Inter-lens. Non foliated, intensely magnetite-biotite altered porphyritic meta-volcanic rocks are cut by calcite veins, progressing to brecciation (Figure 27). Coarse, brecciated euhedral apatite grains are primarily infilled by chalcopyrite and calcite before quartz (Figure 29, Figure 34). Pyrite is also seen to be a primary infill mineral of fractured apatite while euhedral pyrites are present within calcite (Figure 29c).

Elongate lenses of recrystallised quartz ( $\pm$  feldspar) in Mount Fort Constantine Volcanics were interpreted by K. L. Blake et al. (1997) as reflecting primary pumice fragments. Examples in sample EH760\_11 are infilled by chalcopyrite, demonstrating a sheared, primary texture being infilled by mineralisation stage (Figure 29a).

Chalcopyrite replaces calcite (Figure 29a) as well as pyrite in combination with magnetite (Figure 28b) within calcite breccia matrix.

Chalcopyrite is typically present as infill within calcite veins oriented parallel to- sub-parallel and within existing biotite-magnetite foliation. Veins are less commonly observed to cross cut pre-existing fabrics (Figure 30**Error! Reference source not found.**). Birds-wing tension veining was mostly absent from Inter-lens rocks, however calcite lenses associated with minor chalcopyrite mineralisation are common (Figure 31). Calcite lenses trend parallel to and are bound by existing biotite-magnetite foliation, deforming the fabric at the widest point.

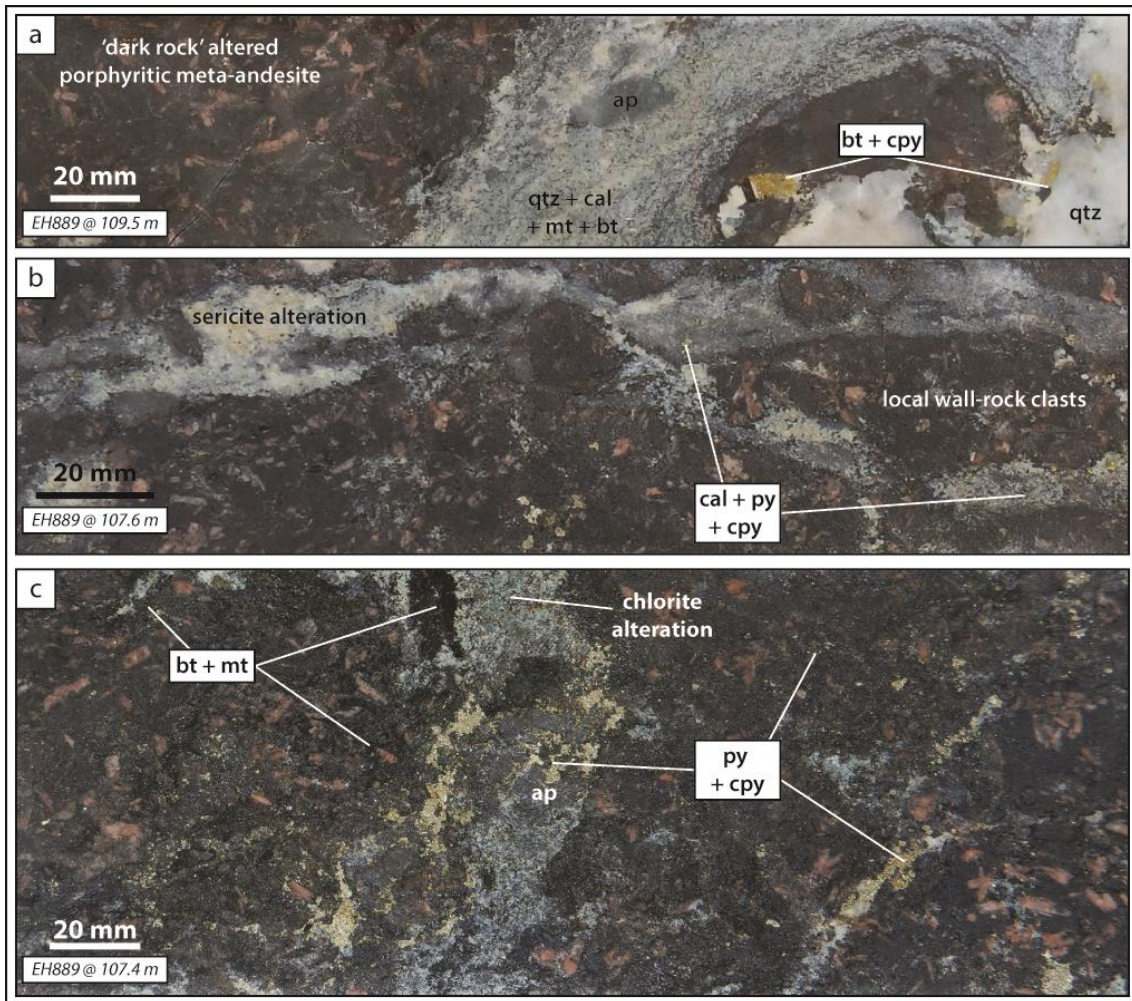


**Figure 27: Representative examples of brecciated porphyritic meta-andesites in a calcite rich matrix similar to the Marble Matrix Breccia and Crackle Vein Breccia at Ernest Henry.** a) a 30 mm wide, diffuse vein of quartz (qtz) + calcite (cal) contains minor magnetite (mt) + biotite (bt) with coarse apatite (ap); b) calcite rich vein contains clasts of local porphyritic meta-andesite wall-rock; minor infill chalcopyrite (cpy) associated with calcite and magnetite; c) fractured apatite in calcite vein infilled by sulphides.

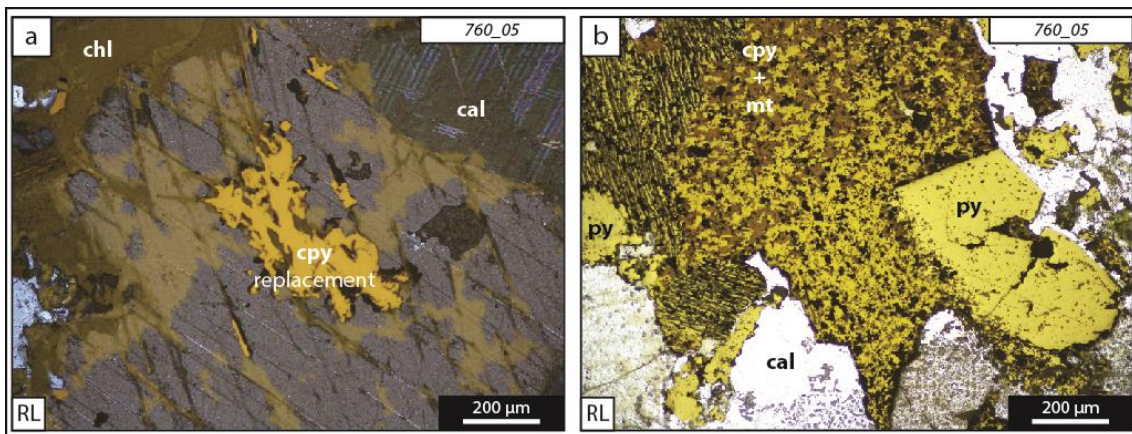


**Figure 28: Chalcopyrite replacement textures.** A) chalcopyrite (cpy) replaces calcite along a cleavage set; b) magnetite (mt) and chalcopyrite replace pyrite (py) in calcite vein.



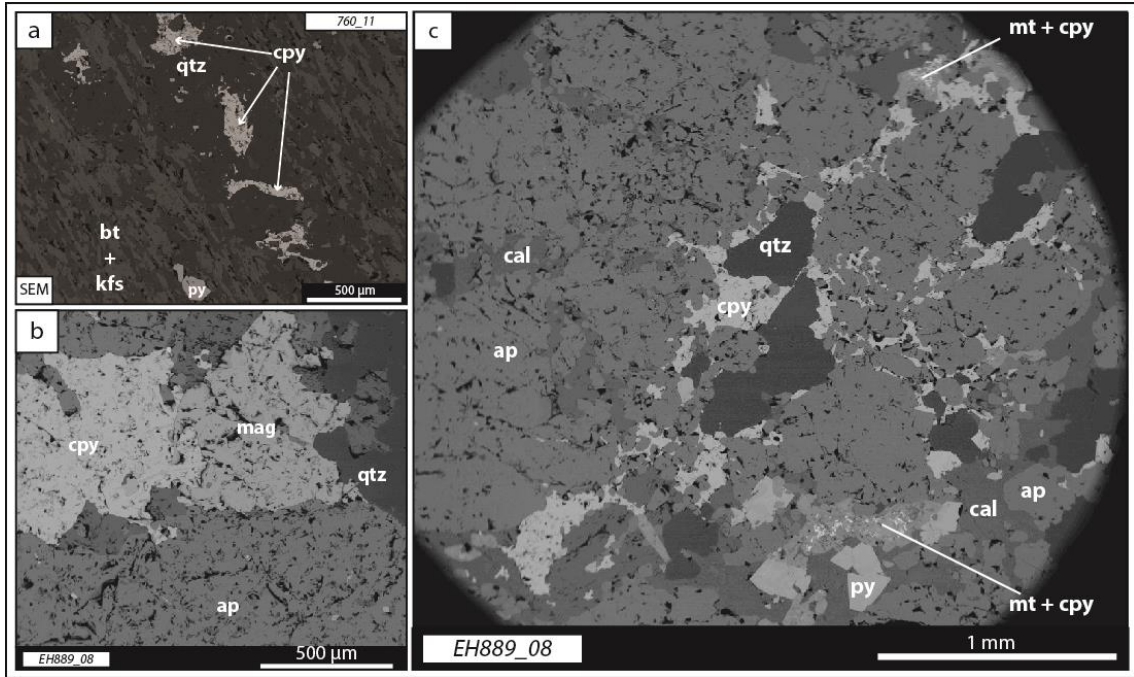


Figure 29: Chalcopyrite infill textures a) chalcopyrite (cpy) infilling quartz (qtz) lens in foliated metavolcanic; b) chalcopyrite directly infills fractured apatite in veins and the calcite-rich matrix; c) chalcopyrite is inter-grown with magnetite in parts.

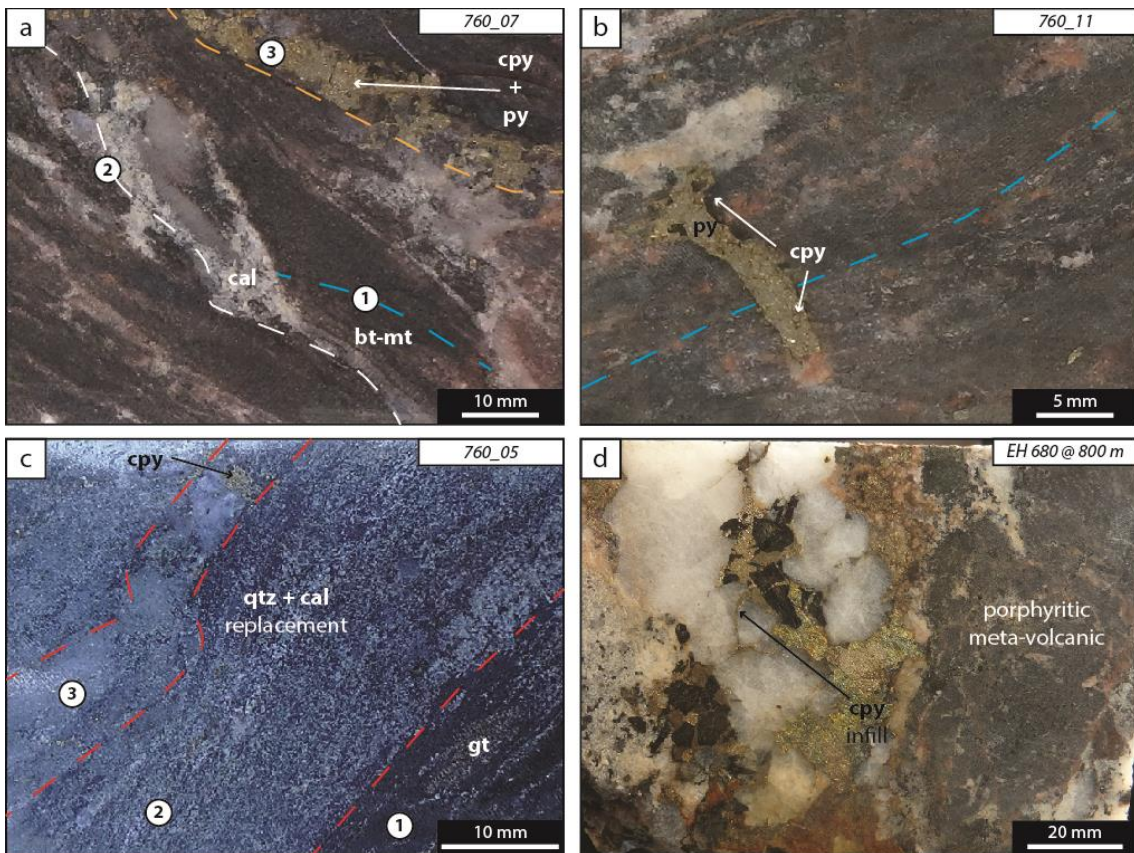
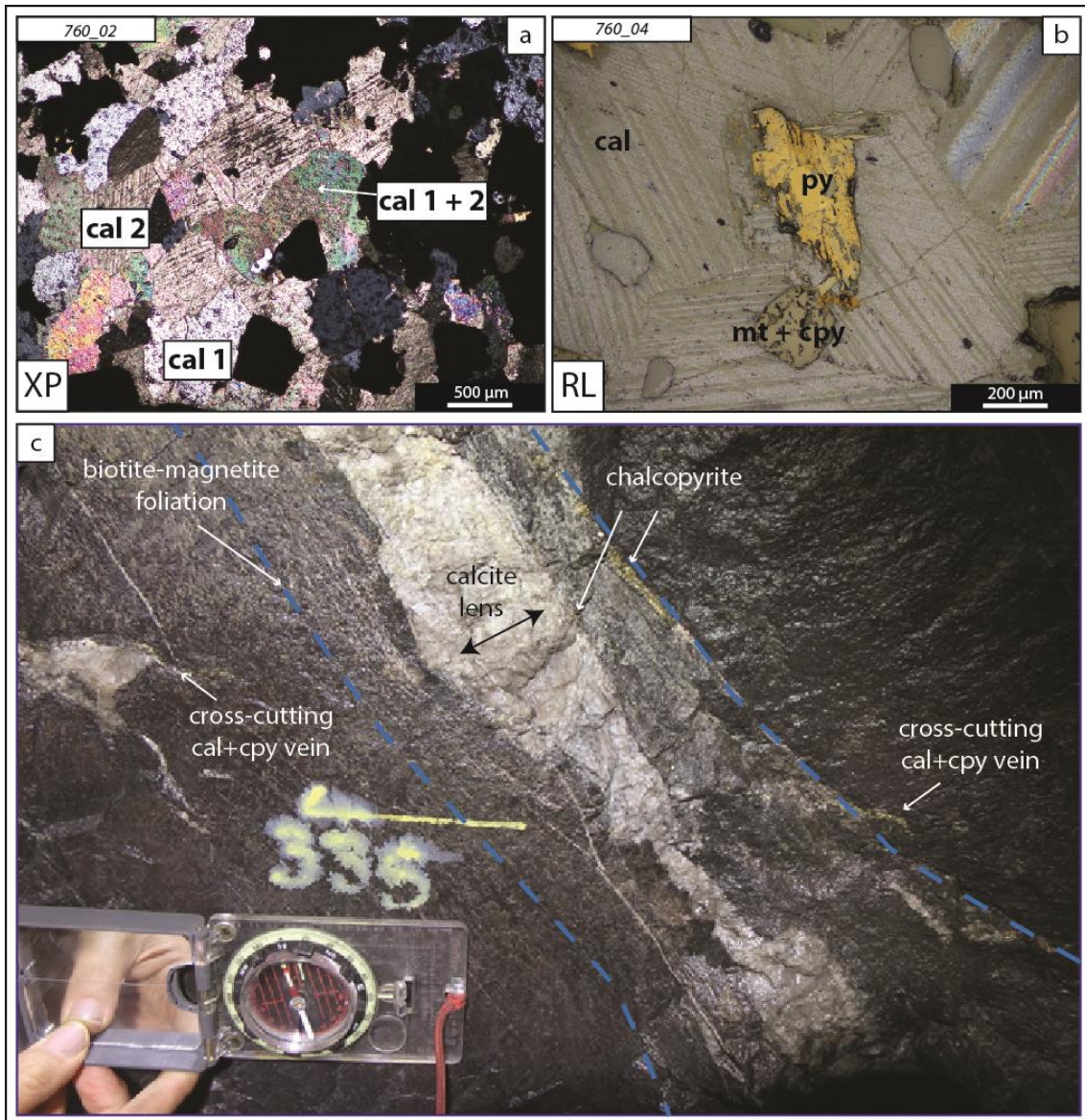


Figure 30: examples of chalcopyrite mineralisation cross cutting pre-existing fabrics.





**Figure 31: Mineralisation stage calcite textures; a) Multiple generations of calcite inter-grown, may indicate recrystallisation of calcite b) calcite replaces pyrite in latest stage in paragenesis, calcite contains inclusions of chalcopryite (cpy) and magnetite (mt) at a triple point; c) weakly mineralised calcite lenses underground parallel to and within pre-existing biotite-magnetite foliation. Compass for scale. Notice fine chalcopryite veins cutting biotite-magnetite foliation.**

## SERICITE

Fine grained muscovite or ‘Sericite’ alteration is identified by a pale to off-white colour with a very soft texture which can be easily scratched away with a finger nail.

Retrograde sericite was observed mostly replacing vein calcite. Groundmass feldspars

and phenocrysts were most intensely replaced in selvages of calcite-quartz vein boundaries in biotite-magnetite altered rock meta-volcanics (Figure 26g, h).

## CHLORITE

Chlorite alteration is interpreted as retrograde replacement, observed most commonly in calcite veins and calcite-rich matrix of breccias. Chlorite pseudomorphs biotite, pyrite and calcite in veins and pseudomorph biotite in groundmass (Figure 32). Chlorite is also observed stable with fine grained muscovite (sericite) replacing massive feldspars, interpreted as recrystallised groundmass (Figure 23c).

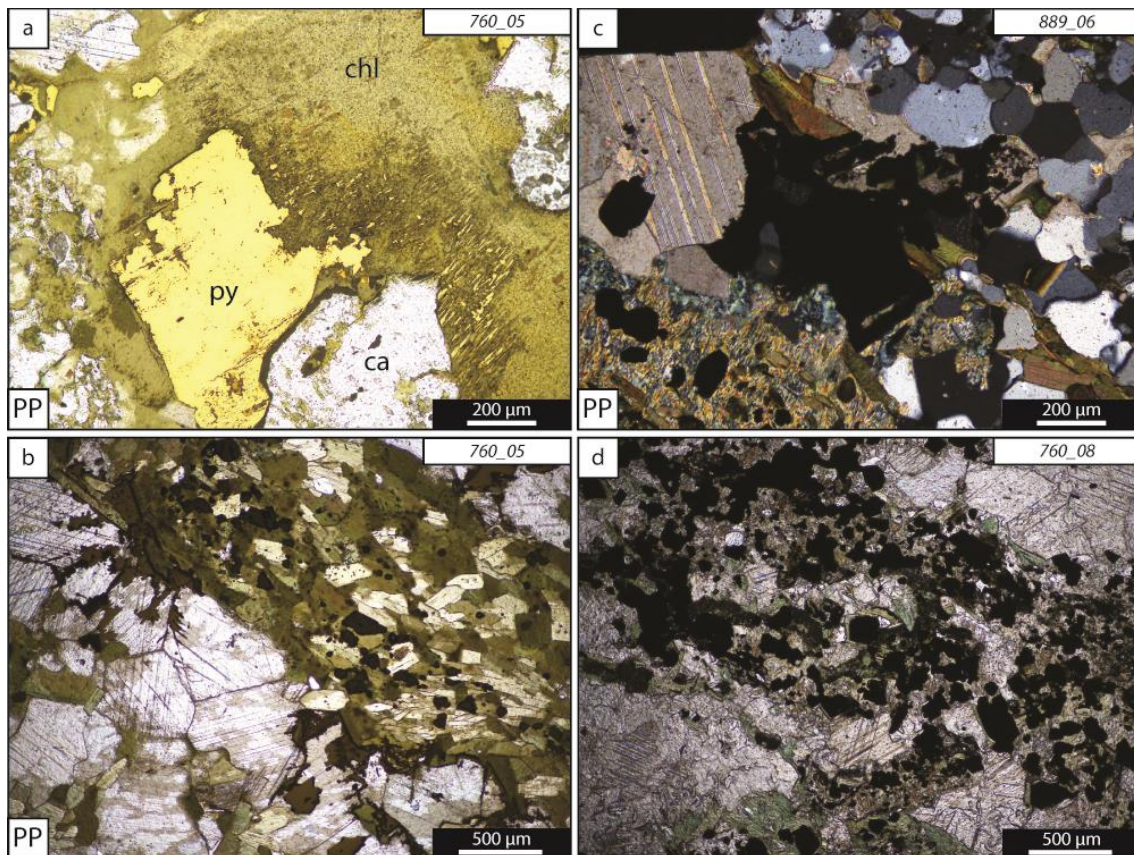


**Figure 32: Representative examples of chlorite alteration in the Inter-lens. a) chlorite (chl) replacing pyrite (py) in a calcite vein; b) chlorite-muscovite replacement of massive feldspar; c) chlorite replacement of interstitial biotite in a calcite vein; d) chlorite replacement of biotite in calcite vein.**



**Table 6: Summary of alteration stages and mineral textures observed in the Inter-lens**

<i>Alteration Stage</i>	<i>Mineral</i>	<i>Field Relations</i>	<i>Textures</i>	
<b>Stage 1</b> <i>Albitisation</i>	Albite	Replaces primary volcanic groundmass and phenocrysts Phenocrysts aligned to foliation in parts	replacement	
<b>Stage 2</b> <i>Magnetite + Biotite</i>	Magnetite	Replaces albite Subhedral in clast groundmass	replacement	
	Biotite	Replaces albite Relic grains in clast groundmass	schistose in parts	
<i>Potassic Feldspar</i>	K-feldspar	Replaces albite Replaces biotite in groundmass	replacement	
<i>Biotite-garnet schists</i>	Garnet	Porphyroblastic	Fractured	
	Biotite	Background mineral	Schistose	
	K-feldspar porphyroblasts	Porphyroblastic in biotite schist and quartz veins.	fractured	
<i>Biotite strain shadows</i>	biotite	Infills strain shadows of breccia clasts Replaces k-feldspar at clast boundary	Infill schistose	
<i>Post-shearing</i>				
<b>Stage 3</b> <i>Mineralisation</i>	chalcopyrite	Anhedral grains with calcite and magnetite	Infill replacement	
	magnetite	Breccia clast boundary in strain shadow assoc. with pyrite	replacement	
	apatite	Euhedral porphyroblasts	brecciated	
		Vein infill		
	calcite	relic grains in quartz background replaces biotite	Infill replacement	
	quartz	Indiscriminately texturally destructive	replacement	
	pyrite	vein infill Euhedral associated with calcite	fractured infill	
	Fine grained muscovite	replaces feldspar groundmass and phenocrysts, vein calcite	replacement	
	<i>Retrograde</i>	chlorite	Pseudomorph calcite, biotite and pyrite	replacement
		Fine grained muscovite	Fine grained muscovite inter-grown with chlorite. Replaces calcite in veins	replacement



### Mineral Liberation analysis (MLA) Maps

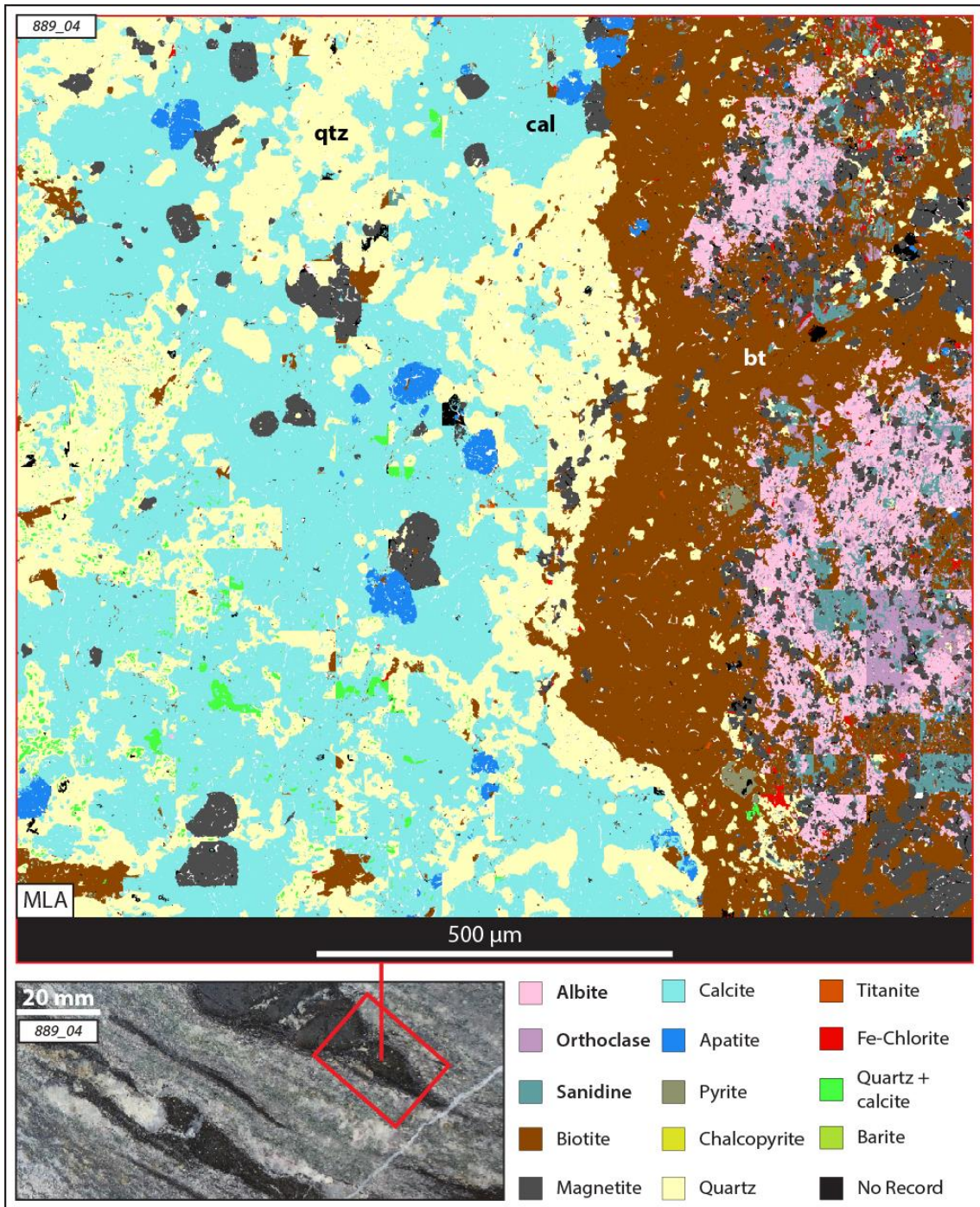


Figure 33: MLA of EH889\_04 with hand sample inset. Pink-purple zone to the right represent feldspar groundmass of altered volcanics with variable sodic and potassic species composition with anastomosing biotite rims. MLA identifies albite ( $\text{NaAlSi}_3\text{O}_8$ ), orthoclase ( $\text{KAlSi}_3\text{O}_8$ ) and sanidine ( $\text{KAlSi}_3\text{O}_8$ ) feldspars, however due to complex alteration textures individual species are poorly defined. Notice infill and replacement textures are pervasive and mineral grains do not appear to be fractured, brecciated or sheared.



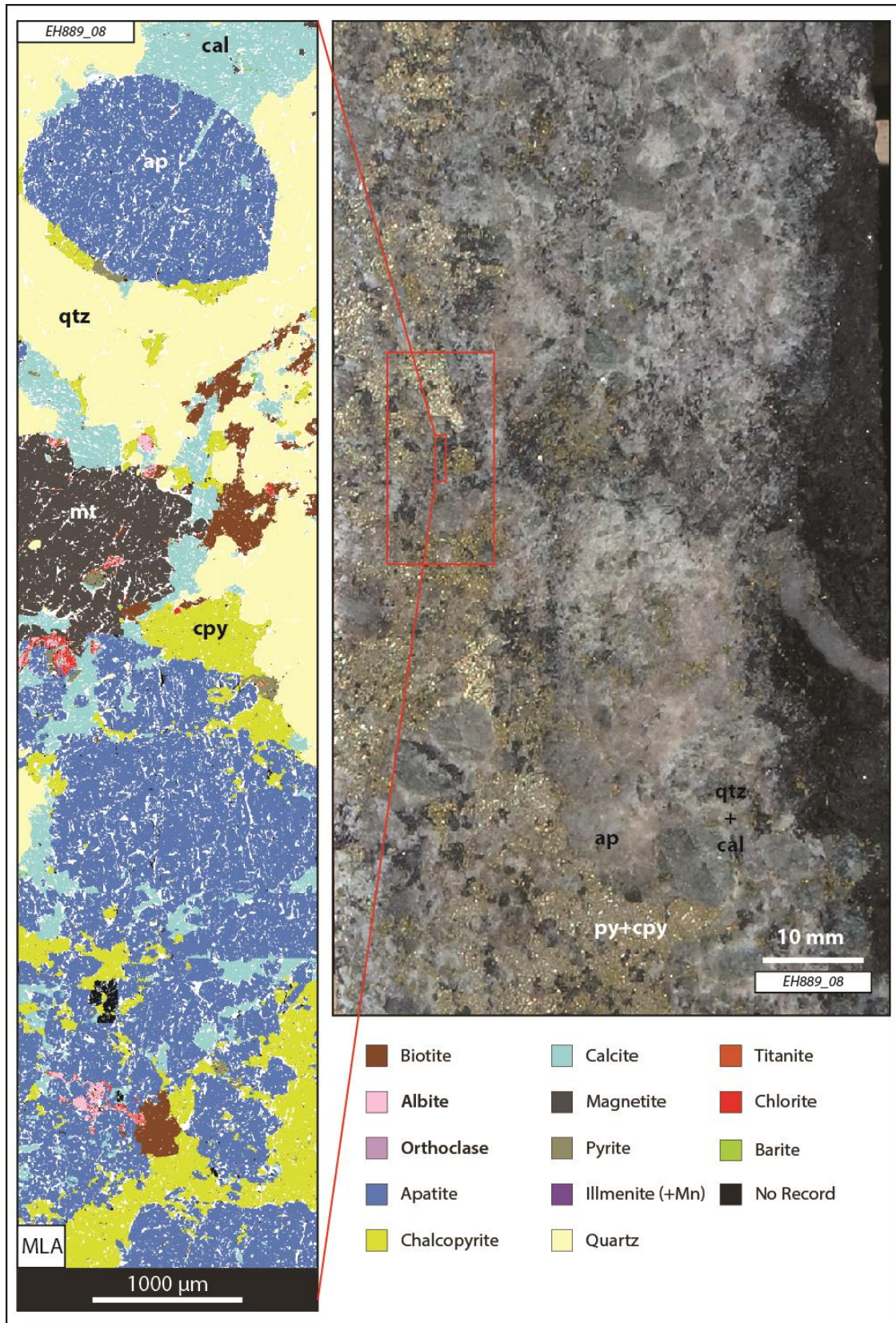


Figure 34: MLA of EH889\_08 Chalcopyrite abundances increases away from wall-rock. Euhedral apatite grains are brecciated and subsequent infill textures dominate. Sulphides are noticeably not sheared.



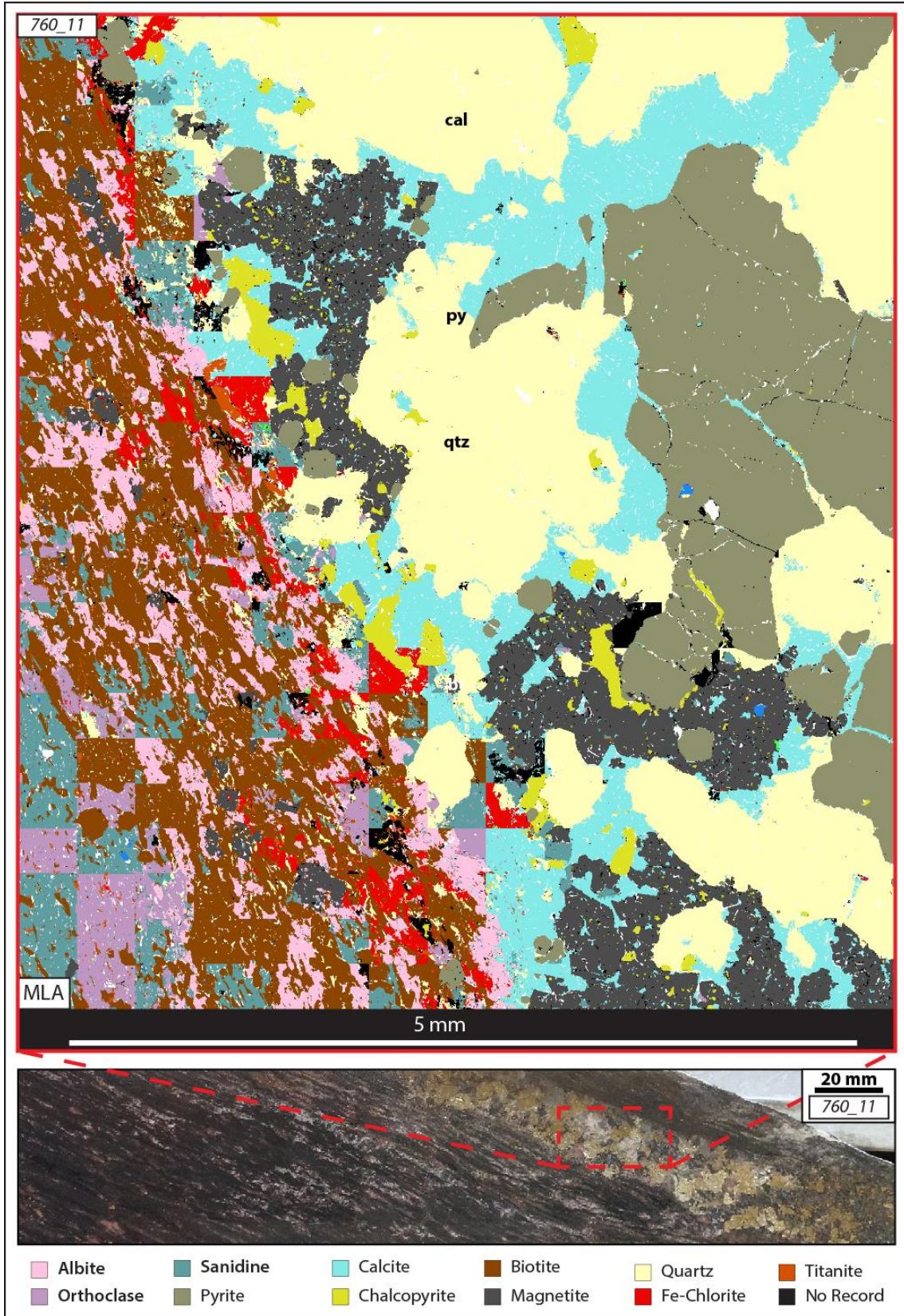


Figure 35: MLA image of EH760\_11. Fractured euhedral pyrites (py) grains are infilled by calcite (cal), chalcopyrite (cpy) and quartz (qtz). Notice infill and replacement textures are pervasive and mineral grains (except pyrite) do not appear to be fractured, brecciated or sheared.

#### EH889\_04

Analysis of the meta-volcanic groundmass of the breccia clast reveals inter-grown albite ( $\text{NaAlSi}_3\text{O}_8$ ), orthoclase ( $\text{KAlSi}_3\text{O}_8$ ) and sanidine  $\text{K}(\text{AlSi}_3\text{O}_8)$  feldspar species indicating potassic alteration of albite (Figure 33). Groundmass feldspars present highly complex exsolution textures, complicating species identification, hence the term K-feldspar-altered albite is adopted. Trace amounts of barite and chalcopyrite associated with Cu-Au mineralisation stage (Mark et al., 2006) are present in the biotite-rich strain shadow. Calcite and quartz are the dominant minerals in the breccia matrix with minor amounts of euhedral apatite and magnetite grains. Infill and replacement textures are pervasive and mineral grains do not appear to be fractured, brecciated or sheared.

#### EH889\_08

Intensely Biotite-magnetite altered, porphyritic meat-andesite is cut by chalcopyrite-bearing veins. Veining is intense, approaching the development of a calcite-matrix, mosaic breccia. Within the calcite vein, brecciated, euhedral apatite grains are infilled primarily by calcite, chalcopyrite and minor pyrite. Chalcopyrite is most abundant further from the wall-rock. Optical work shows quartz to be late and replaces minerals indiscriminately. Chalcopyrite textures are exclusively infill.

#### EH760\_11

Sample presents intense foliation defined by biotite- and magnetite-altered lenses intercalated with calcite. Fabric is cut by a foliation-parallel vein, dominated by coarse grained, euhedral pyrite calcite and quartz with minor chalcopyrite and magnetite. Coarse euhedral pyrite grains are fractured, infilled primarily by calcite, chalcopyrite and quartz. Notice minerals in vein are not sheared.



Intense fabric defined by inter-grown feldspar and biotite has been observed on meta-volcanic clast boundaries in breccias (Figure 23). SEM reveals elongate quartz-feldspar lenses inter-grown with the biotite are infilled by chalcopyrite, pyrite and magnetite at their cores (Figure 29a).

## DISCUSSION

### **Hypothesis 1: The protolith of the Inter-lens is the same protolith as the Ernest Henry orebody (Mount Fort Constantine Volcanics).**

Prior to this study, the protolith of the Inter-lens had not been established. The most convincing evidence of a protolith was preserved as wall-rock clasts in hydrothermal breccias. Clasts of volcanic rocks displaying porphyritic and trachytic textures were observed throughout the Inter-lens. These meta-volcanic clasts are texturally and mineralogically consistent with meta-andesites of the Mount Fort Constantine Volcanics, strongly supporting the hypothesis that they constitute at least one component of the Inter-lens protolith. However, a large proportion of the Inter-lens has been so intensely altered and replaced that any relic protolith is unrecognisable.

Porphyroblastic garnets in biotite-rich schists are particularly uncommon within the deposit. Garnets have been documented previously, within biotite-rich footwall rocks (Mark et al., 2006) which contain shaly metasedimentary lenses and mafic-intermediate components (Twyerould, 1997). It is reasonable then to expect a minor metasedimentary and/or mafic component is present within the Inter-lens.

## **Hypothesis 2: The paragenesis of the Inter-lens is consistent with paragenesis of the Ernest Henry deposit.**

The Inter-lens exhibited albite replacement of plagioclase groundmass and phenocrysts of primary volcanic rocks. This alteration stage was rarely preserved, due to intense or complete replacement of albite by magnetite-biotite 'dark-rock' and later potassic feldspar. Magnetite-biotite 'dark-rock' alteration (early stage 2) is pervasive, overprinting albite intensely. Magnetite is a dominant mineral in the groundmass, having replaced albite indiscriminately. Biotite alteration was variable, and the most intensely biotite-altered clasts are likely to have had a relatively higher Fe-Mg-rich primary mineral assemblage (pyroxene or amphibole), indicating a mafic-intermediate protolith. Applying isotopic and analytical geochemistry techniques in future works will be able to test this assertion.

Potassic feldspar replaced biotite groundmass. Complex alteration textures in groundmass and phenocrysts of breccia clast reveals inter-grown albite ( $\text{NaAlSi}_3\text{O}_8$ ), orthoclase ( $\text{KAlSi}_3\text{O}_8$ ) and sanidine  $\text{K}(\text{AlSi}_3\text{O}_8)$  feldspar species. Complex alteration textures make certainty in identification of feldspars problematic, hence the umbrella term 'K-feldspar altered albite' is used to interpret these results.

Chalcopyrite is most common in quartz-calcite veins generally composed of calcite + quartz + euhedral apatite + chalcopyrite  $\pm$  pyrite  $\pm$  magnetite. Vein thickness varied between mm scale to developing into a breccia matrix. Calcite lenses associated with minor chalcopyrite were oriented parallel to and within pre-existing biotite-magnetite foliation, deforming the fabric. Fine grained, infilling chalcopyrite in magnetite-biotite altered groundmass, and strain shadows of breccia clasts was common, although chalcopyrite intensity was very low in these features. A preference for calcite-associated chalcopyrite mineralisation was obvious, atypical of the highest grade ore breccia. No

Au-mineralisation was observed. Overall, the paragenesis of the Inter-lens (summarised in Figure 36) is not controversial, and is broadly consistent with the paragenesis of the Ernest Henry deposit described by Mark et al. (2006).

## Inter-lens

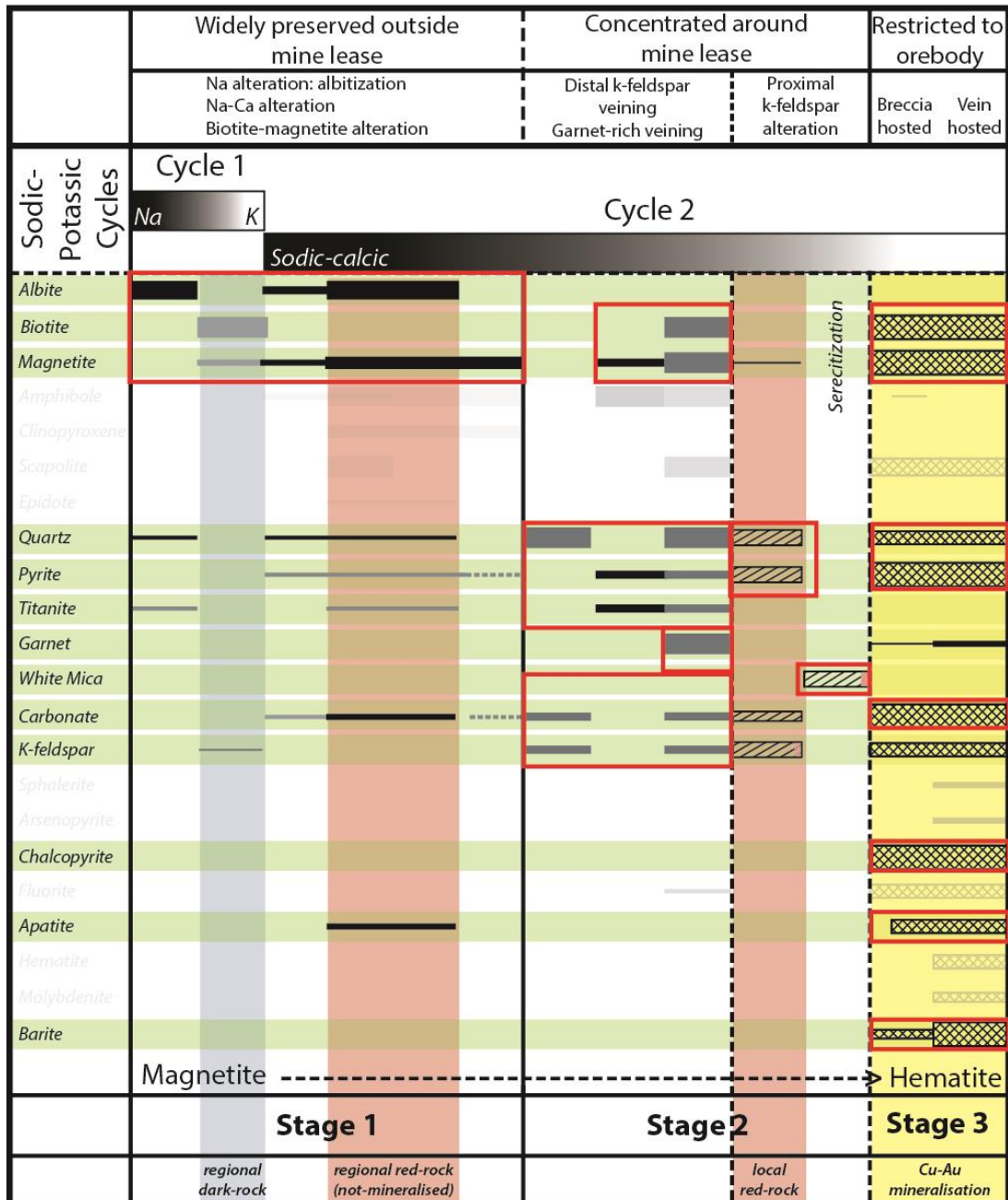


Figure 36: Paragenesis of the Inter-lens with respect to the Ernest Henry ore deposit by Mark et al. (2006). Green highlights minerals identified, red boxes indicate mineral association observed.

### **Hypothesis 3: The formation of the Inter-lens post-dates mineralisation of the Ernest Henry deposit.**

The persistent, anastomosing magnetite-biotite foliation observed throughout the Inter-lens was retained within clasts of brecciated wall-rock, confirming that this fabric formed prior to calcite fabrics. Subsequent fabrics are shown to be broadly parallel to sub-parallel within the earliest fabric. Alignment of breccia clasts and calcite lenses indicating the earliest foliation imposed some control onto the orientation of calcite veining. Cross-cutting veins were abundant, and were used to constrain relative timing of foliation development.

Veins containing chalcopyrite typically parallel to and within, or are cutting across a pre-existing biotite-magnetite foliation. The character of chalcopyrite mineralisation in these veins is mostly infill with minor replacement of calcite and magnetite in some samples. Chalcopyrite grains were not seen to be fractured or sheared in any example in thin section. These cross-cutting relationships and mineral textures provided direct evidence that the pre-existing shear fabrics was overprinted by the mineralisation stage. In thin section, evidence of brecciation, fracturing or rotation of biotite, magnetite, feldspar or chalcopyrite associated with mineralisation stage was absent in the most intensely foliated samples. Instead, calcite, quartz magnetite, chalcopyrite and K-feldspar exhibit replacement and infill textures overprint pre-existing fabrics. Relic biotite grains within the quartz-calcite veins reinforce these interpretations.

Garnet porphyroblasts in biotite rich schists are fractured (brecciated in some cases) which is a texture rarely observed in minerals of the Inter-lens. Mark et al. (2006) assigns garnet growth to within the late stages of pre-ore potassic alteration (stage 2) as part of a garnet-, K-feldspar- and biotite-rich alteration assemblages, consistent with Inter-lens examples. Calcite is shown to replace the schistose biotite in thin section, and



veins containing infill chalcopyrite are seen to cut the quartz-calcite replacement fabric in sample EH760\_03. The interpretation of late Stage 2 syn-deformational garnet growth is well supported, and constrains the latest development of shear fabrics within the Inter-lens.

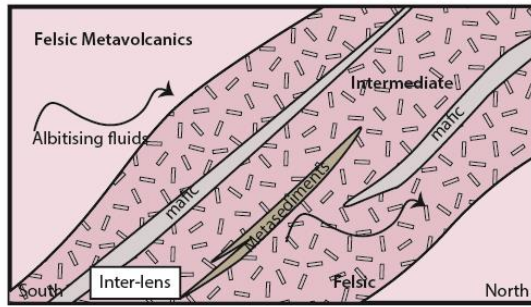
Mineral textures, paragenesis and field relationships provide compelling evidence that the Inter-lens developed a shear structure prior to the onset of Cu-mineralisation.

Shearing of the Inter-lens can be constrained to pre-mineralisation, as fabrics and kinematics were continually observed to be overprinted by Stage 3 and Stage 4 assemblages through veining, infill and replacement processes. Deformation and subsequent infill of minerals representative of late Stage 2 alteration constrain the formation of the shearing texture. General deformation and mineral relationships are presented in Figure 37.

### **Does understanding of the Inter-lens have any implications for the genetic models for the Ernest Henry orebody?**

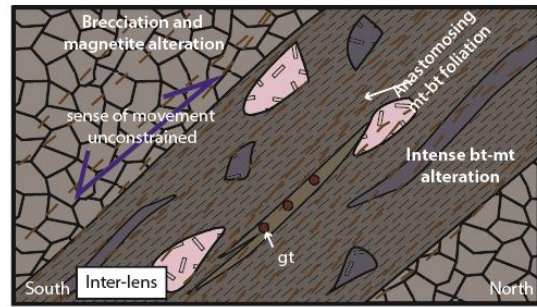
The currently accepted model of the Ernest Henry deposit proposes that release of CO<sub>2</sub> from fluids sourced from enriched mantle or mafic magmas was critical to brecciation and mineralisation. The release of CO<sub>2</sub> under immense pressure is interpreted to have generated 'explosive' fluidised breccias in a model similarly used to describe phenomena such as kimberlite dykes (Oliver et al., 2006). Although interpretations by Oliver et al. (2006) strongly implicate the role of magmatic fluid components in ore mineralisation, it falls short of reasonably excluding chemical milling processes as dominant brecciation mechanism.

Stage 1 - Regional Sodic and Sodic-Calcic alteration of Mount Fort Constantine Volcanics



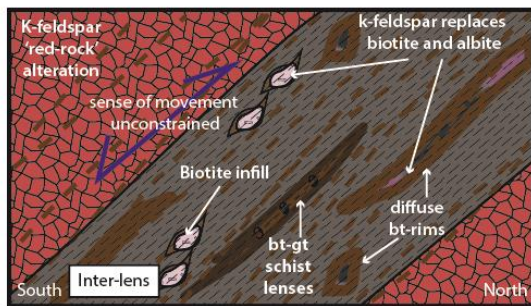
Intercalated felsic, intermediate metavolcanic volcanic rocks with minor mafic-intermediate and shaly metasediments. Albite replacement is indiscriminate and pervasive. Felsic metavolcanics will become ore breccia.

Stage 2 (early)- Magnetite-biotite alteration



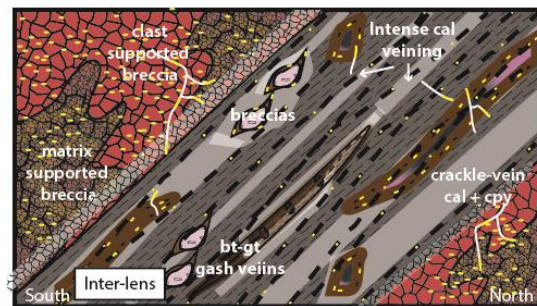
Biotite-magnetite alteration of meta-andesites. Intense foliation of biotite-rich rocks. Foliation anastomosing around lenses of albitised wall rock. Lenses of mafic and albite preserving rock resist foliation.

Stage 2 (late)- Potassic feldspar alteration



K-feldspar replaces biotite and albite indiscriminately. Brecciation of wall rock controlled by existing bt-mt foliation. Porphyroblastic garnets in biotite schists become fractured and overprinted by magnetite veins.

Stage 3- Cu-Au Mineralisation



Magnetite and minor chalcopyrite replaces minerals in existing foliation. Intense brecciation of orebody with infill magnetite-chalcopyrite. Intense calcite veining associated with minor chalcopyrite. Calcite veining controlled by existing fabric, progressing to wholesale wall-rock replacement. Calcite-chalcopyrite veins parallel to and cutting pre-existing fabric.

**Figure 37: Basic geological model representing Inter-lens deformation and overprinting relationships.**

It would seem unlikely that the Inter-lens could exist in the explosive breccia model, unless the formation of the Inter-lens post-dated mineralisation. However, this study has highlighted unambiguously that the tectonic fabrics of the Inter-lens were formed prior to mineralisation. Abundant examples of breccia clasts composed of mostly undeformed, altered meta-volcanic clasts are present within the Inter-lens which most likely formed through persistent, foliation controlled quartz-calcite veining. An alternative hypothesis is therefore proposed in favour of chemical milling processes. Inter-lens rocks are intensely biotite-rich relative to the felsic rocks of the high grade

ore, which may have inhibited the intense clast size reduction observed within the high grade ore breccia and is likely to be a lithological control.

The lateral extent of the Inter-lens remains unconstrained. It is unclear whether the Inter-lens intersects with bounding shear zones at the footwall and hanging wall of the deposit. However, a number of consistencies were identified between the Inter-lens and the biotite-rich rocks of the Hangingwall and Footwall Shear Zones described by Twyerould (1997). These include a) predominantly biotite-rich, strongly foliated rocks with intense and persistent quartz-calcite veining controlled by biotite fabrics and b) main foliations, shear zones and faults dipping moderately  $\sim 40^\circ$  toward the south east (Twyerould, 1997; M. R. Williams et al., 2015). The relationship between the formation of the Inter-lens with respect to the bounding shear zones, and the implications that the Inter-lens may have imposed control onto the formation of the Ernest Henry deposit warrants further investigation.

## CONCLUSIONS

The essential findings of this paper are outlined below:

- The Inter-lens is a pre-mineralisation structure comprised predominantly of biotite-magnetite altered, porphyritic meta-andesite.
- The paragenesis of the Inter-lens is consistent with the Ernest Henry orebody.
- Shear textures within the Inter-lens formed prior to the formation of the high grade ore breccia, and have been overprinted by veining, replacement and infill.
- The currently accepted 'explosive' breccia model at Ernest Henry must be revised, as pre-mineralisation structures such as the Inter-lens are not likely to have been preserved.

## ACKNOWLEDGMENTS

This project was equally challenging and exciting, however, it would not have been possible without the enormous financial support from Mount Isa Mines Research and Development and logistical assistance with fieldwork. Technical expertise, practical advice and enthusiasm for the project provided by Brad Miller, Vanessa Sexton, Dan Ashton and Chloe Conway from the Ernest Henry Geology team was invaluable during this project.

Thank you also to the AusIMM and Playford Trust for their generous scholarship which provided much appreciated support. Thanks also to Ben and Aoife at Adelaide Microscopy who provided invaluable technical support and to Ingham Petrographics for producing such high quality polished thin sections which were essential for this study. I am especially grateful to Dr Richard Lilly for his academic support and geological insight and his Team A.W.E.S.O.M.E.S. crew (Jack (Tuna), Shauna, Sam, Ella). The comradery we developed in the field and on the grind was an enormous benefit during this project.

## REFERENCES









- AUSTIN, J., & BLENKINSOP, T. G. (2008). The Cloncurry Lineament: Geophysical and geological evidence for a deep crustal structure in the Eastern Succession of the Mount Isa Inlier. *Precambrian Research*, 163(1-2), 50-68. doi:10.1016/j.precamres.2007.08.012
- AUSTIN, J. R., & BLENKINSOP, T. G. (2009). Local to regional scale structural controls on mineralisation and the importance of a major lineament in the eastern Mount Isa Inlier Australia: Review and analysis with autocorrelation and weights of evidence. *Ore Geology Reviews*, 35, 298-316.
- BAKER, T. (1998). Alteration, Mineralisation, and Fluid Evolution at the Eloise Cu-Au Deposit, Cloncurry District, Northwest Queensland, Australia. *Economic Geology*, 93, 1213-1236.
- BLAKE, D. H., ETHERIDGE, M. A., PAGE, R. W., STEWART, A. J., WILLIAMS, P. R., & WYBORN, L. A. I. (1990). Mount Isa Inlier - Regional Geology and Mineralisation. In F. E. Hughes (Ed.), *Geology of the Mineral Deposits of Australia and Papua New Guinea* (pp. 915-925). Melbourne: The Australian Institute of Mining and Metallurgy.
- BLAKE, K. L., POLLARD, P. J., & XU, G. (1997). *Alteration and mineralization in the Mount Fort Constantine volcanics, Cloncurry district, northwest Queensland*. Retrieved from
- BLENKINSOP, T. G., HUDDLESTONE-HOLES, C. R., FOSTER, D. R. W., EDMISTON, M. A., LEPONG, P., MARK, G., . . . RUBENACH, M. J. (2008). The crustal scale architecture of the Eastern Succession, Mount Isa: The influence of inversion. *Precambrian Research*, 163, 31-49.



- CLEVERLEY, J. S., & OLIVER, N. H. S. (2005). Comparing closed system, flow-through and fluid infiltration geochemical modelling: examples from K-alteration in the Ernest Henry Fe-oxide-Cu-Au system. *Geofluids*, 5, 289-307.
- DENARO, T. J., RAMSDEN, C., & BROWN, D. (2007). *Queensland Minerals: A Summary of Major Mineral Resources, Mines and Projects*. Queensland Department of Mines and Energy.
- FOSTER, D. R. W., & AUSTIN, J. R. (2008). The 1800-1610 Ma stratigraphic and magmatic history of the Eastern Succession, Mount Isa Inlier, and correlations with adjacent Paleoproterozoic terranes. *Precambrian Research*, 163, 7-30.
- MACKENZIE, W. S., & GUILFORD, C. (1980). *Atlas of rock-forming minerals in thin section*. London ; New York: Longman.
- MARK, G., OLIVER, N. H. S., & WILLIAMS, P. J. (2006). Mineralogical and chemical evolution of the Ernest Henry Fe oxide-Cu-Au ore system, Cloncurry district, northwest Queensland, Australia. *Mineralium Deposita*, 40(8), 769-801. doi:10.1007/s00126-005-0009-7
- OLIVER, N. H. S., CLEVERLEY, J. S., MARK, G., POLLARD, P. J., FU, B., MARSHALL, L. J., . . . BAKER, T. (2004). Modeling the Role of Sodic Alteration in the Genesis of Iron Oxide-Copper-Gold Deposits, Eastern Mount Isa Block, Australia. *Economic Geology*, 99, 1145-1176.
- OLIVER, N. H. S., RUBENACH, M. J., FU, B., BAKER, T., BLENKINSOP, T. G., CLEVERLEY, J. S., . . . RIDD, P. J. (2006). Granite-related overpressure and volatile release in the mid crust: fluidized breccias from the Cloncurry District, Australia. *Geofluids*, 6(4), 346-358. doi:10.1111/j.1468-8123.2006.00155.x
- PAGE, R. W. (1988). Geochronology of Early to Middle Proterozoic Fold Belts in Northern Australia: A Review. *Precambrian Research*, 40/41, 1-19.
- PAGE, R. W., & SUN, S.-S. (1998). Aspects of geochronology and crustal evolution in the Eastern Fold Belt, Mt Isa Inlier. *Australian Journal of Earth Sciences*, 45, 343-361.
- PAGE, R. W., & SWEET, I. P. (1998). Geochronology of basin phases in the western Mt Isa Inlier, and correlation with the McArthur Basin. *Australian Journal of Earth Sciences*, 45(2), 219-232. doi:10.1080/08120099808728383
- POLLARD, P. J. (2006). An intrusion-related origin for Cu-Au mineralization in iron oxide-copper-gold (IOCG) provinces. *Mineralium Deposita*, 41(2), 179-187. doi:10.1007/s00126-006-0054-x
- RYAN, A. J. (1998). Ernest Henry Copper-Gold Deposit. In D. A. Berkman & D. H. Mackenzie (Eds.), *Geology of Australian and Papua New Guinean Mineral Deposits* (pp. 759-768). Melbourne: The Australian Institute of Mining and Metallurgy.
- SPIKINGS, R. A., FOSTER, D. A., KOHN, B. P., & LISTER, G. S. (2001). Post Orogenic (<1500 Ma) thermal history of the Proterozoic Eastern Fold Belt, Mount Isa Inlier, Australia. *Precambrian Research*, 109, 103-144.
- TWYEROULD, S. C. (1997). *The geology and genesis of the Ernest Henry Fe-Cu-Au deposit, NW Queensland, Australia*. (Doctor of Philosophy), University of Oregon.
- WILLIAMS, M. R., HOLWELL, D. A., LILLY, R. M., CASE, G. N. D., & McDONALD, I. (2015). Mineralogical and fluid characteristics of the fluorite-rich Monakoff and El Cu-Au deposits, Cloncurry region, Queensland, Australia: Implications for regional F-Ba-rich IOCG mineralisation. *Ore Geology Reviews*, 64, 103-127. doi:10.1016/j.oregeorev.2014.05.021
- WILLIAMS, P. J., BARTON, M. D., JOHNSON, D. A., FONTBOTÉ, L., DE HALLER, A., MARK, G., & OLIVER, N. H. S. (2005). Iron Oxide Copper-Gold Deposits: Geology, Space-Time Distribution, and Possible Modes of Origin. *Economic Geology, 100th Anniversary Volume*, 371-405.

**APPENDIX A: DESCRIPTION OF HOST ROCKS AT ERNEST HENRY.**

Adapted from Ryan (1998) and Mark et al. (2006) and from internal communication,  
Ernest Henry Mining.

<p>Altered Metadiorite (Di)</p>	<p>Medium- (1-3 mm) to coarse-grained (5-10 mm), mesocratic to leucocratic with equigranular appearance. Metamorphic mineralogy of plagioclase, hornblende, magnetite, titanate, quartz and K-feldspar is largely retained.</p>	
<p>Fine &amp; Coarse Grained Albitite (FGAB/CGAB)</p>	<p>Massive fine grained and coarse grained albitized rocks with intermediate volcanic and volcaniclastic protolith. Fine grained variants are typically dull grey to white colour with a sugary texture. A greater range of colour is seen in coarser grained variants. Darker coloured versions contain minor opaques and biotite, with altered versions of igneous intrusions or (diiorite) dykes observed in core.</p>	
<p>Weakly- to Moderately- &amp; Strongly-Foliated Schist (SCH3/SCH4)</p>	<p>Interpreted as original intermediate volcanics, biotite-rich rocks display strong tectonic fabrics transitioning from SCH3 to SCH4. Common to the bounding shear zones. Form anastomosing cleavage around pods of competent quartz/albitized rock. Foliation has been subject to varying degrees of biotite/magnetite alteration.</p>	
<p>Porphyritic Intermediate Volcanic (PIV)</p>	<p>The majority of the meta-andesite hosts have a fine-grained groundmass, subhedral to euhedral plagioclase phenocrysts and preserve a variety of igneous textures ranging from glomeroporphyritic, porphyritic, seriate to non-porphyritic (Mark et al., 2006).</p>	
<p>Mafic Volcanic &amp; Meta-Mafic Volcanic/Metasediment (MV/MMV)</p>	<p>Fine grained mafic volcanic/siltstone with strong foliation contains intense biotite and carbonate with abundant pyrite ± minor economic chalcopyrite. Meta-variants contain biotite, amphibole, and moderate pyrite ± trace garnet, arsenopyrite and minor chalcopyrite.</p>	
<p>Marble Matrix Breccia (MMB)</p>	<p>A carbonate-rich area containing mafic and felsic volcanic clasts in a carbonate-biotite-magnetite-amphibole-chlorite matrix with distinctive swirling texture. Clasts typically possess dark reaction haloes of biotite + magnetite + chlorite (Ryan, 1998).</p>	
<p>Intermediate Volcanic ± Carbonate Banding (IV)</p>	<p>Fine, to medium grained schistose variant of intermediate volcanics with moderate foliation. Distinct to diffuse mineralogical layering is interpreted as foliation vein infill grading into replacement of wall rock. Dominant layering assemblages are carbonate + quartz ± amphibole, biotite + magnetite, and feldspars + quartz + biotite.</p>	
<p>Massive-Crackle Vein &amp; 'Birds-wing' Tension Veined &amp; Matrix Supported, Felsic Volcanic Breccias (FV/FV1/FV2)</p>	<p>Matrix-supported and clast supported breccias (FV2) in felsic volcanics grade to tension veined volcanics (FV1) through to crackle fracture veining and unbrecciated rocks (FV). Matrix is dominantly magnetite-carbonate-sulphide. Clasts are characteristically brick-red in colour, ranging from 2mm to 15mm across (Ryan, 1998).</p>	

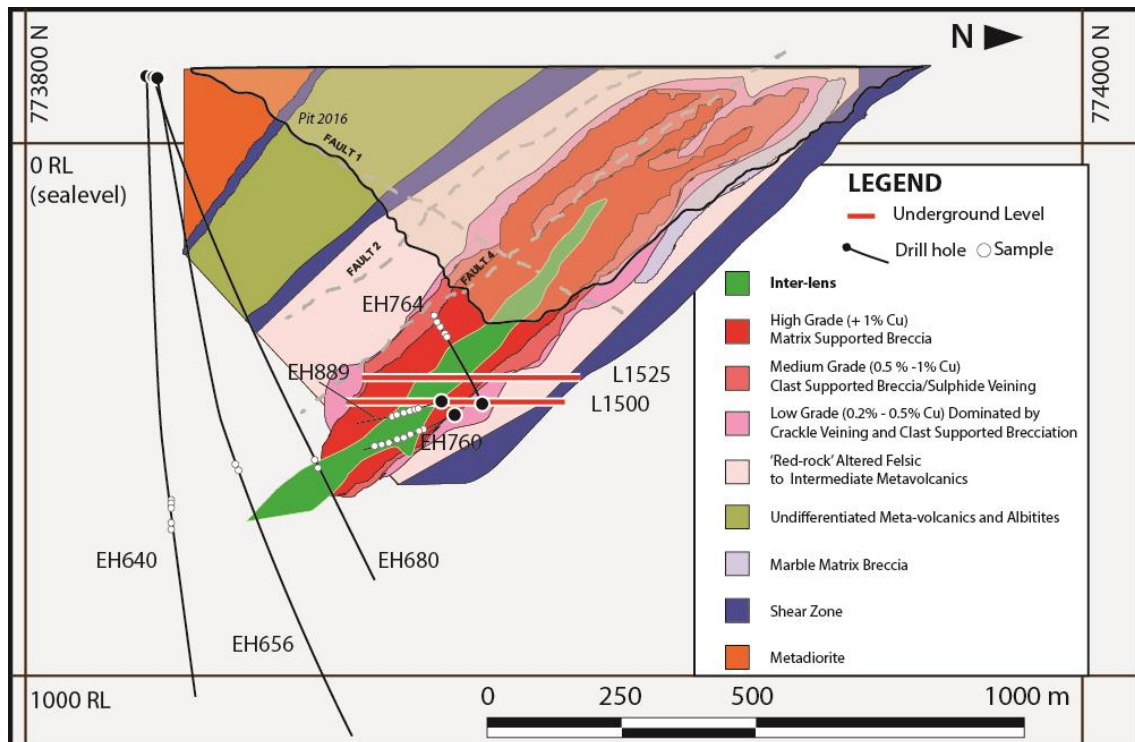
## **APPENDIX B: EXTENDED METHODS**

This study focussed primarily on geological mapping underground at the Ernest Henry mine lease and detailed graphical logging of drill core. Paragenesis of the Inter-lens was then compared with the Ernest Henry paragenesis by Mark et al. (2006). Two underground levels and six drill holes were selected which provided a) good coverage along the strike of the Inter-lens structure and b) long intersections through the structure. Three recently drilled oriented holes were identified (EH760, EH656, EH640).

Structural measurements from exposed features underground were measured with a magnetic declination of 6° E in Cloncurry. Replicating in-situ measurements in 3 oriented drill holes using a Marjex Core Orientation Frame was undertaken in a location shielded from magnetic sources. If a structure, such as a pervasive fabric, remained constant in its attitude, representative measurements were taken every 10-15m along a hole.

Alteration style was defined and recorded by identification in hand sample of indicator minerals, such as calcite, magnetite, biotite, hematite-stained K-feldspar and chlorite.

Rock textures were recorded with particular attention focused on foliation and brecciation. Mineral cross cutting relationships were examined, logged and photographed for detailed analysis. Samples representative of hydrothermal alteration stages with clear textural relations were taken for paragenetic analysis from underground and drill core. Where permitted, oriented samples were taken from underground to prepare oriented thin sections to observe potential micro-scale kinematic indicators, and to observe hand samples in natural light.



**Plan of study area in section view. Inter-lens geometry and location interpreted from voids within 0.7% Cu grade shell at Ernest Henry.**

### Core orientation

3 holes were identified as oriented from the mine database. EH760 and EH656 were surveyed using the Reflex GYRO™, a highly accurate electronic instrument which records orientation and inclination of the bore hole to true north. GYRO oriented core is preferred due its effectiveness in magnetised environments. EH640 was surveyed using the Ranger tool and was oriented to the mine north and is less reliable.

### Structural measurements from oriented core

Core was visually inspected to identify what structures were present. The structures most commonly observed were foliation and schistosity, mineral alignment and brittle fractures and veins. Bedding was not likely to be encountered in the metavolcanic and brecciated rocks. If a structure, such as a pervasive fabric, remained constant in its



attitude, representative measurements were taken every 10-15m along a hole. When rapid changes were observed, more frequent measurements were made. Particular attention was made to observe multiple structures and their relations to develop geological context.

Measurements were taken using a Marjex Core Orientation Frame in a location where the compass would not be affected by magnetic sources. Dip and azimuth of the drill hole was set based on survey data from the mine drilling database. Magnetic declination of 6 E in Cloncurry, and 9 E in Adelaide were applied when orienting the frame.

Planar structures were extended using an extension plane fixed to the core with BluTac™. Core was then placed into the frame, with the bottom-of-hole orientation line and arrows facing down, replicating the in-situ orientation of the core. An elastic band was used to stabilise the core. The structural measurements could then be measured with a compass as a geologist would at outcrop.

Although whole core is preferred for conducting structural measurements, access was limited and most commonly half core was available. Measurements were made on half core samples prior to being cut to quarter core to be made into thin sections.



**Application of the Marjex core orientation frame, dip and azimuth are set as recorded by mine survey data. Structural planes are extended to replicate in-situ measurements sheltered from magnetic sources.**

### **Core Logging**

Detailed graphical logging was undertaken using selected drill holes. Intersections of the Inter-lens were logged and could be identified by (often) brittle deformation, and distinct changes in tectonic fabric, lithology and /or alteration styles.

Style of alteration observed was recorded graphically and was identified by the minerals that could be identified in hand sample, such as carbonate, quartz, magnetite, biotite, K-feldspar (red-rock) alteration and chlorite.

Rock textures were logged with particular attention focused on foliation and brecciation. Mineral cross cutting relationships were examined, logged and photographed for detailed analysis. Relationships were and were determined by presence in veins and cross-cutting veins, replacement and infill textures. This data can be assessed against the well documented paragenetic sequence of the Ernest Henry Deposit.

## **Underground**

Underground, in-situ measurements could be taken from exposure features. The lithology has been intensely magnetite altered, which affects the compass close to the surface. After taking measurements, it is important to move away from the rock surface and observe the affect and correct accordingly. Sometimes adjustments of up to 20 degrees were made to dip direction measurements. To mitigate this influence, underground measurements were recorded to the nearest 5°, as per the procedure used within the mine. This should be considered when analysing results from the underground environment. Measurements of oriented samples can validate at the surface. Where permitted, oriented samples were taken from underground and measurements were verified. Oriented thin sections were produced to observe potential micro-scale kinematic indicators, and to observe hand samples in natural light. Sample orientation was recorded by drawing horizontal lines (dip = 0) along surfaces and recording the strike of that line in-situ.

## **Petrography and optical microscopy**

20 thin sections of the Inter-lens and surrounding ore breccia (11 unpolished, 9 polished) were generated by Ingham Petrographics, Ingham, Qld, from samples collected during March 2016. Photomicroscopy and viewing was undertaken at University of Adelaide using an Olympus BX51 System Microscope with a DP21 Microscope digital camera. Mineral identification in thin section was assisted by detailing optical properties as outlined by MacKenzie and Guilford (1980).

## **Scanning Electron Microscope (SEM) and Mineral Liberation Analysis (MLA)**

Mineralogical and textural analysis of protolith and alteration mineralogy was undertaken at Adelaide Microscopy using a FEI Quanta600 Scanning Electron Microscope with the Mineral Liberation Analysis (MLA). Semi-quantitative analysis was undertaken of 9 sections representative of host rock, veins and breccia matrix. MLA maps were produced using the following procedure:

1. Mapped area was selected using MLA software. Map areas were designed to be completed in less than 8 hours.
2. After MLA has produced a classified map, the SEM was used to spot check minerals to verify classes.
3. Accurately classified minerals would be added to an ad-hoc classification database.
4. Minerals that were incorrectly or inaccurately classified would be inspected using the SEM spot check capability. Mineral spectra would be assessed to assign the most accurate mineral name to the class. Optical microscope notes were used to aid identification.
5. After assigning classifying spectra, images would be reclassified and re processed.

This process was repeated until the user was satisfied with the assigned mineral classifications.

Accuracy of mineral identification using MLA is limited by:

- The classes on file in the database
- Complex alteration textures

Minerals with similar chemical and physical properties in proximity.

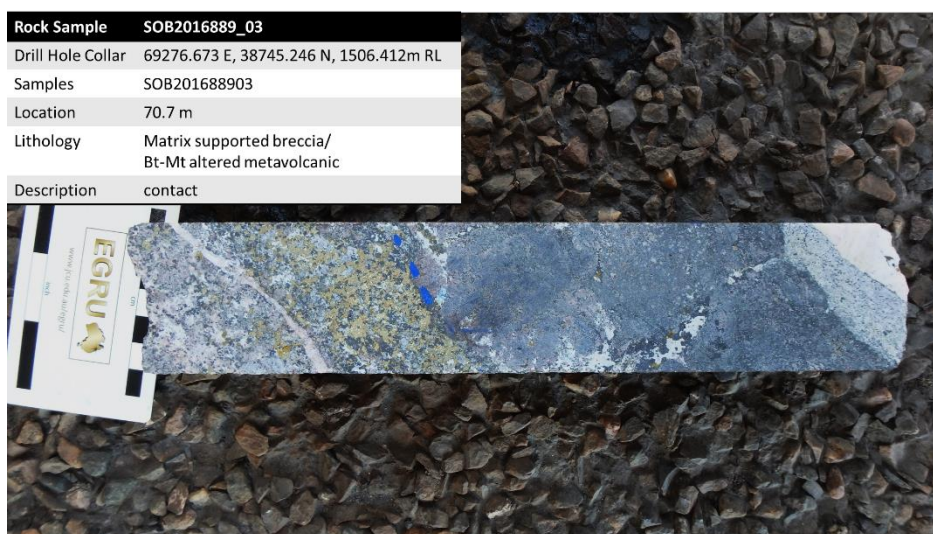
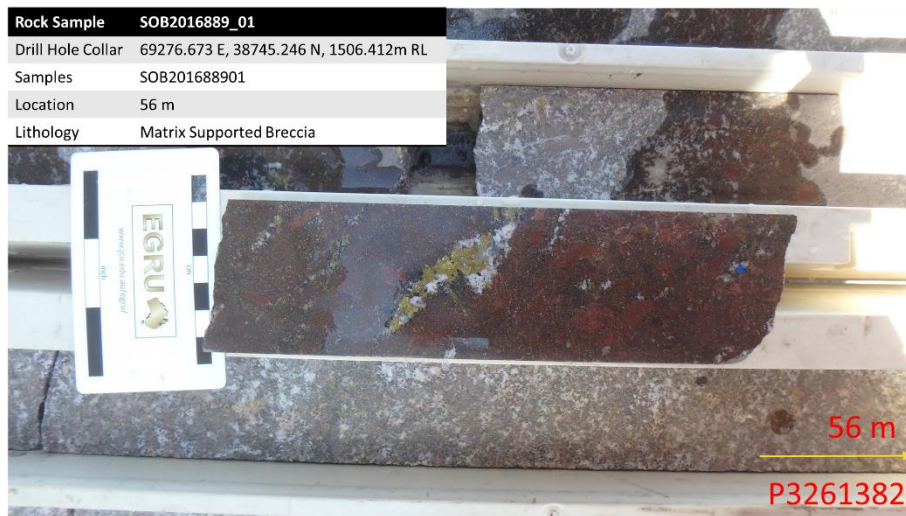


**APPENDIX C: ORIENTED DRILLHOLE STRUCTURAL DATA**

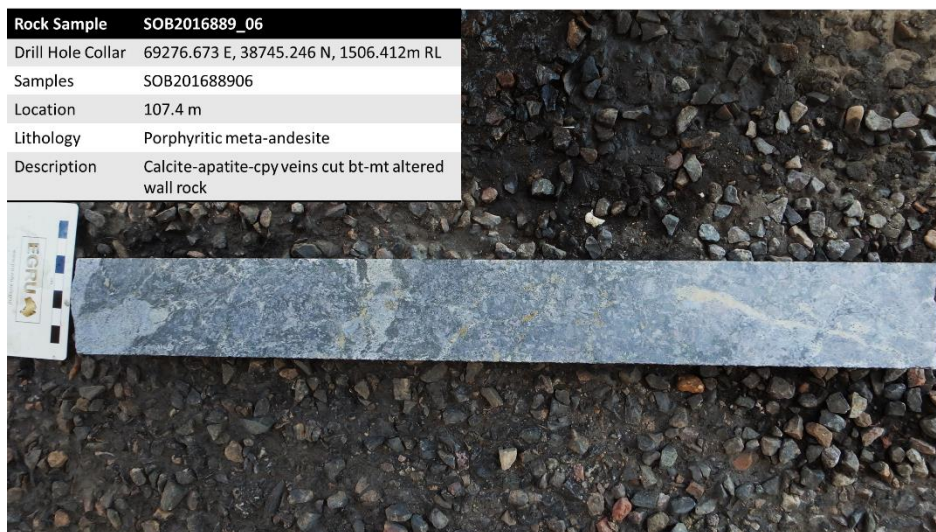
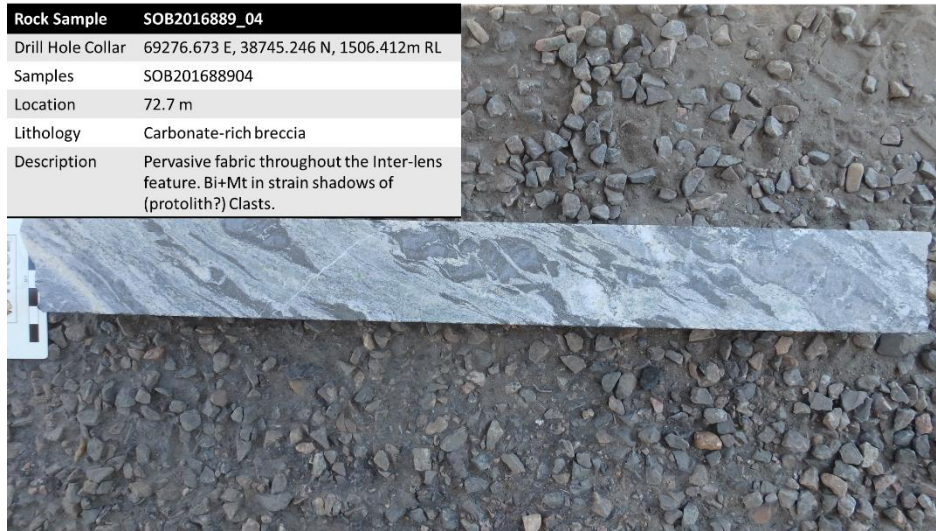
<b>DRILL HOLE ID</b>	<b>DEPTH (M)</b>	<b>DIP ANGLE</b>	<b>DIP DIRECTION</b>	<b>COMMENT</b>
<b>EH760</b>	99.5	30	200	Inter-lens contact
	102.9	40	150	bt-mt fabric
	102.9	85	80	cross-cutting cb vein
	103.8	35	150	bt-mt fabric
	103.8	70	90	cross cutting crack
	105.7	35	150	bt-mt fabric
	105.7	70	60	large cross-cutting vein, filled with chlorite? And carbonate?
	117.8	45	130	bt-mt fabric
	120.5	25	120	bt-mt fabric
	120.5	25	120	sigmoidal fabric axial trend, fabric parallel
	123.5	40	150	fabric, Gt inclusions in mt/bi appears to show 2 fabrics, but it could be oriented and clast boundaries or a crenulation
	124.8	70	140	Mt vein filled with cal cross cuts
	129.7	50	130	garnet in vein/sigmoidal
	137.6	35	130	bt-mt fabric
	142.4	50	145	bt-mt fabric
	146	45	140	bt-mt fabric
	149.4	40	145	bt-mt fabric
	149.4	40	145	bt-mt fabric
	149.4	30	140	bt-mt fabric
	149.4	30	180	fabric in cal
	149.4	28	140	mineralised vein
	151.2	30	30	bt-mt fabric
	158.6	40	140	bt-mt fabric
	159.3	88	200	cross cutting chlorite vein N/S sub-vertical strike
	159.3	40	40	fabric (messy zone)
	173.3	40	145	bt-mt fabric
	176	40	125	bt-mt fabric
	179	40	140	bt-mt fabric
	181	40	155	sigmoidal axis
	187.1	50	140	bt-mt fabric

<b>DRILL HOLE ID</b>	<b>DEPTH (M)</b>	<b>DIP ANGLE</b>	<b>DIP DIRECTION</b>	<b>COMMENT</b>
<b>EH656</b>	695.5	88	196	very late cal vein, cross cuts pink vein
	695.5	58	15	pink vein cross cut by white cal vein
	702.8	44	64	carbonate birds-wings
	702.8	54	140	biotite fabric foliation which is cross cut by carbonate birds-wings
	707	45	155	fabric clast and biotite foliation
	720	47	170	fabric defined by clast orientation and biotite foliation
	726.5	36	278	pink vein
	<b>EH640</b>	754.5	48	110
759.5		52	133	fabric defined by foliation
778		50	63	carbonate vein 2.5cm width
778		52	62	carbonate fabric, is parallel to the cal vein
778		54	62	magnetite vein set
791		48	174	fabric in carbonate
799		32	230	late carbonate vein micro fracture
799		55	100	thick carbonate vein
799		72	118	fabric in magnetite and biotite schistosity
814		52	270	fabric in carbonate
814		51	264	bt-mt fabric
822		63	310	bt-mt fabric
822		88	236	mineralised vein
824		47	265	magnetite and carbonate rich vein defining fabric with clast orientation
838		60	100	fabric schistosity in clasts
838		30	130	fabric schistosity in clasts
847.3		44	115	fabric by orientation of biotite grains schistosity
849.7		30	290	carbonate vein
849.7		30	110	carbonate vein
849.7		82	250	mineralised cal vein micro fracture

## APPENDIX D: SAMPLES AND DESCRIPTIONS.









<b>Rock Sample</b>	<b>SOB2016889_07</b>
Drill Hole Collar	69276.673 E, 38745.246 N, 1506.412m RL
Samples	SOB201688907
Location	113.3 m
Lithology	Porphyritic meta-andesite
Description	Calcite-apatite-cpy veins cut bt-mt altered wall rock



<b>Rock Sample</b>	<b>SOB2016889_08</b>
Drill Hole Collar	69276.673 E, 38745.246 N, 1506.412m RL
Samples	SOB201688908
Location	115.1 m
Lithology	
Description	Comments: matrix texture (vein?) and infill dominate. Infill sulphides, try to the pale, creamy mineral, texture is representative of identify111-116m interval



<b>Rock Sample</b>	<b>SOB2016889_09</b>
Drill Hole Collar	69276.673 E, 38745.246 N, 1506.412m RL
Samples	SOB201688909
Location	125.7 m
Lithology	Matrix supported breccia
Description	Contact zone, representative sample of contact, seek to find in orientated core later.



Rock Sample	SOB2016760_01
Drill Hole Collar	69315.98 E, 38764.04 N, 1477.661 m RL
Samples	SOB2016760_01
Location	99.5 m
Lithology	Matrix supported breccia/foliated meta-andesite
Description	Contact



Rock Sample	SOB2016760_02
Drill Hole Collar	69315.98 E, 38764.04 N, 1477.661 m RL
Samples	SOB2016760_02
Location	103.8 m
Lithology	Albitised metavolcanic
Description	Sigma clast with infill biotite



Rock Sample	SOB2016760_03
Drill Hole Collar	69315.98 E, 38764.04 N, 1477.661 m RL
Samples	SOB2016760_03
Location	113.3 m
Lithology	Gt-bt vein
Description	Gt-bt-vein in quartz-calcite matrix, cut by quartz vein + cpy





Rock Sample	SOB2016760_04
Drill Hole Collar	69315.98 E, 38764.04 N, 1477.661 m RL
Samples	SOB2016760_04
Location	113.8 m
Lithology	Bt-gt schist
Description	Biotite fabric drapes garnets



Rock Sample	SOB2016760_05
Drill Hole Collar	69315.98 E, 38764.04 N, 1477.661 m RL
Samples	SOB2016760_05
Location	120.5 m
Lithology	Cb-matrix breccia
Description	Ori sample



Rock Sample	SOB2016760_06
Drill Hole Collar	69315.98 E, 38764.04 N, 1477.661 m RL
Samples	SOB2016760_06
Location	129.7 m
Lithology	Gt-bt schist
Description	Petro sample







<b>Rock Sample</b>	<b>SOB2016760_10</b>
Drill Hole Collar	69315.98 E, 38764.04 N, 1477.661 m RL
Samples	SOB2016760_10 (mislabelled as 670_10)
Location	189 m
Lithology	Foliated meta-andesite
Description	Calcite cuts foliation

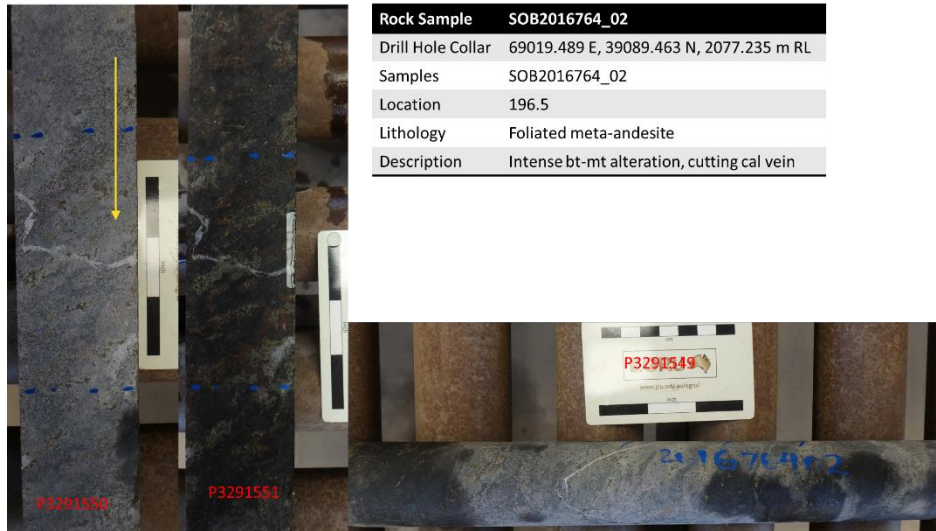


<b>Rock Sample</b>	<b>SOB2016760_11</b>
Drill Hole Collar	69315.98 E, 38764.04 N, 1477.661 m RL
Samples	SOB2016760_11 (mislabelled as 670_11)
Location	178.8 m
Lithology	Foliated meta-andesite
Description	Foliation parallel cpy-cal-py vein



<b>Rock Sample</b>	<b>SOB2016764_01</b>
Drill Hole Collar	69019.489 E, 39089.463 N, 2077.235 m RL
Samples	SOB2016764_01
Location	187 m
Lithology	Foliated meta-andesite
Description	contact





Rock Sample	SOB2016764_02
Drill Hole Collar	69019.489 E, 39089.463 N, 2077.235 m RL
Samples	SOB2016764_02
Location	196.5
Lithology	Foliated meta-andesite
Description	Intense bt-mt alteration, cutting cal vein



Rock Sample	SOB2016764_03
Drill Hole Collar	69019.489 E, 39089.463 N, 2077.235 m RL
Samples	SOB2016764_03
Location	217 m
Lithology	Foliated meta-andesite
Description	Bt-mt altered,

Rock Sample	SOB2016680_01
Drill Hole Collar	69246.16 E, 38152.19 N, 2160.591 m RL
Samples	SOB2016680_01
Location	765.5 m
Lithology	Clast supported breccia
Description	In quartz vein, look to confirm and characterise in thin section, proximal to contact.





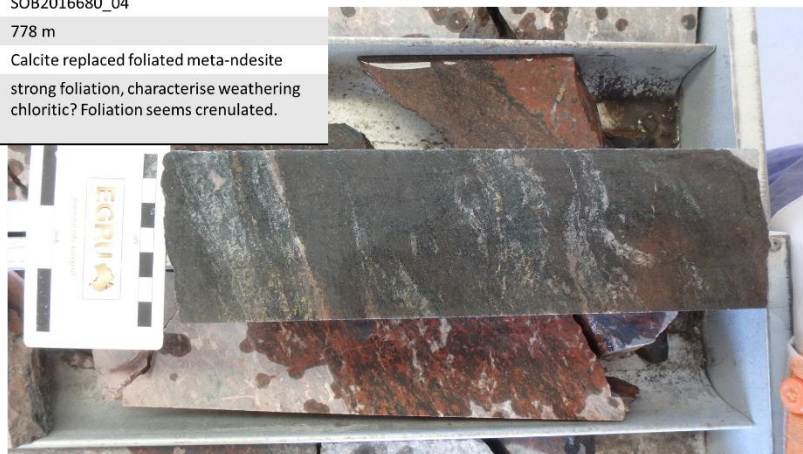
<b>Rock Sample</b>	<b>SOB2016680_02</b>
Drill Hole Collar	69246.16 E, 38152.19 N, 2160.591 m RL
Samples	SOB2016680_02
Location	766 m
Lithology	Clast supported breccia
Description	Magnetite vein, mineralisation, close to contact



<b>Rock Sample</b>	<b>SOB2016680_03</b>
Drill Hole Collar	69246.16 E, 38152.19 N, 2160.591 m RL
Samples	SOB2016680_03
Location	768 m
Lithology	Foliated meta-andesite
Description	Contact from above



<b>Rock Sample</b>	<b>SOB2016680_04</b>
Drill Hole Collar	69246.16 E, 38152.19 N, 2160.591 m RL
Samples	SOB2016680_04
Location	778 m
Lithology	Calcite replaced foliated meta-andesite
Description	strong foliation, characterise weathering chloritic? Foliation seems crenulated.







<b>Rock Sample</b>	<b>SOB2016656_01</b>
Drill Hole Collar	69163.632 E, 38180.579 N, 2160.64 m RL
Samples	SOB2016656_01
Location	695.5 m
Lithology	Meta-andesite
Description	<ul style="list-style-type: none"><li>• ORI sample</li><li>• Fabric and vein</li></ul>

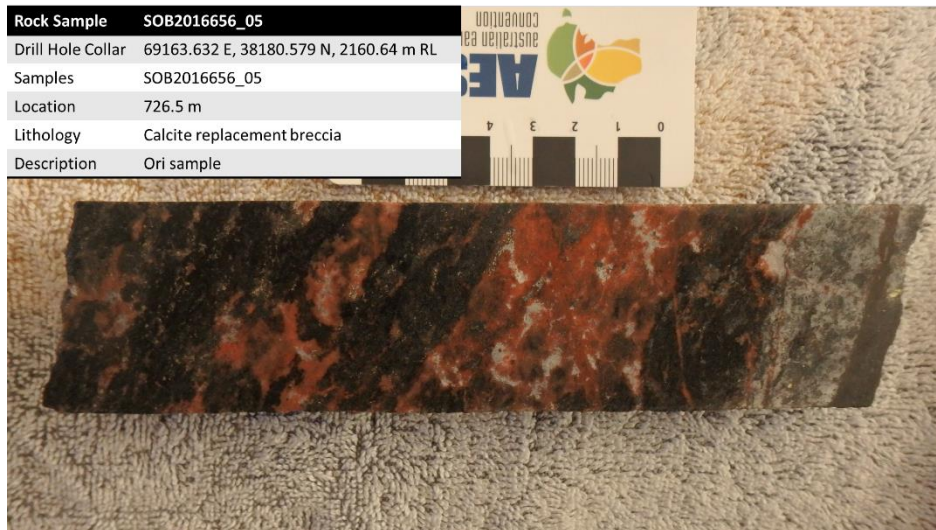


<b>Rock Sample</b>	<b>SOB2016656_02</b>
Drill Hole Collar	69163.632 E, 38180.579 N, 2160.64 m RL
Samples	SOB2016656_02
Location	703 m
Lithology	Foliated meta-andesite
Description	<ul style="list-style-type: none"><li>• Ori sample</li></ul>



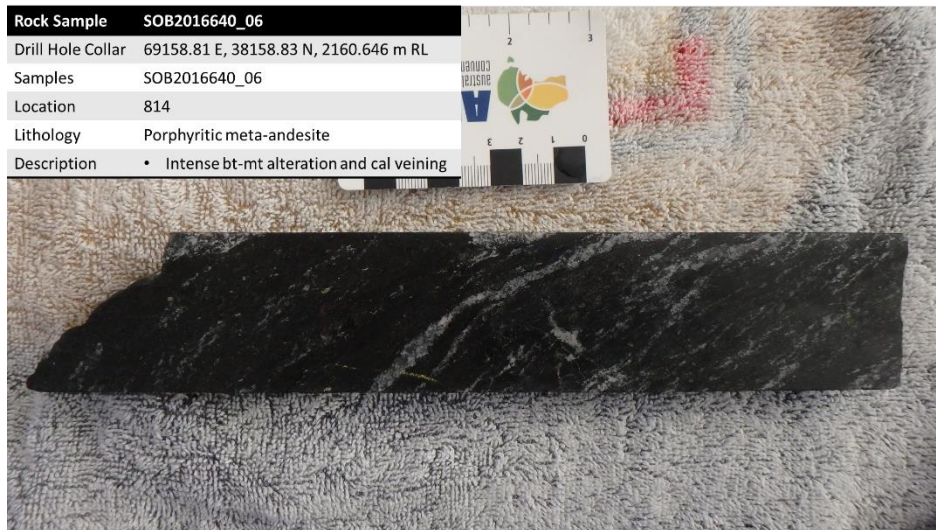
<b>Rock Sample</b>	<b>SOB2016656_03</b>
Drill Hole Collar	69163.632 E, 38180.579 N, 2160.64 m RL
Samples	SOB2016656_03
Location	707 m
Lithology	Calcite-matrix breccia
Description	Elongate clasts define fabric









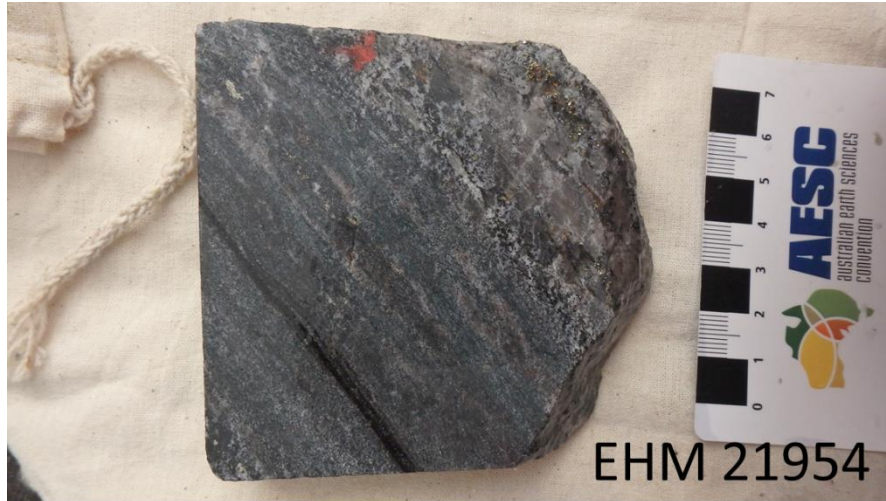








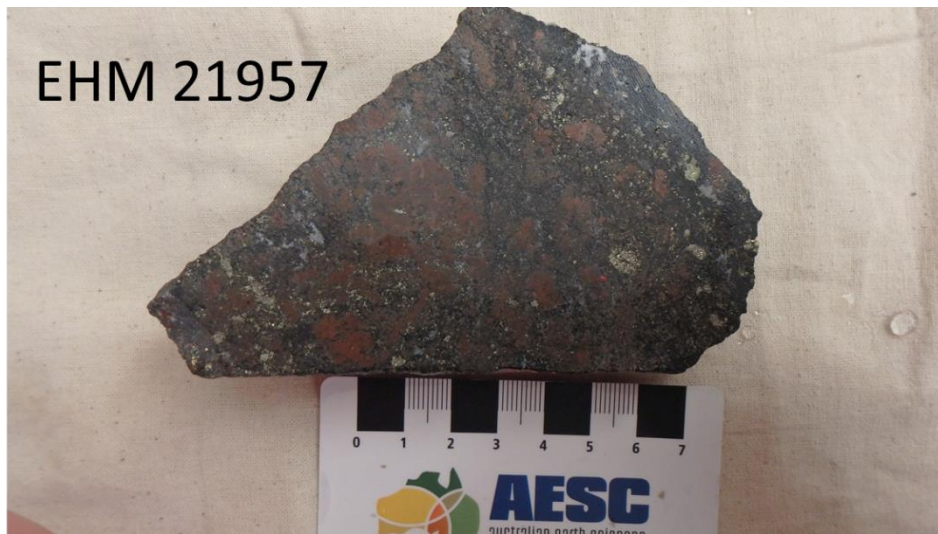




EHM 21954

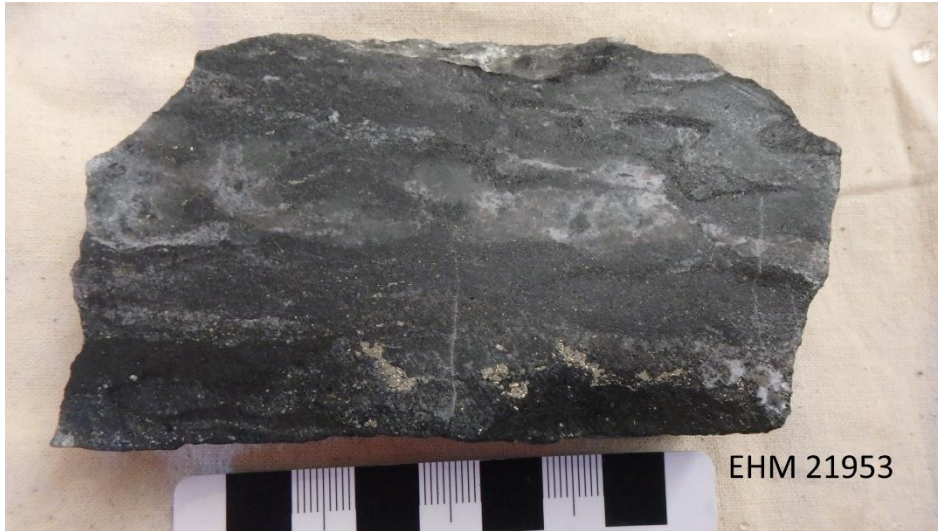


EHM 21955



EHM 21957





## **APPENDIX E: CORE LOGGING SUMMARY**

EH656: Dominated by biotite-rich rocks with persistent magnetite-biotite foliation and intense, foliation parallel quartz-calcite veining. Intermittent zones of breccias have intermediate volcanic clasts that preserve biotite-magnetite foliation. Veins containing chalcopyrite and quartz-calcite cut fabrics at moderate to deep angles.

EH640: Biotite-rich rocks with persistent magnetite-biotite foliation and intense, foliation parallel quartz-calcite veining dominate. Quartz veins upto 20mm thick cut the fabric at shallow angles. Dominant fabric develops a sigmoidal texture in the central parts of the Inter-lens. Local breccias with elongate, aligned clasts and elongate phenocrysts are observed in lower parts associated with distinct magnetite veins. Orientation of veins were generally sub horizontal to the dominant fabric.

EH760: Intensely foliated, biotite-rich rocks hosted minor disseminated chalcopyrite mineralisation. In the central parts of the Inter-lens, the dominant fabric gave way to intense quartz-calcite veining, which displays patchy zones of chaotic folding. The dominant magnetite-biotite fabric was regularly truncated at shallow angle by calcite veins which contained chalcopyrite. Calcite veins of a later stage cut the fabric subvertically.

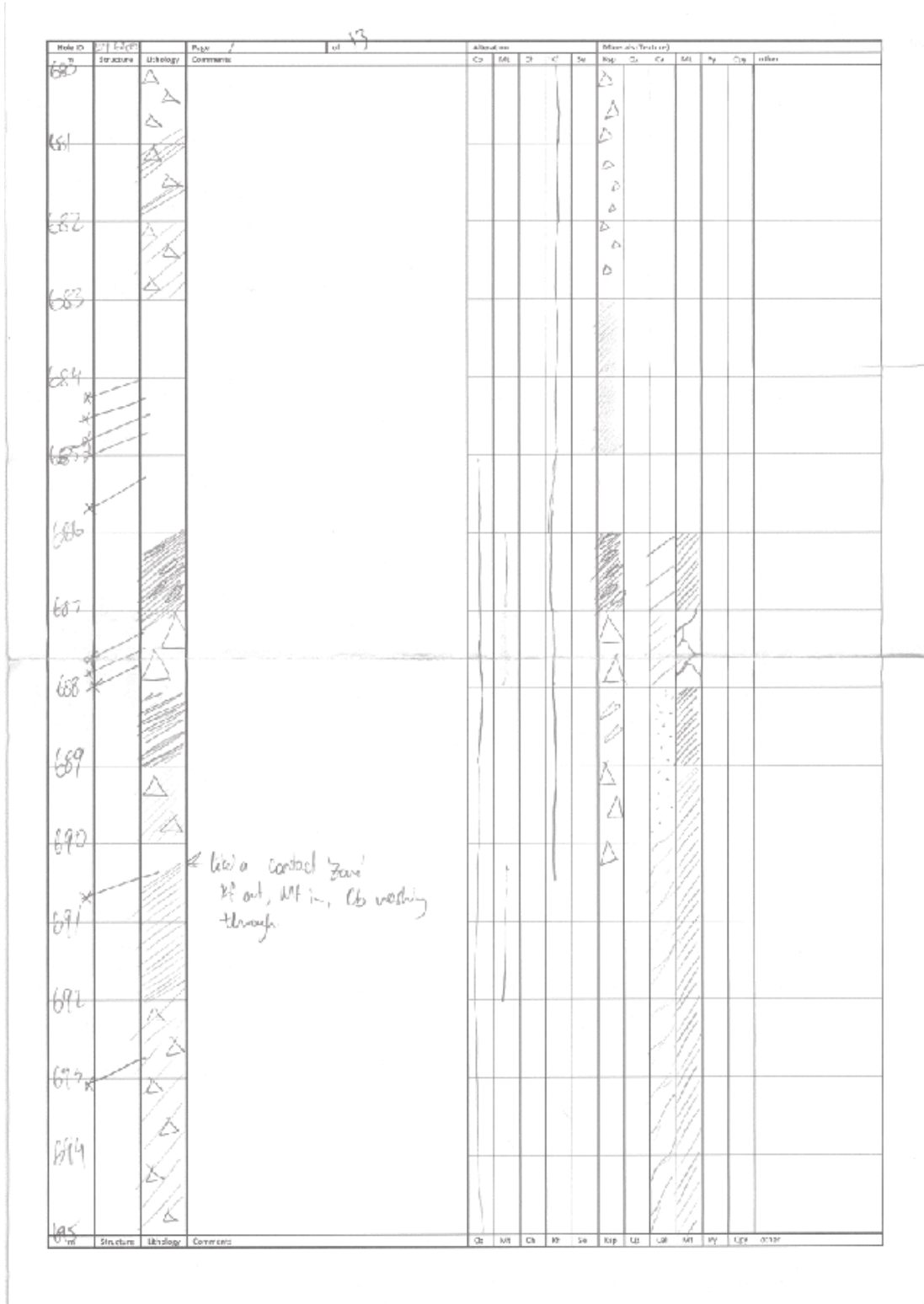
EH889: Tectonic fabric is expressed predominantly by oriented clasts in metasomatic breccias. Porphyritic textures show alignment of phenocrysts and amygdales in parts.

EH764: Calcite interbanded with biotite-magnetite foliation is dominant. Patchy zones of calcite tension veining appear in more brecciated zones.

EH680: Discontinuous magnetite-biotite veins and bands are texturally dominant with local elongate clasts. Secondary crackle brecciation overprinting previous breccias is common and tectonic fabric is less intense to absent in these zones.

**APPENDIX F: GRAPHICAL DRILLHOLE LOGS.**

**EH640**















HOLE ID	Depth	Structure	Lithology	Page No	Comments	Mineralization					Minerals (Texture)									
						La	Ni	Cu	Pb	Zn	Asp	Mal	Chl	Py	Py	Py	Other			
757					mt fabric pink grain oriented & grain															
758																				
759																				
760					← OPI SAMPLE ← OPI SAMPLE & CPY															CPY in zone forming Sediment
761																				
762																				
763																				
764																				
765																				
766																				
767																				
768																				CPY smaller to mt fabric, in the mt fabric zones
769																				
770																				

Core ID	Lithology	Face / Contents	Alteration					Minerals / contents					
			Cl	Wt	Ch	Hf	Se	Epi	Op	Qz	Wt	Py	Other
771													
772													
773													
774													
775													
776													
777													
778		← OPS SAMPLE											
779													
780													
781													
782													
783													
784		← OPS SAMPLE											
785													

File ID	STATUS	LIBRARY	Page	1 of 3	Element					Minerals (Trace %)									
					Ca	Mg	Ch	Al	Si	Fe	Qz	Ca	Mt	Py	Cpx	Other			
786																			
787																			
788																			
789																			
790																			
791																			
792																			
793																			
<del>794</del>																			
795																			
796																			
797																			
798																			
799																			
800																			

← OPI Sample

← OPI Sample



Hand #	Geo		Prop	Comments	Abundant					Minerals: Textures						
	Structure	Micrology			Q	Mt	Ch	Il	Sc	Sp	Ep	Pl	Ol	Mt	Py	Sp
800																
801				Partial fault zone.												
802																
803																
804																
805																
806																
807																
808																
809																
810																
811																
812																
813																
814																
815																

Hole ID	STATION	ELEVATION	Page 102 103	Mineral					Minerals, Textures									
				Zc	Mt	Ch	Pf	Sa	Ep	Qz	Cl	Mt	Px	Cpx	Other			
815																		
816																		
817																		
818																		
819																		
820																		
821																		
822																		
823																		
824																		
825																		
826																		
827																		
828																		
829																		
830																		

← ORE SAMPLE  
003



← ORE SAMPLE

← ORE SAMPLE

Core ID	Structure	Lithology	Page 11 of 13	Mineralization					Minerals (Features)						
				Ca	Mg	Cu	Pb	Zn	Asp	Mal	Chl	Py	Sph	Other	
830															
831															
832															
833															
834															
835															
836															
837															
838															
839															
840															
841															
842															
843															
844															
845															

Zone ID	Structure	Minerals	Comments	Amorphous					Minerals (Square)								
				Ca	Mg	Ch	Fe	Se	Ep	Ca	Cal	Mt	Fy	Gpr	Other		
845																	
846			Structure very chaotic: appears to be intracrystalline - thin texture														
847																	
848			← 847-8 DP2 thin Retained (fractured?)														
849			← sample for thin section														
850			← <del>DP2</del> sample														
851			← <del>DP2</del> Anorthite? 10-16														
852																	
853																	
854																	
855			← <del>DP2</del> infill / kein D2/cb + opt. p.c. 10-15														
856																	
857																	
858																	
859																	
860																	



How D of B	Structure	Lithology	Comments	A. Inclusions					B. Minerals/Textures									
				Cl	Mt	Ch	K	Sp	Kfs	Pl	Pa	Alb	Py	Qtz	Other			
860																		
861																		
862																		
863																		
864																		
865																		
866																		
867																		
868																		
869																		
870																		
871																		
872																		
873																		
874																		

Similar to  
 Zone immediately  
 at contact in 869 et al.  
 except this zone is  
 extra size (for most).  
 Bandow contact is difficult  
 to identify, look for  
 brittle contact.

probably  
 meta-volcanic  
 laces base  
 (pink grey)

871-2 Contact? (end of  
 Lower zone?)  
 As kind of fabric seems  
 to terminate beyond the  
 Qz vein.

disseminated  
 in Cl/Pl  
 matrix  
 intal.

EH656

Hole ID	S.M.	P.L.	Name	ID	Abund.					Microfossil					
					Ch	Mt	Cl	St	Sp	Cal	Gr	Cal	Mt	Sp	Other
675			CLAY @ Core												
676		△													
677		△													
678		△													
679		△													
680		△													
681		△													
682		△	<p>↳ = would think this fabric is likely clay, but could be an extensive contact/boundary. ↳ ↑↑ ch with</p>												
683															
684			<p>↳ on other lens, see face ↳ increase in 687. But no fossils! ← photo does not show the same, lens is ok.</p>												
685															
686		△	<p>↳ logged as contact c. O.A. 687 are from lens below (not contact boundary)</p>												
687		△													
688		△													
689		△													
690		△													

Hex D	Structure	SCL Etiology	Page 3 Comments	of	Attribution					Material/Texture							
					Cs	MR	Dr	C	Se	MR	Dr	Cs	MR	Dr	Other		
689																	
690																	
691																	
692																	
693																	
694																	
695																	
696																	
697																	
698																	
699																	
700																	
701																	
702																	
703																	
704																	
705																	
706																	

← ORE SAMPLE  
 [696-697] - behind vein

← [691 SAMPLE] [691-692]  
 fabric anomaly

Height	Structure	Lithology	Page 5 Concrete	or	Stratigraphy					Materials (Percentage)									
					Cl	Mt	Ca	Rf	Se	Rsp	Op	Cl	Mt	Pr	Ccr	Other			
705																			
706																			
707																			
708																			
709																			
710																			
711																			
712																			
713																			
714																			
715																			
716																			
717																			
718																			
719																			
720																			

~~[20165503]~~  
 Maximum, around Cl/Mt  
 Some coarse volcanic clasts  
 which associated, around  
 the fire mural.  
 [20165503]

FIRE SAMPLE 2016 65604



Hole ID #	Structure	ESL Lithology	Page Comments	#	Minerals Occurences															
					Ch	MT	Ch	MP	Se	Kfs	Co	Gal	Ms	Px	Qtz	Other				
720																				
721																				
722																				
723																				
724																				
725																				
726			← end of core, cut & sampled																	
727			← BMS sample (20665005) Fabric & Pink?																	
728																				
729																				
730																				
731																				
732																				
733																				Trace Sp. of P <sup>+</sup> - 1st fabric
734																				
735																				
736																				
737																				
738																				
739																				
740																				
741																				
742																				
743																				
744																				
745																				
746																				
747																				
748																				
749																				
750																				
751																				
752																				
753																				
754																				
755																				
756																				
757																				
758																				
759																				
760																				
761																				
762																				
763																				
764																				
765																				
766																				
767																				
768																				
769																				
770																				
771																				
772																				
773																				
774																				
775																				
776																				
777																				
778																				
779																				
780																				
781																				
782																				
783																				
784																				
785																				
786																				
787																				
788																				
789																				
790																				
791																				
792																				
793																				
794																				
795																				
796																				
797																				
798																				
799																				
800																				

Hole ID	Structure	Lithology	Page Layer(s)	or	Stratigraphy					Lithology (Remarks)									
					U1	U2	U3	U4	U5	U6	U7	U8	U9	U10					
735																			
736																			
737																			
738																			
739		Δ																	
740		Δ																	
741		Δ																	
742																			
743																			
744		Δ																	
745		Δ																	
746																			
747																			
748		Δ																	
749																			
750																			
n	Structure	Lithology	Comments		Ob	Mt	Ch	Rf	Sc	Ksp	Co	Col	Mt	Fy	Gpy	Other			

← Can Change fill? qtz in CB section  
 E+S (phac).

Hole ID	Structure	Lithology	Page	or	Alterations					Minerals / Trace								
					Cl	MT	Ch	Hf	Se	Ksp	Qtz	Cal	MT	Py	Chc	Other		
750																		
751																		
752																		
753																		
754																		
755																		
756																		
757																		
758																		
759																		
760																		
761																		
762																		
763																		
764																		
765																		

8 in place 8 of 8  
 likely linked to  
 - Cl increasing  
 - Silica increase  
 - brittle zone  
 - fabric veining  
 - breccia texture some in  
 - Spherals occurring  
 in clastic material

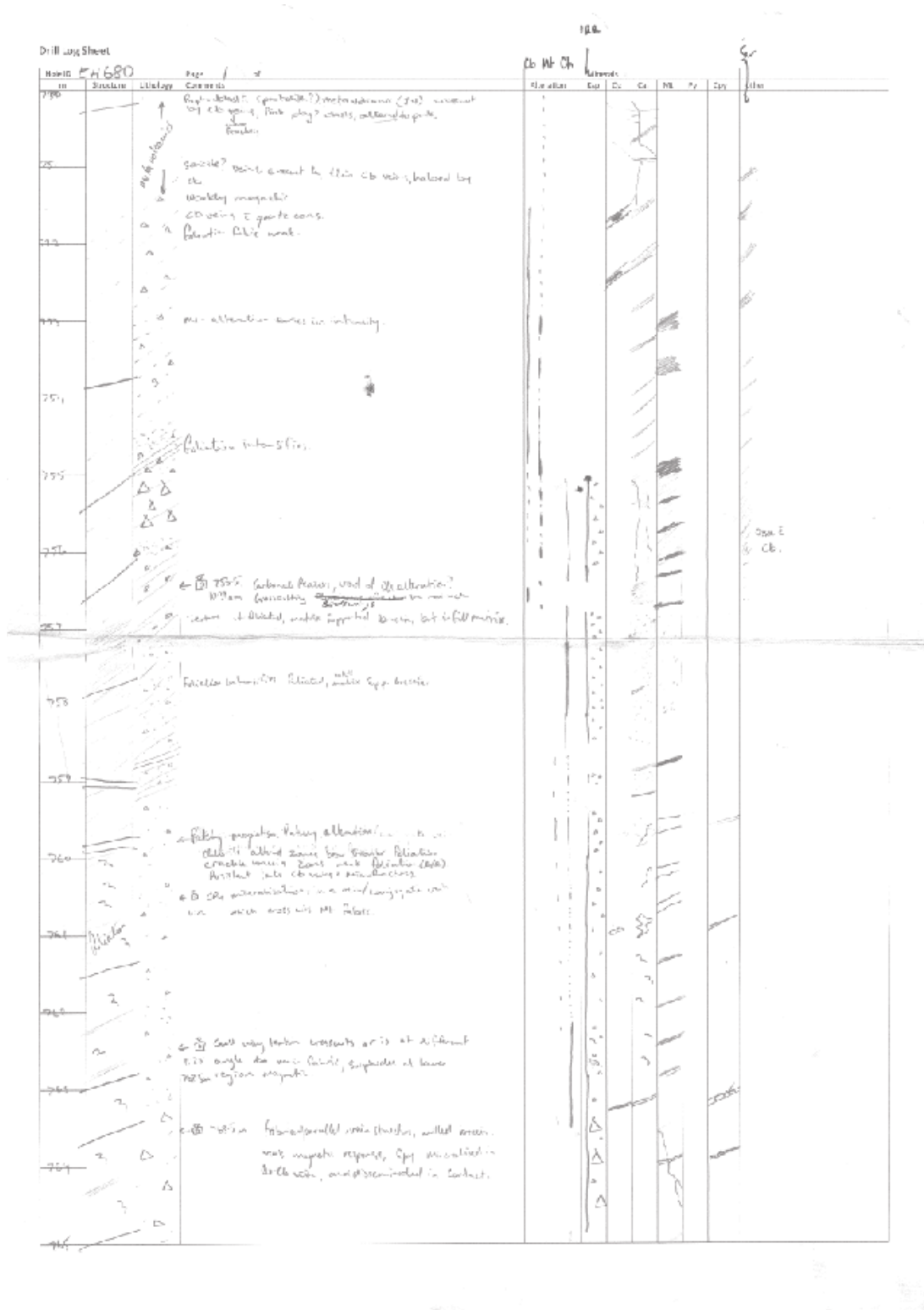
scoping  
 either to  
 mt fabric  
 or in  
 clastic matrix

Node ID	Structure	Lithology	Facies	Comments	Alteration					Minerals (Texture)									
					LD	MT	CF	CT	SA	Py	Ch	MT	Py	Ch	Other				
765																			
766					beyond this point, lens tend out of the Inter-lens.  ↓ MT ↑ Mt? ↑ cb ↑ py cgs  beyond 780, Mt nodules appear as MSFV etc.														
767																			
768																			
769																			
770																			
771																			
772																			
773																			
774																			
775																			
776																			
777																			
778																			
779																			
780																			
781																			
782																			
783																			
784																			
785																			
786																			
787																			
788																			
789																			
790																			
791																			
792																			
793																			
794																			
795																			
796																			
797																			
798																			
799																			
800																			

← Silicates  
 assemblage  
 chlorite  
 in Ch matrix  
 in Mt veins  
 at interface  
 Ch matrix  
 & veins



EH680



Drill Log Sheet

Depth (m)	Structure	Lithology	Page 2 of 2	Comments	Alteration	Minerals	Other				
					Al	Si	Ca	Mg	Fe	Sr	Other
761				760-762m - 100% ...							
762				762-764m - ...							
764				764-766m - ...							
766				766-768m - ...							
768				768-770m - ...							
770				770-772m - ...							
772				772-774m - ...							
774				774-776m - ...							
776				776-778m - ...							
778				778-780m - ...							
780				780-782m - ...							
782				782-784m - ...							
784				784-786m - ...							
786				786-788m - ...							
788				788-790m - ...							
790				790-792m - ...							
792				792-794m - ...							
794				794-796m - ...							
796				796-798m - ...							
798				798-800m - ...							
800				800-802m - ...							
802				802-804m - ...							
804				804-806m - ...							
806				806-808m - ...							
808				808-810m - ...							
810				810-812m - ...							
812				812-814m - ...							
814				814-816m - ...							
816				816-818m - ...							
818				818-820m - ...							
820				820-822m - ...							
822				822-824m - ...							
824				824-826m - ...							
826				826-828m - ...							
828				828-830m - ...							
830				830-832m - ...							
832				832-834m - ...							
834				834-836m - ...							
836				836-838m - ...							
838				838-840m - ...							
840				840-842m - ...							
842				842-844m - ...							
844				844-846m - ...							
846				846-848m - ...							
848				848-850m - ...							
850				850-852m - ...							
852				852-854m - ...							
854				854-856m - ...							
856				856-858m - ...							
858				858-860m - ...							
860				860-862m - ...							
862				862-864m - ...							
864				864-866m - ...							
866				866-868m - ...							
868				868-870m - ...							
870				870-872m - ...							
872				872-874m - ...							
874				874-876m - ...							
876				876-878m - ...							
878				878-880m - ...							
880				880-882m - ...							
882				882-884m - ...							
884				884-886m - ...							
886				886-888m - ...							
888				888-890m - ...							
890				890-892m - ...							
892				892-894m - ...							
894				894-896m - ...							
896				896-898m - ...							
898				898-900m - ...							
900				900-902m - ...							
902				902-904m - ...							
904				904-906m - ...							
906				906-908m - ...							
908				908-910m - ...							
910				910-912m - ...							
912				912-914m - ...							
914				914-916m - ...							
916				916-918m - ...							
918				918-920m - ...							
920				920-922m - ...							
922				922-924m - ...							
924				924-926m - ...							
926				926-928m - ...							
928				928-930m - ...							
930				930-932m - ...							
932				932-934m - ...							
934				934-936m - ...							
936				936-938m - ...							
938				938-940m - ...							
940				940-942m - ...							
942				942-944m - ...							
944				944-946m - ...							
946				946-948m - ...							
948				948-950m - ...							
950				950-952m - ...							
952				952-954m - ...							
954				954-956m - ...							
956				956-958m - ...							
958				958-960m - ...							
960				960-962m - ...							
962				962-964m - ...							
964				964-966m - ...							
966				966-968m - ...							
968				968-970m - ...							
970				970-972m - ...							
972				972-974m - ...							
974				974-976m - ...							
976				976-978m - ...							
978				978-980m - ...							
980				980-982m - ...							
982				982-984m - ...							
984				984-986m - ...							
986				986-988m - ...							
988				988-990m - ...							
990				990-992m - ...							
992				992-994m - ...							
994				994-996m - ...							
996				996-998m - ...							
998				998-1000m - ...							

Check for  
 calcite, and  
 other minerals  
 from the  
 to the  
 Find out  
 in the section



Hole ID	CA structure	Lithology	Page	of	Abundances					Minerals/Textures								
					Ca	Mg	Si	Al	Fe	Sp	Qtz	Pl	Py	Other				
796																		
797																		
798																		
799																		
800																		
801																		
802																		
803																		
804																		
805																		
806																		
807																		
808																		

801-802 infilling behind volcanic

800-801 spt mineralisation in vein

801-802 Condensation zone

802-803 Boundary phase growth

vein  
 Quartz becoming more common  
 large clasts, with cream (Si-alkalid)  
 infill, possible albite  
 kaolinite infilling of  
 veins and to be banding

805-806 infill Ca, S - alteration  
 in Ca vein formation  
 part of a Concord IV

Large mineral inclusions  
 in Ca veins and  
 to be banding



**EH760**

ROMANOS 002

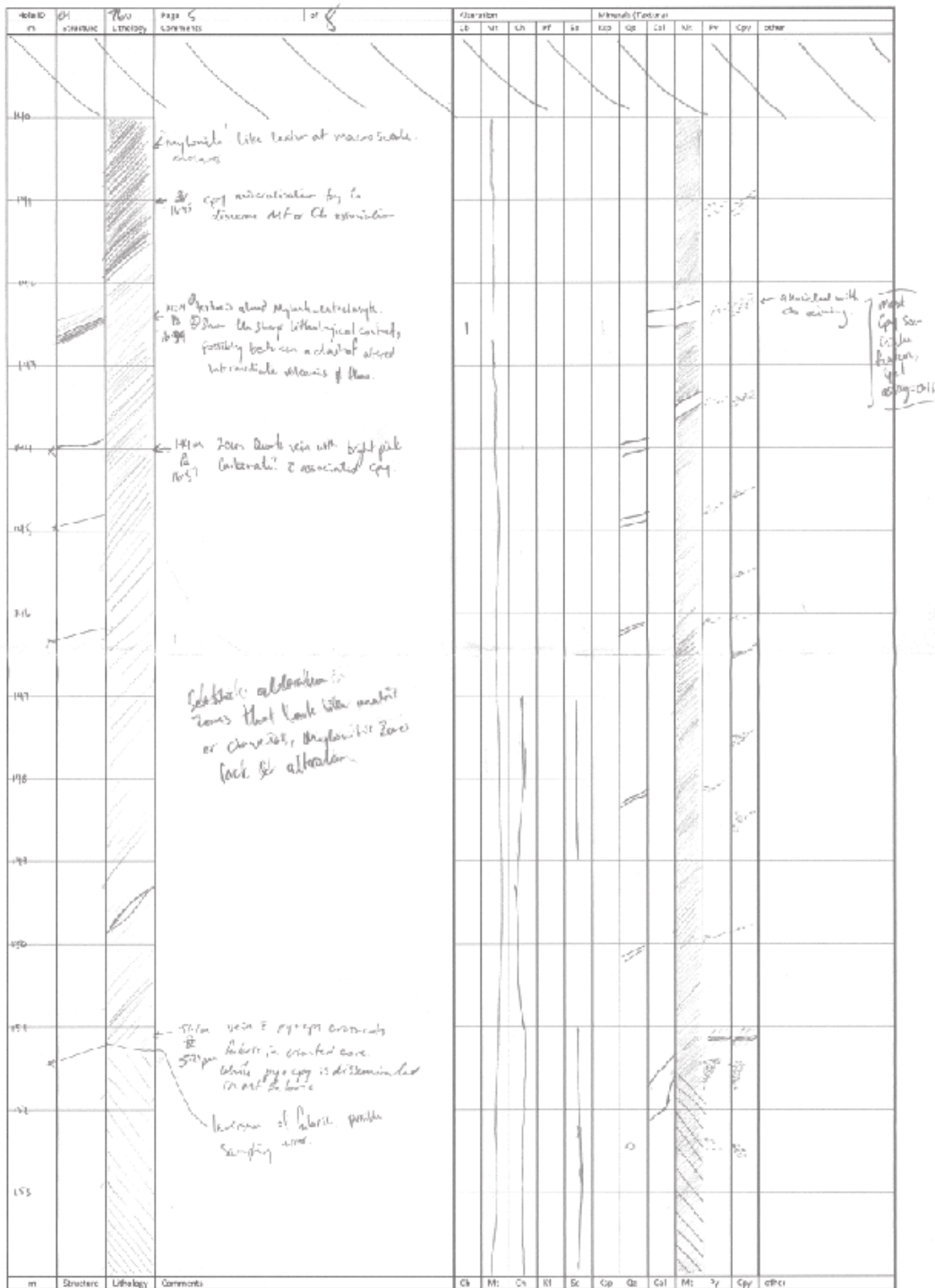
Hole ID	EHT60	Lithology	Page 1	Comments	Orientation					Minerals (For. et al)								
					Lt	Nt	Ln	Pt	St	Rz	Qz	Lil	Kf	Pv	Cpy	Other		
81		Typical coarse Kevy, foliated Wernicke, clast supported breccia Occasional Mt vein. Mostly Mt. Some Cb matrix.																
82																		
83																		
84																		
85																		
86																		
87																		
88																		
89																		
90																		
91																		
92																		
93																		
94																		
95																		
96																		
97																		
98																		
99																		
100																		











Hole #	m	Structure	Lithology	Page # Layers	Minerals					Minerals (Trace)							
					U	Mt	Ls	Rf	Sp	Ap	Lu	Cl	Mt	Py	Gr	Other	
	155			1 or 8													
	156																
	157																
	158																
	160																
	161																
	162																
	163																
	164																
	165																
	166																
	167																
	168																
		Structure	Lithology	Comments	Co	Mt	Cl	Sp	Ap	Lu	Cl	Mt	Py	Gr	Other		

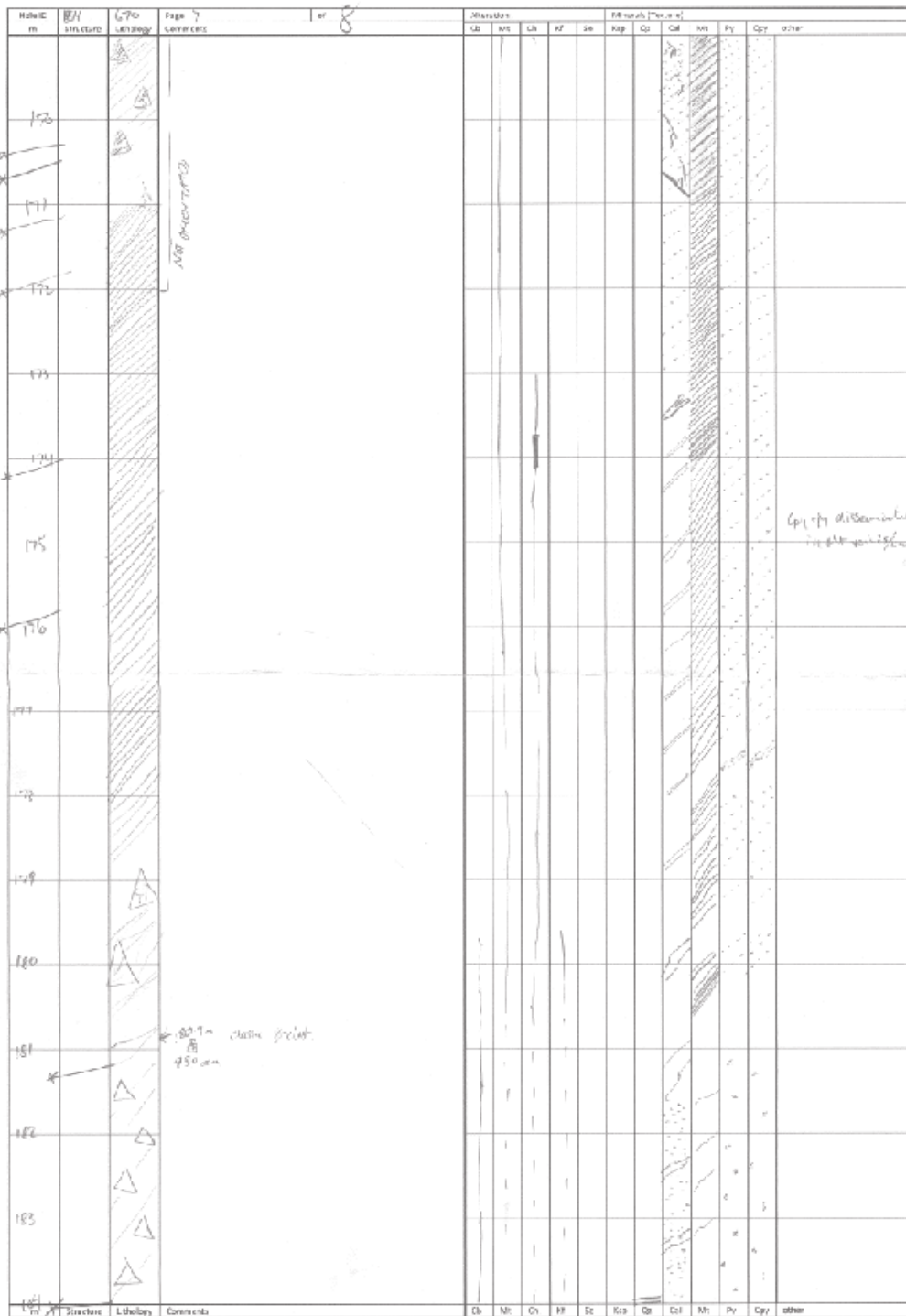
155m  
 156m  
 Apparent break in fabric,  
 massive texture, fractured  
 lot of Qz-Ls veins

157m - Fracture - folded vein?

fabric

check for fold, due to fabric.

165m  
 166m  
 symmetrical folding in  
 orientated con.





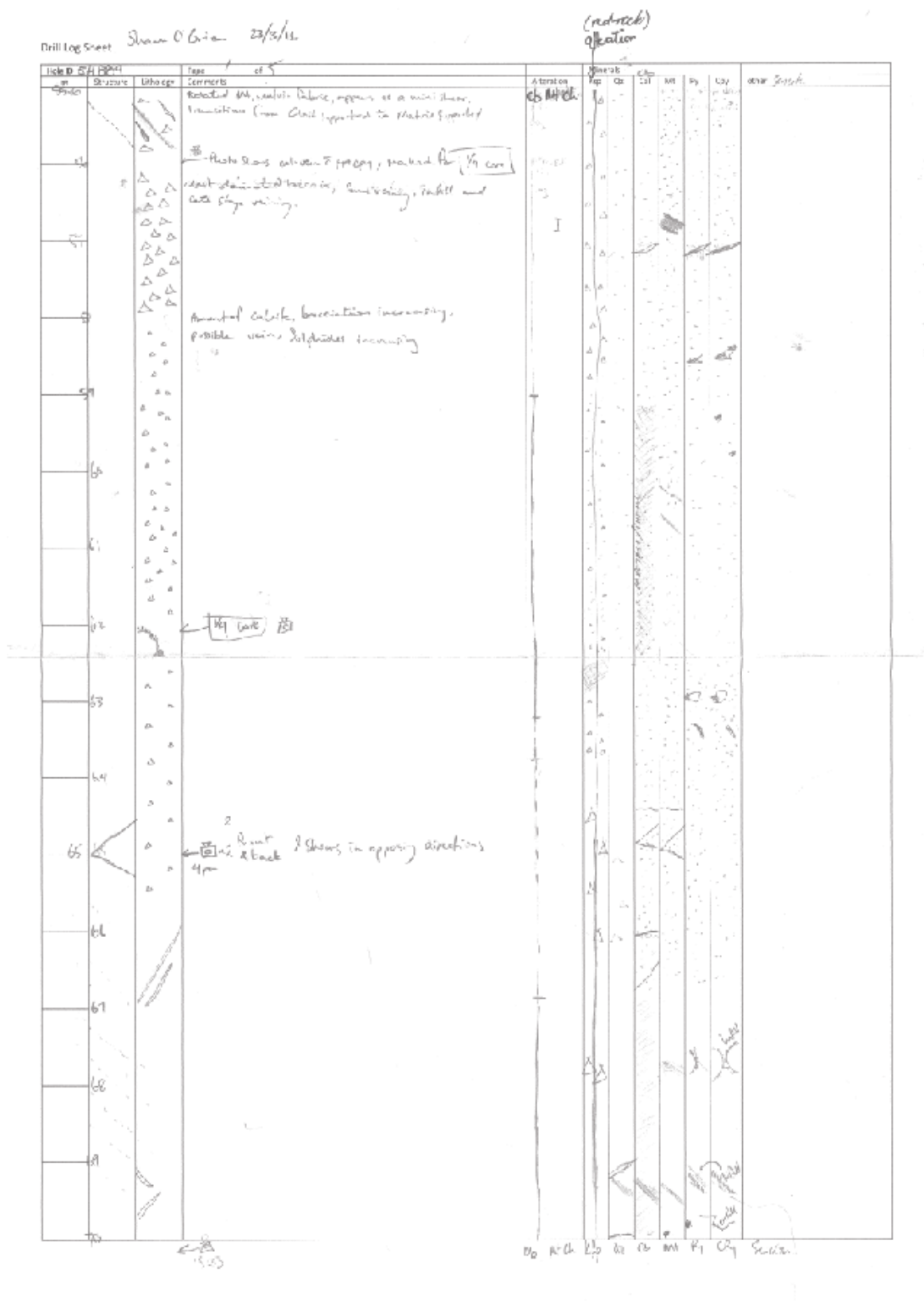






Hole ID	764	UTM Zone	Page 5	of	Minerals					Mineral Texture								
					Ch	Mt	Cl	Qt	Sp	Asp	Tr	Cal	Mt	Pl	Op	Other		
217																		
214																		
212																		
213																		
214																		
215																		
216																		
217																		
218																		
219																		
219.5																		
<p>EOH</p> <p>Not much to take away from this hole.</p> <ul style="list-style-type: none"> <li>- No new relationships</li> <li>- No real break in character, although boundary difficult to define</li> <li>- no gonals</li> <li>- a bit more Fe rich.</li> <li>- varying degrees of brecciation/flow alteration.</li> </ul>																		
in	Strat	Lithology	Comments		Ch	Mt	Cl	Qt	Sp	Asp	Tr	Cal	Mt	Pl	Op	Other		

EH889





Drill Log Sheet

